THE UNIVERSITY OF CHICAGO

THE ROLE OF NICOTINAMIDE N-METHYLTRANSFERASE IN TRIPLE-NEGATIVE BREAST CANCER GENE EXPRESSION AND *IN VIVO* METASTATIC POTENTIAL

A DISSERTATION SUBMITTED TO
THE FACULTY OF THE DIVISION OF THE BIOLOGICAL SCIENCES
AND THE PRITZKER SCHOOL OF MEDICINE
IN CANDIDACY FOR THE DEGREE OF
DOCTOR OF PHILOSOPHY

COMMITTEE ON CANCER BIOLOGY

BY

DENIZ NESLI DOLCEN

CHICAGO, ILLINOIS

DECEMBER 2022

TABLE OF CONTENTS

LIST OF FIGURES

LIST OF TABLES

ACKNOWLEDGMENTS

I would like to thank my PhD advisor Dr. Suzanne Conzen and dissertation committee members Dr. Geoffrey Greene, Dr. Chuan He and Dr. Russell Szmulewitz for their valuable mentorship throughout my PhD. I would also like to thank my family for their unwavering love and support that give me the strength to persevere and motivation to aim towards my biggest dreams.

ABSTRACT

Nicotinamide N-methyltransferase (NNMT) methylates nicotinamide (vitamin B_3) to convert it into 1-methylnicotinamide (1-MNA) using the universal methyl donor S-adenosylmethionine (SAM) also utilized by DNA and histone methyltransferases. This enzymatic reaction has first been proposed as an excess nicotinamide removal mechanism as 1-MNA is excreted in urine; however, there is now strong literature support for NNMT's role in regulating hepatocyte/adipocyte cellular metabolism and cancer cell phenotypes through SAM-depletion induced DNA/histone hypomethylation and associated alterations in the expression of metabolic genes and tumor-promoting genes.

Here, I report a novel association between triple-negative breast cancer (TNBC) NNMT expression and TNBC gene expression along with *in vivo* metastatic potential. TNBC is an aggressive disease that comprises approximately 15% of all breast cancers, is uniformly treated with chemotherapy due to lack of ER/PR/HER2 expression and lack of other genetic drivers that commonly occur in the patient population, and therefore has an unmet need for effective targeted therapies. My dissertation research implicates NNMT as a metastasis-promoting protein in TNBC. I report that NNMT expression in TNBC cells is associated with 1) downregulated intracellular SAM levels, 2) upregulated expression of EMT and invasion-promoting genes, 3) downregulated expression of anabolic genes, and 4) increased probability of visceral metastasis formation in xenograft mouse models. I also report that NNMT-depletion in TNBC cells significantly decreases the probability of visceral metastasis formation *in vivo* while specifically upregulating the liver tropism of TNBC cells. Finally, remainder of my dissertation investigates and discusses NNMT-regulated cellular mechanisms that are pharmacologically targetable along with NNMT to mitigate overall and liver-specific TNBC metastasis formation as a potential therapeutic strategy.

CHAPTER 1

INTRODUCTION

1.1 LITERATURE REVIEW ON NICOTINAMIDE

Nicotinamide (NAM) is a water-soluble form of vitamin B_3 and is a major precursor for nicotinamide adenine dinucleotide (NAD^+) and thereby ATP production (1). NAM cannot be produced endogenously by human cells and is acquired through consumption of meat, fish, legumes, mushrooms, nut and grains. Majority of research interest in NAM biology lies in the role of oral NAM supplementation in reducing the incidence of non-melanoma skin cancers (NMSCs). In a phase 3 randomized clinical trial, oral NAM supplementation was shown to be safe and effective in reducing the incidence of new NMSCs in high-risk patients (2). NMSCs are caused primarily by exposure to ultraviolet (UV) radiation. UV radiation to skin cells results in DNA damage that triggers the ATP-intensive DNA repair process; however, inadequate levels of cellular ATP would dampen DNA repair and increase the incidence of cancer-causing genomic alterations in the inadequately repaired DNA. UV radiation increases the risk of skin cancer by simultaneously damaging DNA and inhibiting DNA repair by depleting NAD^+, which is an essential cofactor for ATP production. As NAM is a major NAD^+ precursor, NAM supplementation is hypothesized to support DNA repair following UV exposure by increasing cellular NAD+ levels and thereby supporting ATP production needed to drive the highly ATP-dependent DNA repair process.

In summary, NAM's support of DNA repair is thought to reduce tumorigenesis and NAM supplementation reduces the rate of new NMSC formation in patients. However, the effect of NAM on NMSC incidence disappears upon cessation of oral supplementation (2). Further research is needed to elucidate the cellular mechanisms contributing to the tumor-suppressive role of NAM.

1.2 LITERATURE REVIEW ON NICOTINAMIDE N-METHYLTRANSFERASE

NAM can be modified in cells with the addition of a methyl group to its pyridine ring, and research interest in NAM methylation began in the 1940s with the identification of methylated vitamin B_3 metabolites in rodent urine (reviewed in (3)). Subsequently, nicotinamide N-methyltransferase (NNMT) was discovered to be a methyltransferase that consumes the universal methyl donor S-adenosyl methionine (SAM) for methylation of NAM, converting NAM to 1-methylnicotinamide (1-MNA) which is subsequently excreted in urine (Figure 1.1) (4). Levels of intracellular molecules are tightly regulated to maintain cellular homeostasis, and methylation serves as the predominant excess NAM clearance pathway under physiological conditions. Even though NNMT's biological significance has long been attributed to its mechanism of action in clearing excess nicotinamide, there is now a significant body of literature demonstrating that NNMT's enzymatic activity affects a multitude of cellular physiological and pathological processes which I will review in this chapter.

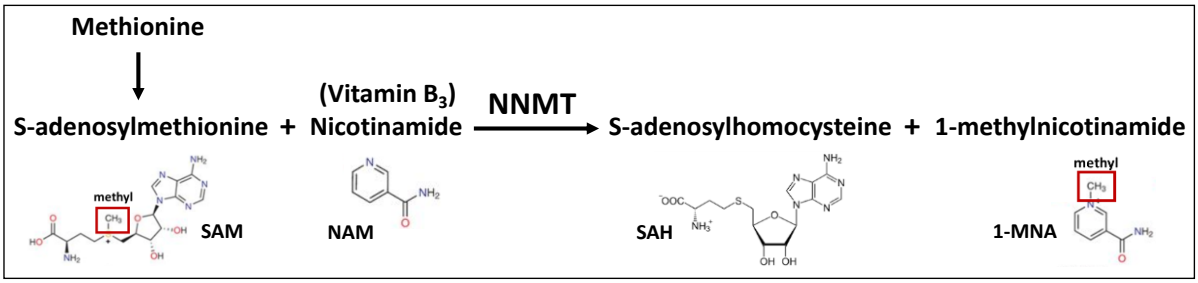

Figure 1.1 NNMT mechanism of action in NAM methylation. SAM is the universal methyl donor participating in most methylation reactions in cells and is synthesized from methionine. NNMT utilizes the methyl group on SAM to methylate the pyridine ring on NAM, converting SAM into S-adenosylhomocysteine (SAH) and NAM into 1-methylnicotinamide (1-MNA), which is excreted in urine. NAM methylation by NNMT is an irreversible reaction.

NNMT gene is comprised of three exons and two introns on human chromosome 11 and mouse chromosome 9. The human NNMT locus encodes a protein of 264 amino acids; alternative NNMT exons and splice variants have been uncovered by RNAseq, but their biological

significance remains to be experimentally validated. The NNMT protein is relatively conserved across mammals and only expressed in certain tissues. Liver exhibits the highest level of NNMT expression among human tissues, and lower levels of expression are found in a few other tissues including adipose, breast, skeletal muscle and lung (The Human Protein Atlas, Figure 1.2). NNMT expression is increased in the Parkinsonian brain, adipose tissue of obese individuals, and several human epithelial cancers (5-12). In addition, STAT3, HNF1, ZEB1 and CEBPβ transcription factors have been shown to mediate increased NNMT expression in cancer cells (10, 13, 14). Beyond these findings, understanding on how NNMT promoter activity and NNMT expression is regulated in mammalian tissues remains limited.

Apart from excess vitamin B_3 removal, NNMT's broader biological significance has initially been established in the fields of obesity, insulin resistance and diabetes research. In one study, NNMT expression in white adipose tissue (WAT) and liver has been shown to be upregulated in a mouse model of diet-induced obesity and insulin resistance (15). In the same

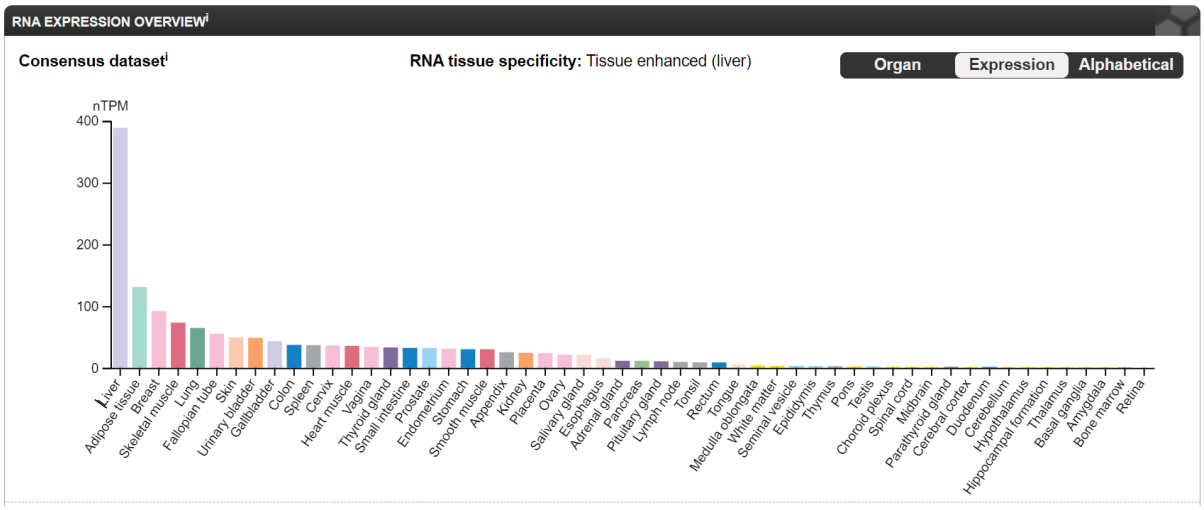

Figure 1.2. RNA expression level of NNMT in different human tissues (The Human Protein Atlas).

study, NNMT depletion in WAT and liver by treatment with an antisense oligonucleotide was shown to protect against the development of diet-induced obesity and insulin resistance. In a

different study, combined NNMT inhibition and reduced-calorie diet have been shown to normalize body composition and liver adiposity parameters in diet-induced obese (DIO) mice to levels observed in age-matched lean diet control mice (16). Importantly, two human studies demonstrated that WAT NNMT expression is regulated in human insulin resistance and type 2 diabetes and that plasma 1-MNA correlates with increased adipose tissue NNMT expression and the degree of insulin resistance (17, 18). These findings all together suggest that NNMT inhibition may provide a novel therapeutic approach for managing insulin resistance and diabetes. Mechanisms by which NNMT could contribute to these metabolic disorders need to be further elucidated, and small molecule inhibitors are in development for effective and selective inhibition of NNMT as a therapeutic approach to these pathologies.

There is accumulating literature investigating the molecular mechanisms by which NNMT regulates metabolism, and recent research findings have also started to establish a role for NNMT in promoting cancer cell phenotypes. By consuming the major NAD^+ precursor NAM and the universal methyl donor SAM with its enzymatic activity, NNMT has the potential to affect the activity of the NAD^+-dependent enzymes and SAM-dependent methyltransferases. Below are cellular processes NNMT has been shown to affect in physiological and pathological contexts with relevant references to primary research literature (reviewed in (3, 19-21)).

1) NAD^+ is an important cofactor that is used by cells to donate electrons to the mitochondrial complex 1 in the electron transport chain and thereby generate ATP. NNMT-induced nicotinamide depletion can result in NAD^+ depletion and thereby causing ATP shortage and affecting the cellular energetic state. *There is already an established role for nicotinamide supplementation in reducing UV exposure-induced skin cancer incidence potentially by providing NAD^+/ATP for the energy-intensive DNA repair processes*

required to maintain DNA integrity following UV exposure. Additionally, BRCA1 depletion in ovarian cancer cells has been shown to upregulate NNMT expression, resulting in decreased mitochondrial respiration and reduced ATP levels, which sensitized these cells to agents that inhibit mitochondrial metabolism and to agents that inhibit glucose import (22).

2) Sirtuin enzymes use NAD^+ as a co-substrate for histone deacetylation and thereby epigenetically regulate metabolic gene expression. NNMT-induced nicotinamide depletion can result in NAD^+ depletion and thereby decrease sirtuin-mediated histone deacetylation affecting metabolic gene expression and cellular metabolic state. *In one study, NNMT knockdown in mouse white adipose tissue and liver has been shown to protect against diet-induced obesity by augmenting cellular energy expenditure through increasing intracellular NAD^+ and SAM levels and thereby altering NAD+-dependent SIRT1 signaling and histone methylation-regulated metabolic gene expression (15). In another study, NNMT overactivation in mouse liver has been shown to decrease NAD^+ levels in the liver and inhibit NAD+-dependent SIRT3 activity, resulting in decreased liver fatty acid oxidation and associated formation of fatty liver (23).*

3) Poly-ADP-ribosyltransferases (PARPs) use NAD^+ as a co-substrate for ADP ribosylation reactions. One of the most important examples is PARP1's role in DNA repair. NNMT-induced nicotinamide depletion can result in NAD^+ depletion and thereby decrease PARP1 activity and DNA repair capacity. *There is only one relevant study that showed that cancer stem cell (CSC) NNMT expression is associated with enhanced resistance to radiation-induced damage and suggested that high NNMT activity in the CSCs could affect the cellular damage resistance by regulating nicotinamide levels and*

thereby DNA repair mechanisms (24). This study, however, did not provide any experimental evidence to support this claim.

4) Most methyltransferases including DNA, histone and protein methyltransferases in mammalian cells use SAM as the methyl donor to methylate their targets. There is a growing body of literature showing that NNMT activity in hepatocytes, adipocytes and cancer cells depletes intracellular SAM resulting in global DNA and histone hypomethylation associated with altered metabolic and tumor-promoting gene expression. DNA and histone hypomethylation-induced gene expression changes have been shown to affect hepatocyte/adipocyte energy metabolism and promote tumorigenic phenotypes in cancer cells belonging to multiple solid tumors. *In one study, higher NNMT expression in ovarian cancer and kidney cancer cells have been associated with decreased repressive histone methylation and upregulated expression of tumor-promoting genes (i.e., SNAI2) in association with increased in vitro motility (25). In another study, higher NNMT expression in mesenchymal glioblastoma stem cells (GSCs) has been shown to promote DNA hypomethylation, increase expression of mesenchymal genes, promote in vitro growth and cell renewal, and promote in vivo tumor growth (26). In another study, expression of NNMT in cancer-associated fibroblasts (CAFs) led to SAM depletion associated with widespread gene expression changes in the tumor stroma that supported ovarian cancer tumor growth in vivo (27). As the last example, one study has shown that higher NNMT expression in glioblastoma cells depletes SAM, decreases the tumor suppressor PP2A methylation and thereby activation in association with decreased sensitivity to radiation treatment (28).*

5) Finally, NNMT's enzymatic product 1-MNA has long been thought as an

inactive metabolite destined to be secreted outside of the cell and excreted out of the body in urine. However, there is a growing body of literature that established 1-MNA as an active metabolite affecting hepatocyte metabolism and cancer cell phenotypes. *In one study, both higher NNMT expression in hepatocytes and 1-MNA supplementation has been shown to increase SIRT1 protein expression in hepatocytes in association with increased glucose output and decreased cholesterol production (29). In another study, higher NNMT expression in colorectal cancer cells and 1-MNA supplementation has been shown to enhance 5-fluorouracil (5-FU) resistance through reducing ROS and thereby inhibiting the ASK1-p38 MAPK pathway, which reduces 5-FU-induced apoptosis (30).*

In summary, NNMT has been brought to the forefront of research to comprehensively investigate NNMT-regulated molecular mechanisms that contribute to normal physiology and pathological conditions including metabolic disorders and cancer to devise novel and effective treatment strategies with small molecule inhibitors of NNMT.

1.3 RATIONALE FOR STUDYING NNMT'S ROLE IN TRIPLE-NEGATIVE BREAST CANCER BIOLOGY

All breast cancers (BCs) occur in the mammary gland terminal ducts and lobules and are divided into two main histological subtypes: pre-invasive (in situ) and invasive (Figure 1.3) (reviewed in (31)). Pre-invasive BC comprises 5-10% of all BCs and have not yet invaded beyond the boundaries of the ducts and lobules at the time of diagnosis. Invasive BC is one of the leading causes of death in women, comprises the majority of all BCs and have invaded beyond the boundaries of the ducts and lobules at the time of diagnosis. Early breast cancer that is contained in the breast or that has only spread to the axillary lymph nodes is considered curable as improvements in multimodal therapy led to increasing probability for cure in approximately 70-

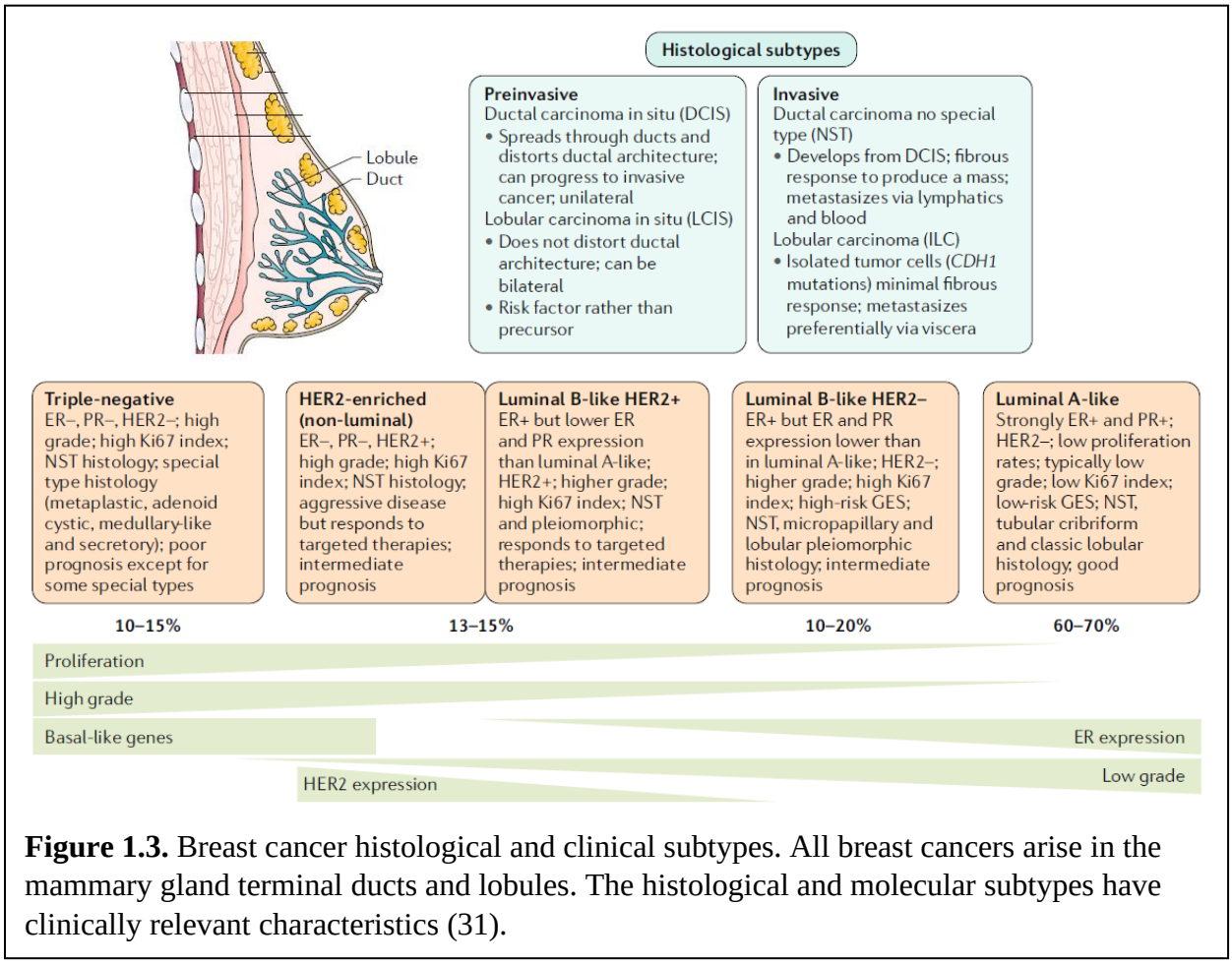

Figure 1.3. Breast cancer histological and clinical subtypes. All breast cancers arise in the mammary gland terminal ducts and lobules. The histological and molecular subtypes have clinically relevant characteristics (31).

80% of patients. On the contrary, advanced (metastatic) breast cancer is not considered curable with current treatment strategies.

Breast cancer is a heterogenous disease, and the most clinically relevant method of dividing it into subtypes is based on whether a breast tumor expresses the estrogen receptor (ER), progesterone receptor (PR) or the HER2 growth factor receptor as there are effective inhibitors for ER, PR and HER2 that are used to treat BCs (Figure 1.3). Triple-negative breast cancer (TNBC) is an aggressive disease that comprises approximately 15% of all BCs and is uniformly treated with chemotherapy due to lack of ER/PR/HER2 expression (reviewed in (32)). TNBC exhibits high intra-tumoral and inter-tumoral molecular heterogeneity, resulting in a lack of pharmacologically targetable driver mutations that commonly occur in the patient population. PARP inhibition in addition to DNA-damaging chemotherapy is still the most promising targeted therapy for approximately 10% of the TNBC patient population with BRCA-deficient tumors that are sensitive to DNA repair inhibition. TNBC therefore has an unmet need for the identification of novel and targetable molecular mechanisms that commonly occur in the patient population.

Out of all BC subtypes, TNBC is the most responsive the chemotherapy and a significant portion of early-stage TNBC patients achieve long-term survival following chemotherapy. However, TNBC patients with tumors that are not responsive to chemotherapy have the worst survival outcomes among all BC patients due to progressing and incurable metastatic disease. Molecular mechanisms that contribute to TNBC chemoresistance and metastatic progression need to be identified to devise more effective treatment strategies to improve patient survival and quality of life.

The major goal of my dissertation research was to investigate whether NNMT has a role in TNBC biology and subsequently determine potential NNMT-regulated and targetable molecular

mechanisms contributing to TNBC progression and metastasis. Below are findings that altogether constitute my rationale for studying NNMT in the context of TNBC biology.

1) NNMT has been shown to promote TNBC phenotypes *in vitro*; however, studies describing NNMT-induced *in vivo* mechanisms and phenotypes are lacking. *In one in vitro study, NNMT via 1-MNA production has been shown to inhibit reactive oxygen species (ROS)- induced autophagy by suppressing the AMPK-ULK1 pathway in association with increased cell viability in patient-derived BC cell lines including the MDA-MB-231 TNBC cell line (34). In another in vitro study, NNMT has been shown to increase chemoresistance in a SIRT1-dependent manner in patient-derived BC cell lines including the MDA-MB-231 TNBC cell line (33).*

2) Upper tertile of tumor *NNMT* mRNA expression in untreated and early-stage ER-negative BCs is associated with a significantly worse probability of recurrence free survival (RFS) and distant metastasis-free survival (DMFS), suggesting a role for NNMT in ER-negative BC progression and metastasis (Figure 1.4, KMplot). Due to a scarcity of PR-negative BCs in the publicly available KMplot dataset, TNBC patient size is also too small to perform *NNMT* mRNA expression-associated survival analysis. However, TNBC is considered a subgroup of ER-negative BCs for clinical purposes as both TNBC and ER-negative BC lack ER expression, which is an important molecular driver and therapeutic determinant in BC. Another important BC molecular driver and therapeutic determinant is the presence of tumor HER2 expression. ER-neg/HER2-neg BC patient size in the KMplot dataset is conducive to statistically meaningful survival analysis; therefore, I performed *NNMT* mRNA expression-associated RFS and DMFS analysis on this patient population, as well. In lieu of TNBC patient tumor analysis, both in untreated and early-

stage ER-negative and ER-neg/HER2-neg BCs, upper tertile of tumor *NNMT* mRNA expression is associated with a significantly worse probability of RFS and DMFS, suggesting an ER and HER2- independent role for NNMT in BC progression and metastasis (Figure 1.5, KMplot).

In summary, a multitude of NNMT-induced mechanisms including SAM depletion-induced DNA/histone hypomethylation and associated upregulation of tumor-promoting genes have been shown to promote tumorigenic phenotypes in various solid tumors including breast cancer. There is evidence suggesting a role for NNMT mechanism of action in TNBC biology; however, NNMT-induced TNBC *in vivo* mechanisms and phenotypes need further experimental elucidation.

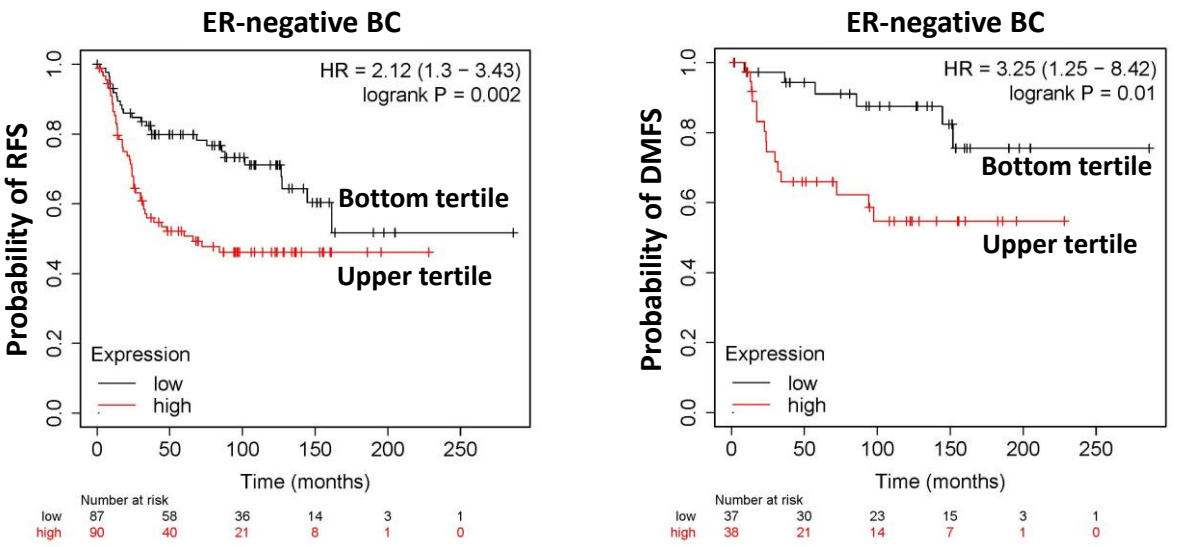

Figure 1.4. Upper tertile of NNMT expression in untreated, early-stage ER-negative BCs is associated with a significantly worse probability of recurrence free survival (RFS) and distant metastasis-free survival (DMFS), suggesting a role for NNMT in ER-negative BC progression and metastasis (KMplot).

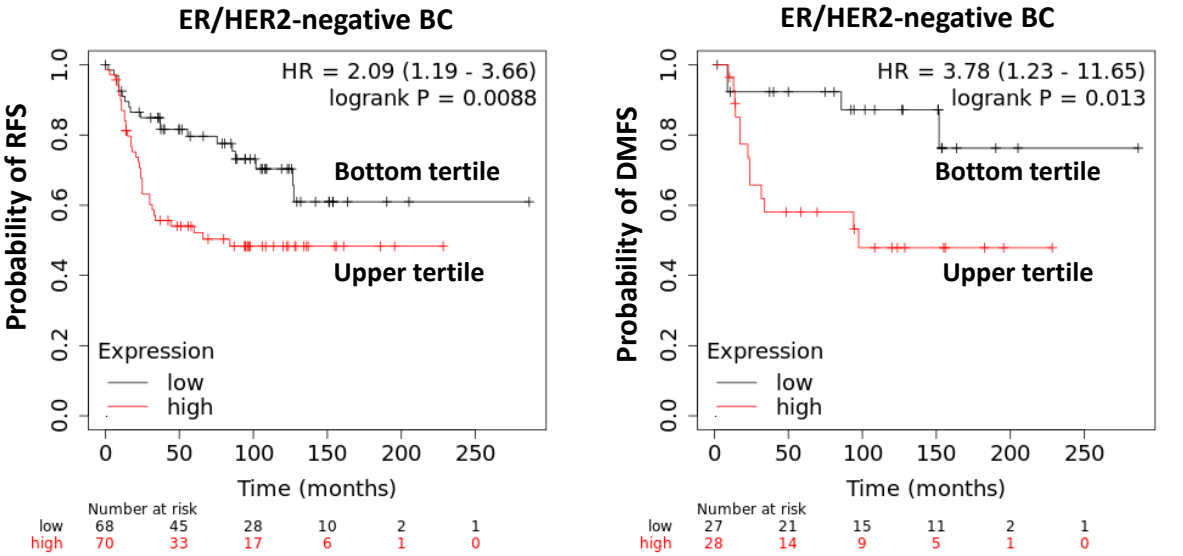

Figure 1.5. Upper tertile of NNMT expression in untreated, early-stage ER-neg/HER2-neg BCs is associated with a significantly worse probability of recurrence free survival (RFS) and distant metastasis-free survival (DMFS), suggesting an ER and HER2-independent role for NNMT in BC progression and metastasis (KMplot).

CHAPTER 2

MATERIALS AND METHODS

2.1 Cell Lines and Reagents

2.1.1 Cell Lines and Media

The MDA-MB-231 and SUM159PT cell lines were generous gifts from Dr. Olufunmilayo Olopade (The University of Chicago). All cell lines were routinely authenticated using short tandem repeat profiling at the University of Arizona and tested for mycoplasma contamination using the ATCC Universal Mycoplasma Detection Kit (ATCC). MDA-MB-231 cells were maintained at 37°C and 5% CO_2 in DMEM (Gibco) supplemented with 4.5 g/L D-glucose, 4mM L-glutamine, 110 mg/L sodium pyruvate, 1% Penicillin/Streptomycin (Corning) and 10% FBS (Gemini Bio). SUM159PT cells were maintained 37°C and 5% CO_2 in DME/F-12 (Sigma) supplemented with 0.1545 g/L calcium chloride (Sigma), 0.365 g/L L-glutamine (Sigma), 0.05905 g/L L-leucine (Sigma), 0.09125 g/L L-lysine (Sigma), 0.0612 g/L magnesium chloride (Sigma), 0.04884 g/L magnesium sulfate (Sigma), 1.2 g/L sodium bicarbonate (Sigma), 100 uM L-methionine (Sigma), 1% Penicillin/Streptomycin (Corning) and 10% FBS (Gemini Bio).

For *in vitro* experiments conducted in physiological methionine concentration, MDA-MB-231 cells were cultured in glutamine-, methionine- and cystine-depleted DMEM (Gibco) supplemented with 4.5 g/L D-glucose, 4mM L-glutamine (Sigma), 110 mg/L sodium pyruvate (Sigma), 0.2 mM L-Cystine 2HCl (Sigma), 15 uM L-methionine (Sigma), 1% Penicillin/Streptomycin (Corning) and 5% FBS (Gemini Bio). For *in vitro* experiments conducted in physiological methionine concentration, SUM159PT cells were cultured in the

same DME/F-12 (Sigma) formulation with only different concentrations of L-methionine (15 uM) and FBS (5%).

2.1.2 Derivative Cell Lines

pLKO-Tet-On lentiviral vector (Addgene cat # 21915) was used for doxycycline-inducible shRNA-mediated NNMT depletion in MDA-MB-231 and SUM159PT cell lines. Three shRNA oligos targeting unique sequences on exon 1 of human *NNMT* mRNA (Table 2.2) were cloned into the pLKO-Tet-On vector as described in the Tet-pLKO manual available on the Addgene website. 6 million HEK293T cells (< 20 passages) were plated onto 10-cm poly-D-lysine coated tissue culture plates (Corning) in 10 ml of standard growth medium (DMEM with 10% FBS). On the next day, medium on the HEK293PT cells was replaced with 6 ml of DMEM with 10% FBS 1 hour before transfection. For one 10-cm plate, 36 ul of Fugene transfection reagent (Roche) was added directly into 600 ul of OptiMEM medium (Gibco) and incubated for 5 minutes at room temperature. 4 ug of the pLKO-Tet-On vector with shControl, shNNMT-1, shNNMT-2 or shNNMT-3 sequences was mixed with 9 ug of ViraPower lentiviral packaging mix (ThermoFisher) in 50 ul of OptiMEM. DNA mixture was added to the diluted Fugene reagent and incubated for 30 minutes at room temperature. 700 ul of the DNA/Fugene mixture was then added dropwise onto cells in the 10-cm plate, and cells were incubated at 37°C. On the following day, medium was changed to 6 ml of DMEM with 20% FBS per plate and cells were incubated at 37°C for 48 hours to generate lentivirus. At the end of 48 hours, lentiviral particle-containing medium from each plate was removed, filtered, and concentrated with Lenti-Pac lentivirus concentration solution (GeneCopoeia) according to manufacturer's instructions. Concentrated lentiviral particles were aliquoted, titered and stored at -80°C until further use. To generate stable doxycycline-inducible shRNA-expressing cells, 300,000 MDA-MB-231 and 300,000 SUM159PT cells were

plated onto 6-well plates (one well per shRNA) in 2 ml of standard growth medium. On the next day, medium was replaced with 2 ml of standard growth medium without any antibiotics and supplemented with 10 ug/ml polybrene (Sigma) and shControl, shNNMT-1, shNNMT-2 or shNNMT-3 lentiviral particles at an MOI of approximately 0.5. Cells were incubated for 12-14 hours (overnight) at 37°C with polybrene and lentiviral particles. Medium on the cells was then replaced with 2 ml of standard growth medium without any antibiotics, and cells were let to recover for 24 hours from the stresses of transduction. Because the pLKO-Tet-On lentiviral vector provides puromycin resistance, cells were cultured in standard growth medium supplemented with puromycin (Sigma, 2.25 ug/ml for MDA-MB-231 cells, 1.25 ug/ml puromycin for SUM159PT cells) and selected for puromycin resistance for 14 days to generate MDA-MB-231-shControl, MDA-MB-231-shNNMT1, MDA-MB-231-shNNMT2, MDA-MB-231-shNNMT3, SUM159PT-shControl, SUM159PT-shNNMT1, SUM159PT-shNNMT2, SUM159PT-shNNMT3 cell lines. These cell lines were maintained with constant puromycin selection and treated with 100 ng/ml doxycycline (Sigma) for a minimum of 72 hours to induce shRNA expression for efficient *NNMT* knockdown.

pLL-CMV-rFLuc-T2A-mRFP-mPGK-Puro lentiviral vector (System Biosciences cat # LL320) was used to generate stable Luciferase-expressing MDA-MB-231-shControl, MDA-MB-231-shNNMT1, SUM159PT-shControl, and SUM159PT-shNNMT1 cells for *in vivo* bioluminescence imaging. The puromycin resistance gene was replaced with the neomycin resistance gene in the LL320 vector by System Biosciences. Lentiviral particles for the LL320-neomycin vector were generated with HEK293T cells using the pPACKH1 HIV lentivector packaging kit (System Biosciences) according to manufacturer's instructions. Concentrated lentiviral particles were then generated as previously described. To generate stable Luciferase-

expressing cells, 300,000 MDA-MB-231-shControl, MDA-MB-231-shNNMT1, SUM159PT-shControl or SUM159PT-shNNMT1 were plated onto 6-well plates and transduced as previously described with LL320-neomycin lentiviral particles. Transduced cells were then cultured in standard growth medium supplemented with G-418 (Sigma, 2 mg/ml) and selected for neomycin resistance for 14 days to generate MDA-MB-231-shControl-Luc, MDA-MB-231-shNNMT1-Luc, SUM159PT-shControl-Luc and SUM159PT-shNNMT1-Luc cell lines. These cell lines were maintained with constant puromycin and G-418 selection. Luciferase-based bioluminescence in these cell lines was confirmed with The Luciferase Assay System (Promega).

2.2 Protein Analyses

2.2.1 Protein Extraction

For all *in vitro* experiments concluding in protein analysis, cells were cultured in their standard growth medium supplemented with 5% FBS, 15 uM methionine, appropriate selection antibiotic and 100 ng/ml doxycycline to induce shRNA expression and downstream protein expression changes for 8 days prior to protein extraction. Medium was replaced every 48 hours, and protein was extracted exactly 48 hours post-final medium change from ~90% confluent 10-cm dishes. For protein extraction, cells were washed once with and scraped into ice-cold 1X PBS followed by centrifugation at 5,000g for 2 minutes at 4°C. Supernatant was removed and RIPA Lite (Formula: 7.5ml 5M NaCl, 3.0ml 0.5M Na_2HPO_4, 2.0ml NaH_2PO_4, 1.0ml 0.5M EDTA, 12.5ml 20% TX-100, 1.05g NaF in 250ml) containing Phos-stop (Roche) and Complete Mini (Roche) was added onto the remaining cell pellet followed by thorough mixing with pipette and 30-minute incubation on ice for cell lysis and protein extraction. Cell lysates were spun down at 13,000 rpm for 10 min at 4°C and supernatant containing total protein was collected and stored at -80°C. Protein concentration in each sample was quantified with The Pierce BCA Protein Assay

Kit (ThermoFisher).

Approximately 100 mg of each flash frozen xenograft tumor was homogenized manually in 300 ul of ice-cold RIPA Lite containing Phos-stop (Roche), Complete Mini (Roche), 2 ug/ml Aprotinin (Sigma), 5 mM EDTA (Invitrogen), 1 mM sodium orthovanadate (Sigma), 1 mM PMSF (Sigma), 5 mM NaF (Sigma), and 1 mM benzamidine hydrochloride (Sigma) and then maintained at constant agitation for 2 hours at 4°C. Tumor lysates were spun down for 20 minutes at 12,000 rpm at 4°C and supernatant containing total protein was collected and stored at -80°C. Protein concentration in each sample was quantified with The Pierce BCA Protein Assay Kit (ThermoFisher).

2.2.2 Western Blotting

Per each lane of an SDS-PAGE gel, 30 ug of cell line or xenograft tumor total protein extract was denatured in 1X Laemmli Buffer (BioRad) for 5 minutes at 95°C. Denatured protein extracts were immediately loaded onto 10% SDS-polyacrylamide gels, resolved at 80V until the dye front passes the stacking gel and then at 100V until the dye front reaches the bottom of the gel. For proteins less than 80 kDa in size, SDS-PAGE gels were transferred to nitrocellulose membranes at 200 mA for 90 minutes at 4°C. For proteins greater than 80 kDa in size, SDS-PAGE gels were transferred to nitrocellulose membranes at 100 mA for 30 minutes followed by 300 mA for 30 minutes at 4°C. Membranes were blocked in 5% BSA-containing 1X TBST for 1 hour at room temperature, incubated with primary antibody in 5% BSA-containing 1X TBST (Table 2.1), then washed three times with 1X TBST. Membranes were then incubated with fluorescently labeled secondary antibodies for 1 hour in 5% BSA-containing 1X TBST, then washed three times with 1X TBST. Proteins were detected with either an Odyssey imaging system (LI-COR) or ChemiDoc imaging system (BioRad).

2.3 RNA Analyses

2.3.1 RNA Extraction

For all *in vitro* experiments concluding in RNA analysis, cells were cultured in their standard growth medium supplemented with 5% FBS, 15 uM methionine, appropriate selection antibiotic and 100 ng/ml doxycycline to induce shRNA expression and downstream gene expression changes for 6 days prior to RNA extraction. Medium was replaced every 48 hours, and RNA was extracted exactly 48 hours post-final medium change from ~90% confluent 10-cm dishes. For total RNA extraction, The RNAeasy Mini Kit with optional DNAse digestion (Qiagen) was used according to the manufacturer's protocol.

Approximately 100 mg of each flash frozen xenograft tumor and liver metastatic nodule was placed in 2 ml of ice-cold RLT buffer (Qiagen) containing 2-Mercaptoethanol (BME) (10ul of BME for every 1 ml of RLT buffer), and total RNA from each tissue was extracted using the Tissue Lyser II homogenizer (Qiagen) and The RNAeasy Midi Kit with optional DNAse digestion (Qiagen) according to manufacturer's protocol.

The concentration of harvested RNA was quantified using a Qubit 4 Fluorometer (ThermoFisher) and Qubit RNA Broad Range Assay Kit (Invitrogen) according to manufacturer's protocol. RNA integrity score (RIN) of each total RNA sample was determined using a Tapestation 4150 (Agilent) and High Sensitivity RNA Screentape Assay (Agilent) according to manufacturer's protocol.

2.3.2 RNAseq Library Preparation

Total RNA samples with a RIN score ≥9 were selected for library preparation at The McDermott Center Next Generation Sequencing (NGS) Core at UT Southwestern Medical Center. At the NGS core, RNA-sequencing libraries were prepared from 4µg total DNAse-treated RNA

with the TruSeq Stranded Total RNA LT Sample Prep Kit from Illumina. Poly-A RNA was purified and fragmented before strand-specific cDNA synthesis. cDNA was then A-tailed and indexed adapters were ligated. After adapter ligation, samples were PCR amplified and purified with Ampure XP beads, then validated on the Agilent 2100 Bioanalyzer. Indexed RNAseq libraries were quantified with Qubit before being normalized and pooled, and sequencing was performed on the NextSeq 500 (Illumina) in 100bp, single-end runs. All biological replicates of all experimental conditions within an individual experiment were run on the same flow cell to minimize run effects, and sequencing data were returned in the fastq format.

2.3.3 RNAseq Analysis

All RNAseq data were analyzed by The McDermott Center for Human Growth and Development Bioinformatics Lab at UT Southwestern Medical Center. Fastq files were quality checked using fastqc (v0.11.2). Reads from each sample were mapped to the GRCh38/hg19 reference human genome using STAR (v2.5.3a). Read counts were generated using featureCounts and the differential expression analysis was performed using edgeR. Ingenuity Pathway Analysis (Ingenuity systems) of differentially expressed genes (DEGs) was performed to identify functional pathways that are significantly altered under among experimental conditions. RNAseq reads of the xenograft primary tumors and liver metastatic nodules excised from NSG mice were aligned to both human and mouse reference genomes and reads aligning to the mouse genome were excluded from further analysis.

2.4 shRNA and *In Vivo* Imaging Plasmids

2.4.1 Plasmid Production and Validation

pLKO-Tet-On lentiviral vector (Addgene 21915) was received as a bacterial plasmid stock, which was streaked onto LB agar plates with the appropriate selection antibiotic and incubated

overnight at 37°C. Individual bacterial colonies that formed on these agar plates were selected and grown in LB medium with the appropriate selection antibiotic at 37°C. Plasmid isolation was then performed using the ZymoPURE II Plasmid Midiprep Kit (Zymo Research). Isolated plasmids were validated with restriction enzyme digestion followed by gel electrophoresis to confirm the presence of DNA bands at expected sizes. Three shRNA oligos targeting unique sequences on exon 1 of human *NNMT* mRNA were cloned into the validated pLKO-Tet-On plasmids, which were transformed into One Shot Stbl3 Chemically Competent *E. coli* (ThermoFisher) with heat shock according to the manufacturer's protocol. Transformed bacteria were streaked onto LB agar plates and individual bacterial colonies were expanded in LB medium with the appropriate selection antibiotic at 37°C. Plasmid isolation was performed using the ZymoPURE II Plasmid Midiprep Kit (Zymo Research). Isolated plasmids were then sent to The McDermott Center Sanger Sequencing Core at UT Southwestern Medical Center for validation of correct shRNA sequence insertion.

pLL-CMV-rFLuc-T2A-mRFP-mPGK-Puro lentiviral vector (System Biosciences cat # LL320) was received as a plasmid stock, which was transformed into One Shot Stbl3 Chemically Competent *E. coli* (ThermoFisher) with heat shock according to the manufacturer's protocol. Transformed bacteria were streaked onto LB agar plates and individual bacterial colonies were expanded in LB medium with the appropriate selection antibiotic at 37°C. Plasmid isolation was performed using the ZymoPURE II Plasmid Midiprep Kit (Zymo Research). Isolated plasmids were then sent to The McDermott Center Sanger Sequencing Core at UT Southwestern Medical Center for sequence validation.

2.5 *In Vivo* Procedures

2.5.1 Orthotopic Implantation of TNBC Cell Lines into NSG Mice

Animal procedures were performed with the approval of the UT Southwestern Medical Center Institutional Animal Care and Use Committee. MDA-MB-231-Luc and SUM159PT-Luc cells with shControl or shNNMT-1 were cultured *in vitro* with 100 ng/ml doxycycline for 3 days to induce shRNA expression. 1 million of doxycycline-treated MDA-MB-231-Luc-shControl and MDA-MB-231-Luc-shNNMT1 cells and 10 million of doxycycline-treated SUM159PT-Luc-shControl and SUM159PT-Luc-shNNMT1 cells suspended in 100 ul of 1X PBS were implanted subcutaneously into the right inguinal mammary fat pads of 7-week-old female NSG mice (Jackson Labs). Animals were initiated on a doxycycline-containing diet (Teklad) 3 days prior to cell implantation, and this diet was maintained until the end of experiment to maintain shRNA expression in primary tumors and metastatic cells. Subcutaneous primary tumor volume was quantified every 2-3 days with an electronic caliper starting from 14 days following cell implantation (tumor volume = (length (mm) × width $(mm)^2$)/2) and primary tumor removal.

2.5.2 TNBC Cell Line Xenograft Primary Tumor Excision

All surgeries were performed aseptically on a sterile surgical field in a biosafety cabinet providing sterile airflow. Sterile surgical attire and sterile tools were used at all times during surgeries. Tumor removal surgery was designed based on published protocols (35, 36) and performed when the length of each MDA-MB-231 and SUM159PT xenograft primary tumor reached but not exceeded 1 cm. Anesthetized mice displaying proper tumor size were placed on sterile surgical towels on a heated plate ventral side up under continuous sedation by administering 2-3% isoflurane via an anesthesia mask. Absence of the foot pinch reflex was checked to confirm that each mouse was properly anesthetized. Eye lubricant was applied to each eye to prevent

dryness while under sedation. 0.5 ml of sterile saline and 2 mg/kg meloxicam were administered via subcutaneous injection in case of blood (fluid) loss during surgery and as pre-emptive analgesic, respectively. Fur was removed by a clipper followed by application of hair removal cream for 30-45 seconds in the entire lower abdominal area. Lower abdomen was then sterilized by application of Betadine solution until dry followed by application of 70% EtOH until dry with sterile cotton-tip applicators for a total of three times. New sterile surgical gloves were worn and while lifting the tumor up on its ventral side with tweezers, incisions were made along the circumference of the tumor with sharp-edged blunt-ended scissors. The tumor and attached skin were then carefully separated and removed from the inguinal mammary gland with small and controlled cuts. Half of the excised tumor was flash-frozen, and the other half was placed in formalin. New sterile surgical gloves were worn, and surgery was continued to remove as much of the inguinal mammary gland as possible with small and controlled cuts to not puncture the peritoneum. When it was concluded that no more inguinal mammary gland tissue remained visible to the naked eye, the surgical incision was tightly and completely closed with wound clip application to the skin. Applied wound clips were carefully observed to confirm that all of them were properly applied and would not come lose. Medium level pressure was applied on the abdomen above the bladder to confirm that urine was able to flow out of the urinary tract and that urinary tract was not obstructed by the placement of wound clips in the lower abdomen. Anesthesia was then terminated, and mice were put in a heated recovery cage and observed until they were securely in sternal recumbency and capable of purposeful movement. Mice were observed every 12 hours and administered 0.5 ml of saline and 2 mg/kg of meloxicam for a total of 72 hours post-surgery. Mice that showed signs of pain (hunching, unwilling to move, failure to groom) 1 hour after surgery or at any later observation timepoint were immediately euthanized. 14 days post-

surgery, wound clips were removed with a wound clip remover.

2.5.3 In Vivo Bioluminescence Imaging

In vivo bioluminescence imaging of the MDA-MB-231-Luc and SUM159PT-Luc xenograft primary tumor and metastatic cells was performed with the AMI-HTX imaging system (Spectral Instruments). All mice in one cage were intraperitoneally injected with 150 mg/kg D-Luciferin (Perkin Elmer). 2 minutes after injecting the last mouse in the cage, anesthesia was induced in an induction chamber with 2-3% isoflurane. Fully anesthetized mice were quickly placed on the heated imaging platform of the AMI-HTX instrument and kept under continuous anesthesia by administering 2-3% isoflurane via a face cone. 8 minutes after injecting the last mouse in the cage with Luciferin, a bioluminescence image with photo overlay was taken with 1 second exposure. Image analysis and normalization of bioluminescence signal among mice in the same comparison group were performed with the Aura Imaging Software (Spectral Instruments).

2.5.4 Histology and Immunohistochemistry

Histological and immunohistochemical staining of the xenograft primary tumors of MDA-MB-231 and SUM159TP cells and NSG mouse organs with their metastatic lesions were performed at the UT Southwestern Medical Center Harold C. Simmons Comprehensive Cancer Center Tissue Management Shared Resource. Harvested tumors and organs were fixed immediately for 24 hours in 10% formalin in PBS (Sigma) and then washed and stored in 70% ethanol for at least 24 hours. Fixed tissues were embedded in paraffin, sectioned into 4 um thick slides, and stained with hematoxylin and eosin (H&E) or with an antibody for Ki67 (CST 9027) or cleaved caspase 3 (CC3; CST 9664) according to internal protocols using the Dako Autostainer Link 48 system. Briefly, for immunohistochemistry (IHC), the slides were baked for 20 minutes at 60°C, then deparaffinized and hydrated before the antigen retrieval step. Heat-induced antigen

retrieval was performed at pH 6 for 20 minutes in a Dako PT Link. The tissue was incubated with a peroxidase block and then incubated with either Ki67 (1:800) or CC3 (1:500) for 35 minutes followed by HRP-conjugated secondary antibody incubation to visualize staining with light microscopy.

2.6 Cellular Metabolite Quantification

2.6.1 Intracellular SAM Quantification

For all *in vitro* experiments concluding in intracellular SAM quantification, cells were cultured in their standard growth medium supplemented with 5% FBS, 15 uM methionine, appropriate selection antibiotic and 100 ng/ml doxycycline to induce shRNA expression and downstream intracellular SAM changes for 5 days prior to metabolite extraction. Medium was replaced every 48 hours, and metabolites were extracted 20-24 hours post-final medium change from ~90% confluent 10-cm dishes. For metabolite extraction, cells were rinsed with 5 ml of ice-cold saline solution once as quickly as possible and then scraped into 1 ml of solution containing 80% HPLC-grade acetonitrile (Sigma), 20% HPLC-grade water (Fisher) and 0.1 nmol/ml d_3-SAM (CDN Isotopes). Cell lysates were transferred into a 1.5 ml Eppendorf tube, flash-frozen in liquid nitrogen and then subjected to three freeze-thaw cycles between liquid nitrogen and 37°C. 9. After the third thaw, cell lysates were vortexed at high speed for 1 min, and then centrifuged at ~20,160g for 15 min in a refrigerated centrifuge. The metabolite-containing supernatant was transferred to a new tube and stored at -80°C. 1000 ng/ml, 500 ng/ml, 250 ng/ml, 125 ng/ml, 62 ng/ml, 31 ng/ml and 0 ng/ml SAM standards (Cayman Chemical) suspended in 80% HPLC-grade acetonitrile (Sigma), 20% HPLC-grade water (Fisher) and 0.1 nmol/ml d_3-SAM (CDN Isotopes) were also prepared and stored at -80°C. Metabolite extracts and standards were given to the UT Southwestern Medical Center CRI Metabolomics facility for absolute SAM quantification with LC-MS/MS.

Endogenous levels of intracellular SAM was quantified by measuring the area under the peak in comparison to deuterated SAM. The following MS transitions and retention time (RT) were used to measure the indicated metabolites: SAM (m/z 399 →250, RT = 16.2 min), d3-SAM (m/z 402→250, RT = 16.2 min). Absolute concentrations of SAM were normalized to 1×10^6 cells for each sample.

2.6.2 Cellular De Novo Cholesterol Synthesis Intermediate Quantification

20-30 mg of flash-frozen xenograft primary tumors and liver metastatic nodules were shaved on dry ice, weighed, transferred to a 1.5 ml Eppendorf and shipped on dry ice to UC San Diego Lipidomics for absolute quantification of free (non-esterified) sterols according to internal LC-MS/MS protocols. Lanosterol, dihydro FF-MAS, dihydro T-MAS and free cholesterol levels in each tissue were provided in the form of ng per mg of tissue.

2.6.3 Cellular Free Cholesterol Quantification

For all *in vitro* experiments concluding in free cholesterol quantification, cells were cultured in their standard growth medium supplemented with 5% FBS, 15 uM methionine, appropriate selection antibiotic and 100 ng/ml doxycycline to induce shRNA expression and downstream free cholesterol changes for 10 days prior to cholesterol extraction. mTOR signaling was inhibited with 1 uM of rapamycin (Sigma) during the last 48 hours of cell culture. *De novo* cholesterol synthesis was inhibited with 1 uM of lovastatin (Selleckchem) during the last 48 hours of cell culture. Mevalonic acid (Sigma) was added to lovastatin-treated cells during the last 48 hours of cell culture. Medium was replaced every 48 hours, and cellular cholesterol was extracted and quantified exactly 48 hours post-final medium change from ~90% confluent 10-cm dishes using the Cholesterol/Cholesterol Ester-Glo Assay (Promega) according to manufacturer's protocol. Absolute cellular free cholesterol concentrations were normalized to 1000 cells for each

sample.

2.6.4 LDL-cholesterol Uptake Quantification

For all *in vitro* experiments concluding in LDL uptake quantification, cells were cultured in their standard growth medium supplemented with 5% FBS, 15 uM methionine, appropriate selection antibiotic and 100 ng/ml doxycycline to induce shRNA expression and downstream LDL uptake changes for 9 days prior to measurement of LDL-cholesterol uptake by cells in less than 90% confluent wells of 6-well plates. Medium was replaced every 48 hours, varying concentrations of fluorescent LDL-Dil cholesterol (provided by UTSW Corbin Lab) were added to cells 24 hours after last medium change, and cells were incubated with LDL-Dil for 6 hours. Cells were then washed once with 1X PBS and suspended in 500 ul of 1X PBS in on ice. Flow cytometry on the suspended cells was performed by the UT Southwestern Medical Center Flow and Mass Cytometry Facility. Data were returned in the form of median LDL-Dil fluorescence level per 10,000 liver cells in each sample.

2.7 Scientific Rigor and Statistical Analysis

All *in vitro* experiments were performed with two or three biological replicates. RNAseq and mass spectrometry on xenograft primary tumors and liver metastatic nodules were performed with the maximum number of available biological replicates to achieve statistical significance. A one-way student's t-test was used to determine significance of differences between two experimental conditions and one-way ANOVA was used to determine significance of differences between multiple experimental conditions. Repeated measures ANOVA was used to determine significance of differences in xenograft primary tumor growth rate.

2.8 Reagent Toolbox

2.8.1 Antibodies

Table 2.1 Antibodies used for Western blot

Antibody target	Company	Catalog number	Incubation conditions
NNMT	Novus Biologicals	NBP2-00537	1:1000 in TBST, overnight 4°C
HMGCS1	Proteintech	17643-1-AP	1:1000 in TBST, overnight 4°C
HMGCR	Novus Biologicals	NBP2-66888	1:1000 in TBST, overnight 4°C
B-actin	CST	3700S	1:2000 in TBST, 30 min RT
B-actin	CST	8457S	1:2000 in TBST, 30 min RT
Rabbit IgG	Invitrogen	PIA32734	1:10,000 in TBST, 1 hr RT
Mouse IgG	Invitrogen	PIA32730	1:10,000 in TBST, 1 hr RT

2.8.2 shRNA Sequences

Table 2.2 shControl and shNNMT sequences

shRNA	Top oligo sequence
shControl	CCGGGGTTAAGTCGCCCTCGCTCGAGCGAGGGCGACTTAACCTTTTT
shNNMT-1	CCGGTGCAGAAAGCCAGATTCTTAACTCGAGTTAAGAATCTGGCTTTCTGCATTTTT
shNNMT-2	CCGGACTCTGCAGAAAGCCAGATTCCTCGAGGAATCTGGCTTTCTGCAGAGTTTTTT
shNNMT-3	CCGGAAGCCAGATTCTTAAGCACCTCTCGAGAGGTGCTTAAGAATCTGGCTTTTTTT

CHAPTER 3

NNMT-ASSOCIATED TNBC GENE EXPRESSION

3.1 Introduction

While NNMT has been associated with cancer and tumorigenic phenotypes, a detailed understanding of NNMT mechanism of action in cancer biology remained limited until The Cravatt Lab provided the first plausible tumor-promoting mechanism for NNMT through SAM consumption; NNMT-induced SAM depletion was found to result in histone hypomethylation associated with increased pro-oncogenic gene expression in cancer cell lines (25). Subsequent studies demonstrated that high NNMT expression results in DNA and PP2A phosphatase hypomethylation associated with increased cancer gene expression and oncogenic kinase activation, respectively, that underlie enhanced tumorigenic phenotypes *in vitro* and *in vivo* (26, 28). While these findings are relevant to multiple solid tumors including glioblastoma, studies investigating whether NNMT affects intracellular SAM levels and thereby SAM-dependent DNA/histone/protein methylation in TNBC cells in association with enhanced tumorigenic phenotypes are lacking. In the first chapter of my dissertation research findings, I will show that NNMT depletes SAM and alters gene expression in patient-derived TNBC cell lines.

3.2 Results

3.2.1 Doxycycline-inducible shRNAs targeting exon 1 of NNMT mRNA provide efficient NNMT protein knockdown.

My first research aim was to determine whether NNMT expression and activity in TNBC cells deplete intracellular SAM. Experimental observation of NNMT-induced SAM depletion would provide a strong rationale to hypothesize that NNMT may influence TNBC gene expression

and thereby tumorigenic phenotypes by SAM-depletion induced DNA/histone hypomethylation and associated transcriptional changes. In order to investigate NNMT-regulated molecular mechanisms, I opted to deplete NNMT in two patient-derived TNBC cell lines (MDA-MB-231 and SUM159PT) with doxycycline-inducible shRNAs targeting unique sequences across the three exons of the *NNMT* mRNA (Figure 3.1). I made the observation that among approximately 20 unique shRNAs that I screened, only the ones that target exon 1 of *NNMT* mRNA provide a sufficient level of knockdown (>50%) at the protein level in MDA-MB-231 and SUM159PT cells (Figure 3.2). The lentiviral backbone plasmid (Addgene 21915) that I cloned the non-silencing control and NNMT shRNA sequences into is selectable by puromycin; therefore, I created puromycin-selected stable MDA-MB-231 and SUM159PT cells with doxycycline-inducible shRNA expression to be used in further experiments (Figure 3.2).

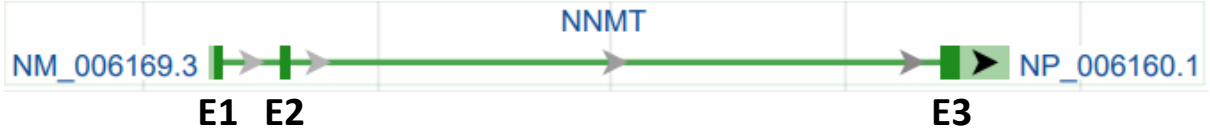

Figure 3.1. NNMT genomic locus on human chromosome 11 (NIH Genome Data Viewer). Human *NNMT* gene has three exons and two introns. E1: exon 1, E2: exon 2, E3: exon 3.

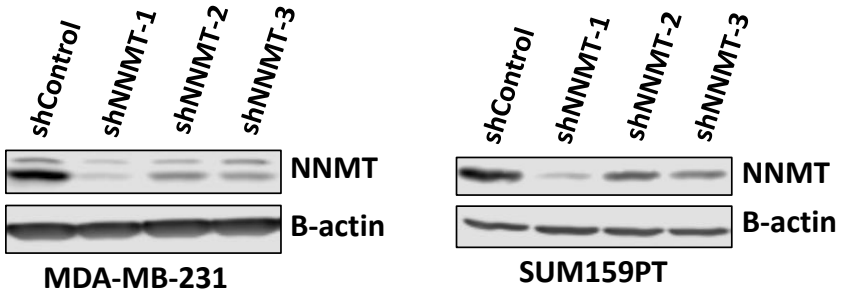

Figure 3.2. Western blots demonstrate that three shRNAs targeting unique sequences on exon 1 of *NNMT* mRNA provide efficient NNMT protein knockdown compared to non-silencing control shRNA in two patient-derived TNBC cell lines. *Cells were under constant puromycin selection and treated with 100 ng/ml doxycycline for at least 72 hours to achieve peak NNMT protein knockdown.*

It is intriguing that only targeting exon 1 of *NNMT* mRNA provides sufficient knockdown

at the protein level. A highly plausible explanation comes from a study that showed the gene-silencing efficiency of siRNA is strongly dependent on the local structure of mRNA at the targeted region (37). An siRNA's complementary sequence must be physically accessible on the target mRNA for the RISC complex-bound siRNA oligo to bind to the target mRNA and for the RISC-complex to then degrade the mRNA. This implies that the region on the mRNA with the shRNA target sequence must have minimal secondary structures to be physically accessible. The 3D conformation with secondary structures that NNMT mRNA adopts in cells is not known; however, based on these findings, I hypothesize that exon 1 of NNMT mRNA may have fewer secondary structures compared to exons 2 and 3, rendering exon 1 more physically accessible and amenable to siRNA binding-mediated degradation.

3.2.2 NNMT depletes intracellular SAM in patient-derived TNBC cell lines.

NNMT's SAM-dependent methyltransferase activity on NAM has the potential to affect the activity of the NAD^+-dependent enzymes and SAM-dependent methyltransferases by consuming the major NAD^+ precursor NAM and the universal methyl donor SAM, respectively. As outlined in the introduction chapters, there is a multitude of cellular processes NNMT-induced NAM and SAM depletion have been shown to affect in physiological and pathological contexts. To begin to investigate NNMT's potential biological significance in TNBC progression, I had two options: 1) determine whether shRNA-mediated NNMT depletion in MDA-MB-231 and SUM159PT cell lines upregulates intracellular nicotinamide and NAD^+ levels, or 2) determine whether shRNA-mediated NNMT depletion in these cells upregulates intracellular SAM levels.

It is important to note that NAM (NAD^+ precursor) and methionine (SAM precursor) levels in the *in vitro* cell culture medium for MDA-MB-231 and SUM159PT cell lines need to be at physiologically relevant concentrations (similar to human plasma concentrations) in order for

shRNA-mediated NNMT depletion to affect their intracellular concentrations. Human plasma NAM concentration has been reported to be in the range of 70 to 275 nM (38), and human plasma methionine concentration has been reported to be approximately 15 uM (39). In contrast, DMEM cell culture medium (MDA-MB-231) contains 33 uM NAM and 200 uM methionine, while HAM'S F12 cell culture medium (SUM159PT) contains 295 nM NAM and 30 uM methionine. Since standard DMEM and HAM'S F12 contain NAM and methionine at supraphysiological concentrations, I searched for commercially available NAM and methionine-free versions of DMEM and HAM'S F12 to be able to add them into these media at physiological concentrations. I only found methionine-free versions of these media that are commercially available and therefore quantified intracellular SAM with mass spectrometry in NNMT-expressing and NNMT-depleted MDA-MB-231 and SUM159PT cells cultured in their standard medium with 15 uM methionine (Figure 3.3).

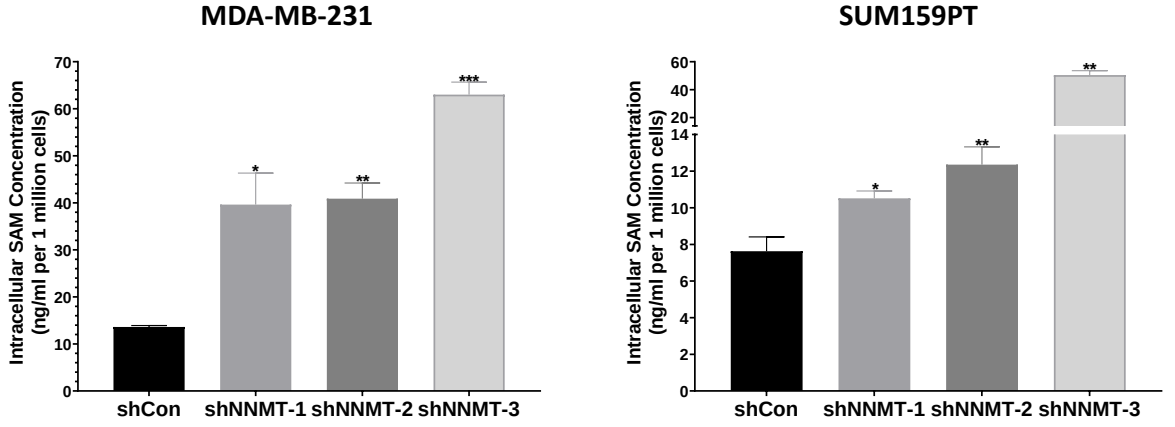

Figure 3.3. Intracellular SAM quantification with mass spectrometry in NNMT-expressing and NNMT-depleted MDA-MB-231 and SUM159PT cell lines show that NNMT depletes SAM levels in these cells. *Cells were under constant puromycin selection and treated with 100 ng/ml doxycycline for 6 days prior to SAM quantification. *p<0.05, **p<0.01, ***p<0.001.*

NNMT depletion with all shRNAs significantly upregulated intracellular SAM concentration in both TNBC cell lines, demonstrating that NNMT depletes intracellular SAM in these cells. It is intriguing that the level of SAM upregulation induced by shNNMT-3 is much

higher compared to the level of SAM upregulation achieved by the other two NNMT shRNAs. One possible explanation is shRNA off-target mRNA binding; however, I determined bioinformatically by using NCBI Nucleotide Blast that all three NNMT shRNA sequences only align to the human *NNMT* transcript. Alternative *NNMT* exons and splice variants have been uncovered by RNAseq whose biological significance remain to be experimentally validated (GTEX Portal; reviewed in (3)); therefore, a more fitting hypothesis is that these NNMT shRNAs may be targeting separate but overlapping groups of *NNMT* transcript variants, resulting in an overall similar phenotype with subtle differences. Importantly, these findings demonstrated that NNMT depletes intracellular SAM in patient-derived TNBC cell lines and provided a strong rationale for investigating potential TNBC phenotypes affected by NNMT-induced SAM depletion.

3.2.3 NNMT expression in patient-derived TNBC cell lines is associated with increased EMT-invasion gene expression and decreased anabolic gene expression.

NNMT-induced SAM depletion can decrease the methylation activity of all SAM-dependent methyltransferases by causing a scarcity in available intracellular methyl units. SAM is the universal methyl donor for almost all methyltransferases in mammalian cells including nucleic acid (i.e., DNA) and protein (i.e., histone) methyltransferases, and NNMT-induced SAM depletion has been shown to result in global DNA and histone hypomethylation and thereby widespread transcriptional changes in gene expression.

CpG DNA methylation is widespread in mammalian genomes with around 70% of CpG dinucleotides being methylated and is a fundamental mechanism of stable gene repression (reviewed in (40)). CpG methylation is significantly enriched in transcriptionally silent heterochromatin and inactive gene promoters. In addition, actively transcribed genes can also

harbor methylated CpGs within their transcribed regions that regulate mRNA alternative splicing. While DNA CpG methylation mostly consists of 5-methylcytidine (5mC), there is a multitude of histone methylation marks with varying affects on gene transcription. Histone methylation predominantly functions by directly recruiting or inhibiting the recruitment of histone-binding proteins (reviewed in (40)). For example, H3K4me3 specifically recruits activating proteins including transcription factors to gene promoters, while inhibiting binding of transcription repressors. In contrast, constitutive heterochromatin is particularly enriched with the repressive modifications H3K9me2 and H3K9me3 that inhibit binding of transcription activators. NNMT-induced SAM depletion and associated DNA and histone hypomethylation can therefore upregulate or downregulate transcription of many genes depending on the nature of DNA and histone methylation marks in their genomic loci.

I performed RNAseq on NNMT-expressing and NNMT-depleted MDA-MB-231 and SUM159PT cells to identify genes that are differentially expressed downstream of NNMT

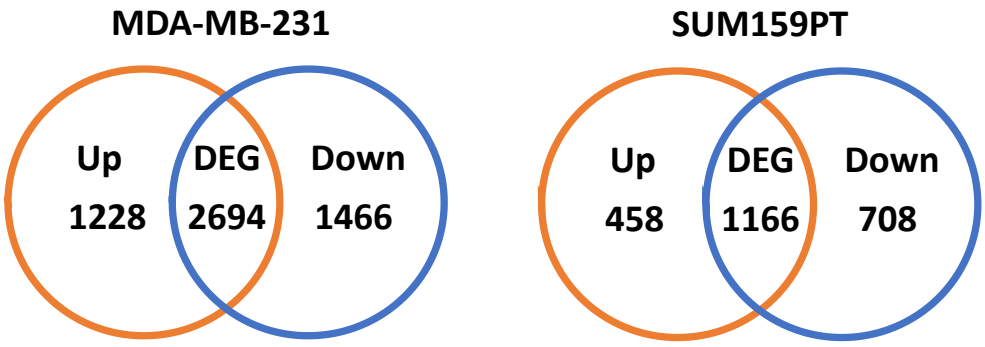

Figure 3.4. Number of all differentially expressed genes (DEG), differentially upregulated genes (Up), and differentially downregulated genes (Down) upon NNMT depletion in patient-derived TNBC cell lines (shNNMT-1 vs shControl). *Cells were under constant puromycin selection and treated with 100 ng/ml doxycycline for 6 days prior to RNA extraction.* *MDA-MB-231(n= 3) DEG filters: shControl TPM>5, FDR<0.05, Log_2FC >0.6 or <-0.6.* *SUM159PT (n=2) DEG filters: shControl TPM>5, FDR<0.1, Log_2FC >0.6 or <-0.6.*

depletion-induced SAM upregulation, which served to generate hypotheses regarding the molecular mechanisms by which NNMT may contribute to TNBC biology. In both cell lines,

NNMT depletion resulted in significant differential gene expression (Figure 3.4). Ingenuity Pathway Analysis (IPA) on NNMT depletion-induced DEGs showed that NNMT expression is associated with increased expression of tumor-promoting genes (Invasion/EMT) and NNMT depletion is associated with increased expression of anabolic metabolism genes (lipogenesis *(cholesterol biosynthesis)*, ribogenesis *(many upregulated large and small ribosomal proteins categorized into EIF2 Signaling)*) in both cell lines (Figures 3.5 and 3.6).

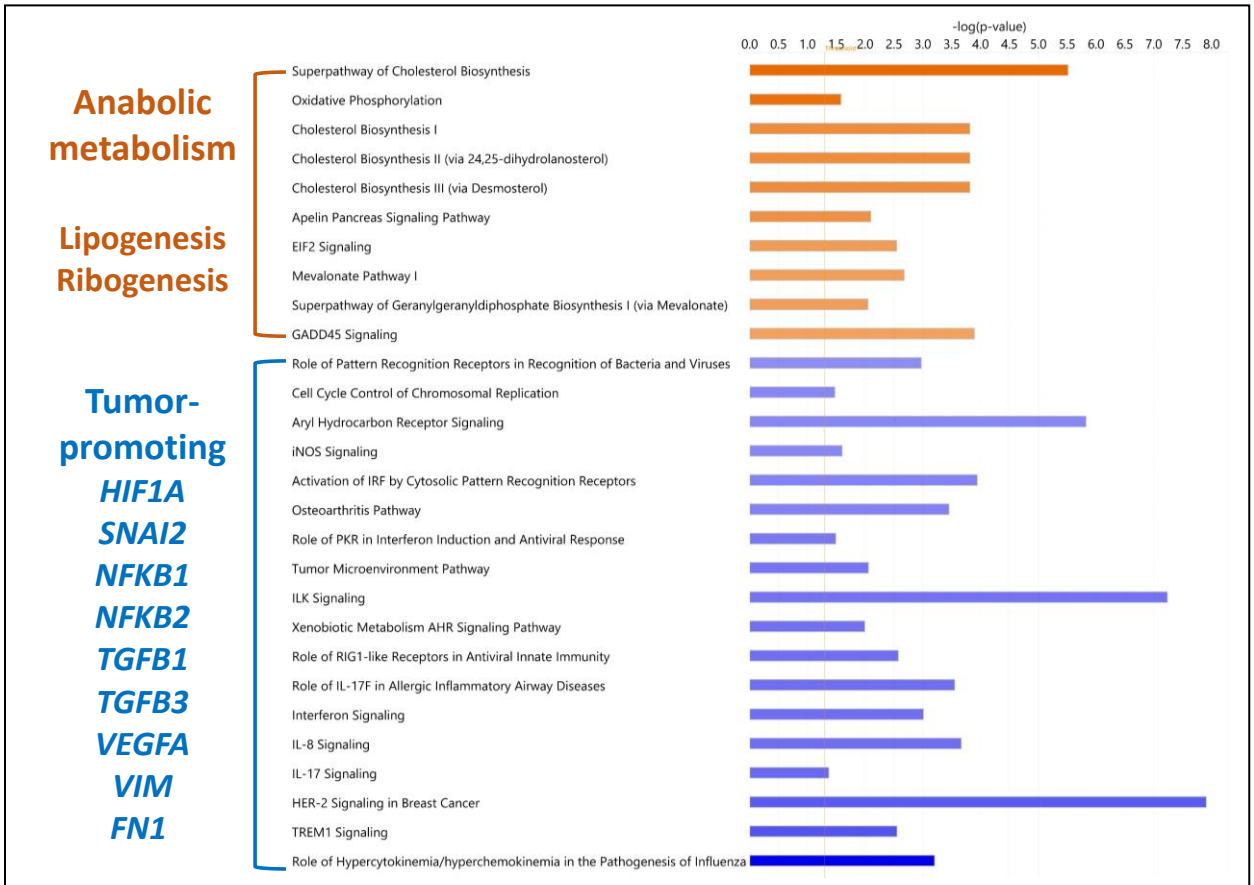

Figure 3.5. IPA canonical pathways whose activation levels are predicted to be upregulated (orange) or downregulated (blue) in association with NNMT depletion-induced DEGs in the MDA-MB-231 RNAseq dataset. *Activation score -log(p-value) > 1.3.*

Furthermore, while the IPA biological pathways that downregulated DEGs are categorized into are predicted to have downregulated activity (blue) and do not seem to be biologically connected, the IPA biological pathways that upregulated DEGs are categorized into are predicted

to have upregulated activity (orange) and fall under anabolic metabolism.

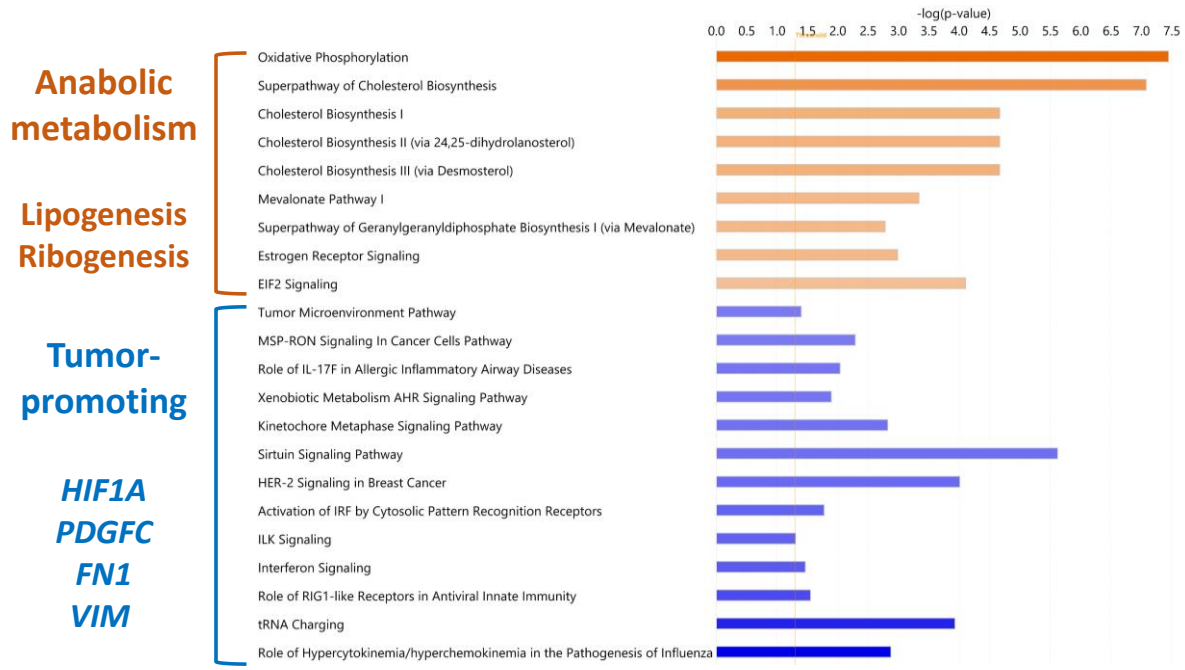

Figure 3.6. IPA canonical pathways whose activation levels are predicted to be upregulated (orange) or downregulated (blue) in association with NNMT depletion-induced DEGs in the SUM159PT RNAseq dataset. *Activation score -log(p-value) > 1.3.*

I formed two hypotheses based on these findings:

1) Genes that were downregulated with NNMT depletion (i.e., Invasion/EMT) may happen to possess repressive DNA and histone methylation in their regulatory regions in these cell lines, and NNMT depletion-induced SAM upregulation may therefore result in an increase in repressive DNA and histone methylation in these regulatory regions resulting in their transcriptional downregulation. In other words, NNMT-expressing cells with SAM depletion would have decreased repressive DNA and histone methylation in the regulatory regions of these genes in association with increased transcription of these genes.

2) NNMT depletion-induced SAM upregulation may upregulate mTOR signaling leading to increased anabolic gene expression. mTORC1 regulates cell growth and metabolism in response to multiple environmental cues including growth factors

and nutrients such as amino acids (41). The Sabatini Lab discovered that SAMTOR acts as a nutrient sensor for SAM in lieu of methionine upstream of mTOR (42). During methionine depletion and thereby SAM depletion, free SAMTOR acts to inhibit mTORC1. When methionine and thereby SAM levels are replete, SAM binds SAMTOR and SAM-bound SAMTOR undergoes conformational changes that inhibits SAMTOR from interacting with the mTORC1 complex, releasing the repression on mTORC1 and activating canonical mTORC1 targets that upregulate anabolism and cell growth. Lipogenesis (cholesterol synthesis) and ribogenesis (EIF2 signaling) pathways in my IPA analysis are canonically downstream of mTORC1 activation.

In summary, these RNAseq findings suggest that SAM may not only act as a methyl donor but also as a nutrient upstream of mTORC1 in the MDA-MB-231 and SUM159PT patient-derived TNBC cell lines. Therefore, altering the level of NNMT expression and activity and thereby SAM levels in these cells may not only affect SAM-dependent methyltransferase activity but also the level of mTORC1 activity.

3.2.4 NNMT expression is associated with tumor-promoting (Invasion/EMT) gene expression in untreated early-stage TNBCs.

I next aimed to determine whether NNMT-associated EMT-invasion and anabolic gene expression in the patient-derived TNBC cell lines have relevance to TNBC patient tumor gene expression. To identify genes whose mRNA expression is significantly correlated with *NNMT* mRNA expression in TNBC patient tumors, I used cBioPortal to perform a co-expression analysis for *NNMT* mRNA in the TCGA untreated and early-stage TNBC tumors (43). I determined that tumor mRNA expression of a set invasion/EMT genes similar to but larger than the invasion/EMT gene set in my *in vitro* RNAseq data is significantly and positively associated with tumor *NNMT* mRNA expression (Figure 3.7). Interestingly, I did not find an association between tumor *NNMT*

mRNA expression and mRNA expression of anabolic metabolism genes in these tumors (data not shown).

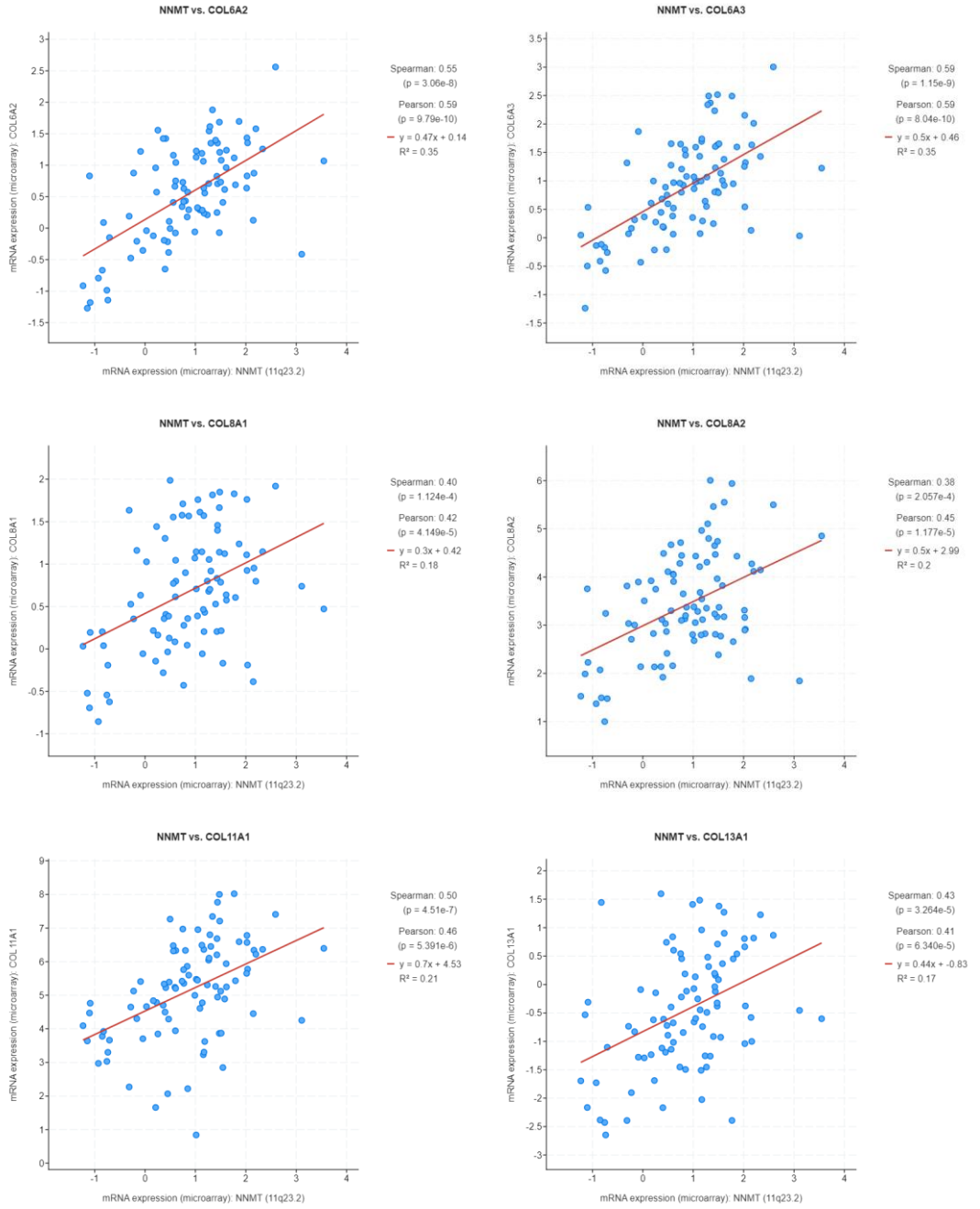

Figure 3.7. cBioPortal co-expression analysis for NNMT mRNA in untreated and early-stage TNBCs in the TCGA dataset demonstrates that tumor *NNMT* mRNA expression is significantly and positively correlated with the tumor mRNA expression of a multitude of tumor-promoting genes that are known to contribute to cancer cell EMT and invasion phenotypes. *X axis of each graph denotes NNMT mRNA expression. Y axis of each graph denotes mRNA expression of another gene. The title of each graph denotes the mRNA whose expression is compared to NNMT mRNA expression. Each graph exhibits a regression line, and associated Spearman and Pearson correlation values with significant p values.*

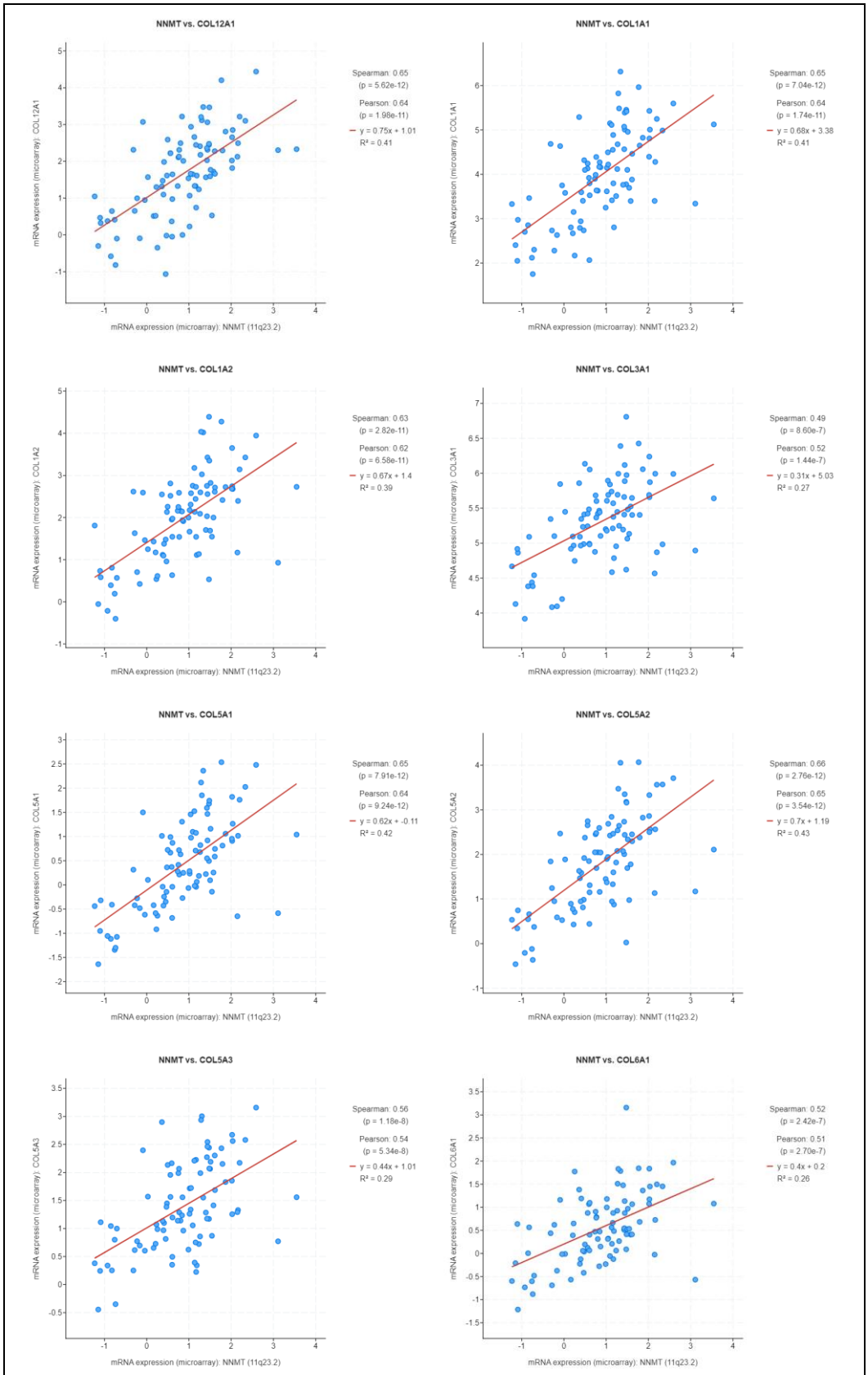

Figure 3.7 Continued.

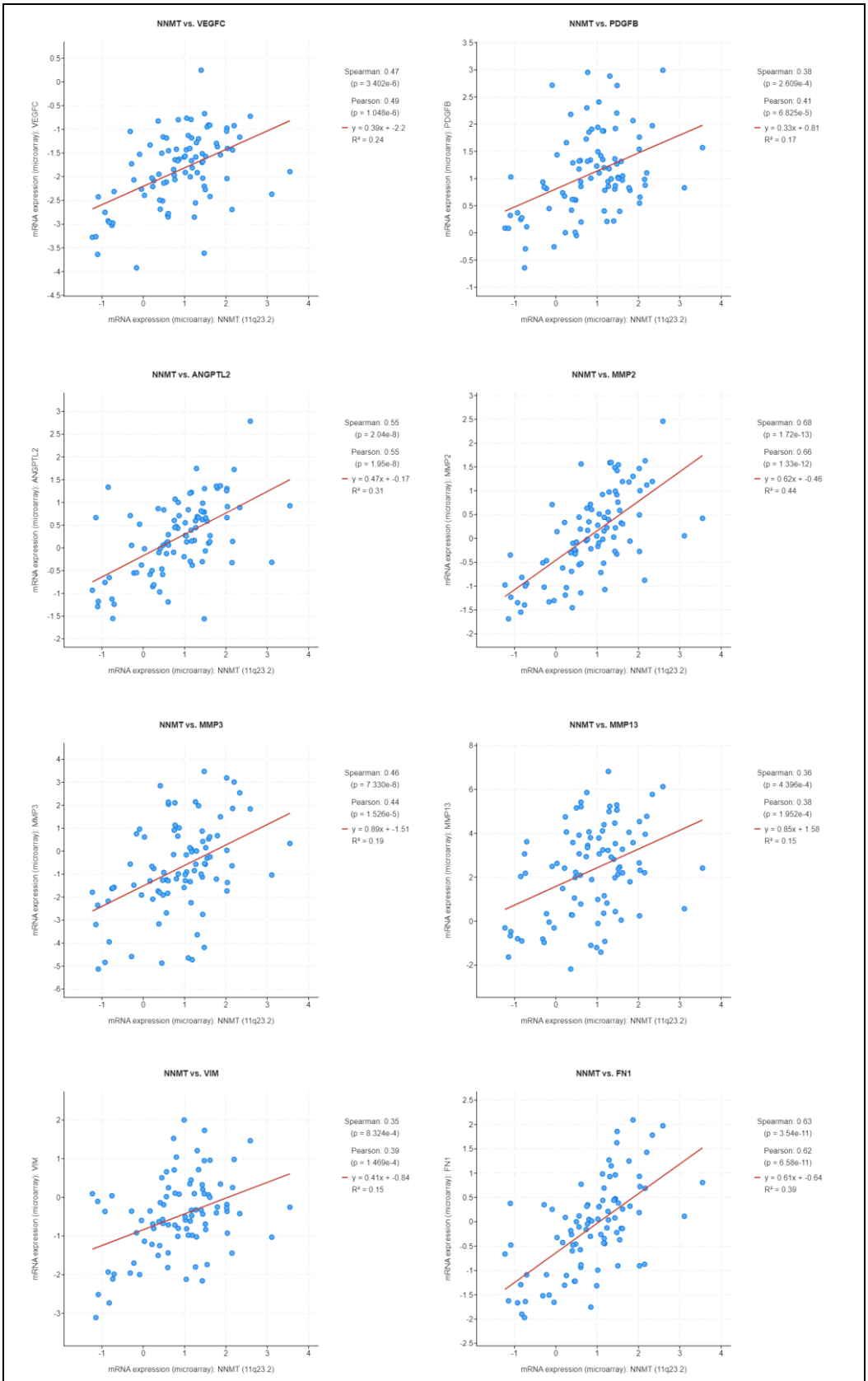

Figure 3.7 Continued.

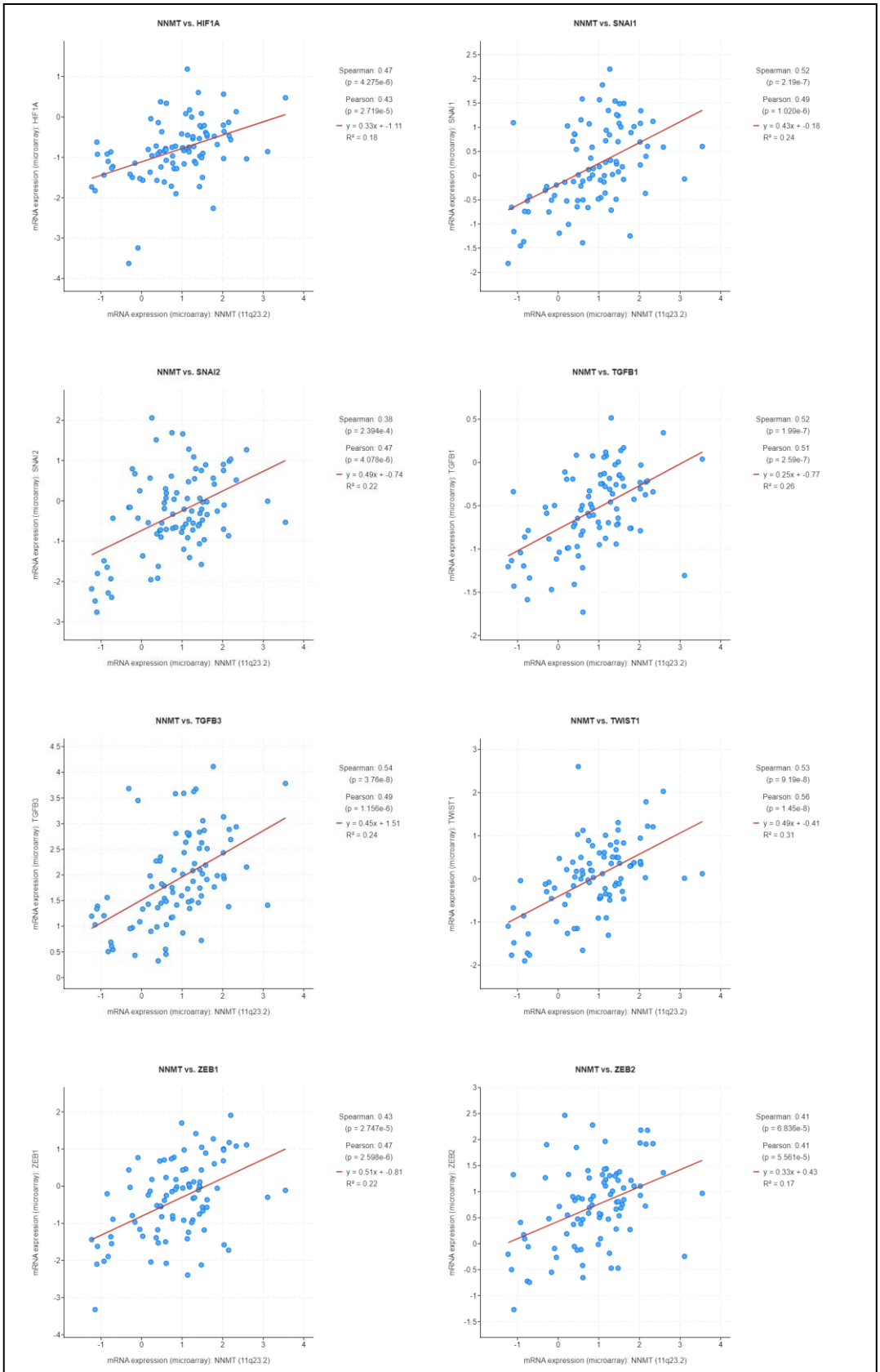

Figure 3.7 Continued.

3.3 Discussion

TNBC is an epithelial cancer and epithelial cells are inherently immotile; therefore, TNBC primary tumor cells need to develop motility and the ability to invade the surrounding stroma to exit the primary tumor site, enter circulation and form distant metastases. The process of becoming motile, invading the surrounding stroma and entering circulation is referred to as invasion, an essential trait of metastatic cancer cells (reviewed in (44)).

EMT (epithelial-to-mesenchymal transition) is a dynamic and reversible process of transdifferentiation of epithelial cells to quasi-mesenchymal states with enhanced stem cell-like properties, motility, and invasive capacity (reviewed in (45)). The EMT program can thus contribute to the overall invasive and thus metastatic capacity of cancer cells and is coordinated by the master transcription factors ZEB1, ZEB2, SNAI1, SNAI2, TWIST1, and TWIST2. These transcription factors induce the expression of hundreds of genes associated with the mesenchymal state (i.e., ECM components (collagen), ECM-degrading enzymes (MMPs), VIM, FN1) and repress genes associated with the epithelial state, and they have been linked to cancer progression and metastasis phenotypes in literature.

HIF1A is a transcription factor that promotes the transcription of genes involved in angiogenesis (i.e., *VEGF*, *ANGPT, PDGF*) and metabolic adaptation to oxygen deprivation (reviewed in (46). HIF1A-mediated angiogenic factor secretion by cancer cells would facilitate the formation of new vasculature in the primary tumor opening the way for tumor cells to enter circulation and later form distant metastases. HIF1A-mediated hypoxia signaling is a feature of most solid tumors including TNBC and is a negative prognostic factor due to its wide array of tumor-promoting effects including therapy resistance, angiogenesis, invasiveness, and metastasis.

My findings in chapter 3 demonstrate that NNMT expression is positively associated with

invasion and EMT gene expression (i.e., *HIF1A, SNAI, VEGF, PDGF, VIM, FN1*) in both patient-derived TNBC cell lines and in untreated early-stage TNBC patient tumors. It is interesting to note that ECM components and ECM-degrading enzymes (MMPs) associated with the EMT state are expressed in the TNBC patient tumors and are positively associated with NNMT expression, but they are not expressed in patient-derived TNBC cell lines cultured *in vitro*. This gene expression difference may be due to the fact that patient tumor cells exists in a complex 3D environment with stromal cells while cell lines cultured *in vitro* exist in a 2D environment deficient of stroma.

I hypothesize that constitutive SAM depletion in high NNMT-expressing TNBC cells result in global DNA and/or histone hypomethylation and associated constitutive overexpression of genes that had possessed transcriptionally repressive DNA and/or histone methylation at their regulatory regions. Some of these genes upregulated downstream of NNMT-induced SAM depletion and repressive DNA/histone methylation depletion may happen to be master regulator genes that promote EMT such as *SNAI2* and genes that promote angiogenesis such as *HIF1A.* Upregulated expression of other genes associated with EMT (i.e., *VIM, FN1, MMPs*) and angiogenesis (i.e., *VEGF, PDGF*) phenotypes may then be explained by the upregulated expression of their upstream regulators (i.e., *SNAI2, HIF1A*).

In addition, NNMT depletion in the TNBC cell lines is associated with increased expression of anabolic metabolism genes; however, *NNMT* mRNA expression in untreated early-stage TNBC patient tumors is not correlated with the mRNA expression of anabolic metabolism genes. This suggests that NNMT does not inherently inhibit anabolic gene expression in TNBC cells and that increased anabolic gene expression may arise artificially as a result of experimentally-induced NNMT depletion and associated SAM upregulation and mTORC1 activation.

Based on these findings, I hypothesized that NNMT-expressing TNBC cells may have enhanced metastatic potential *in vivo* due to increased expression of invasion and EMT-promoting genes. I also hypothesized that depleting NNMT in TNBC cells may decrease their overall metastatic capacity by downregulating the expression of invasion/EMT genes but may also influence their organ tropism by altering their metabolism through upregulating anabolic gene expression and giving these cells unpredictable advantages in unique microenvironments of distant organs that put distinct metabolic demands on the invading metastatic cells (reviewed in (47)). I then set out to address these hypotheses with *in vivo* experiments to begin to establish a biologically significant role for NNMT in TNBC progression.

CHAPTER 4

NNMT-ASSOCIATED TNBC METASTASIS PHENOTYPES

4.1 Introduction

In this chapter of my dissertation, I first aimed to design an *in vivo* experiment that would allow me to determine NNMT's potential role in TNBC primary tumor growth, overall metastatic potential, and organ tropism. Most of the literature on metastatic phenotypes in xenograft mouse models of TNBC uses the highly immunocompromised NSG mouse strain as patient-derived TNBC cell lines are able to form visceral metastases in female NSG mice (48). Therefore, I opted to perform my *in vivo* experiments with this mouse strain. Patient-derived TNBC cell lines form subcutaneous tumors when orthotopically injected into the mammary fat pad of immunocompromised mouse strains (i.e., SCID, NOD.SCID and NSG). However, patient-derived TNBC cell line primary tumor growth in the mammary fat pad of NSG mice is fast, quickly exceeds the limits that are allowed in animal protocols and therefore significantly limits the duration of the experiment. At this stage, if mice have developed any metastases at all, they would be micrometastases. It is therefore essential to surgically remove primary tumors to allow metastasis to progress further in this experimental model (35).

As an alternative strategy, most *in vivo* studies on TNBC metastasis injects TNBC cell lines into the circulation of immunocompromised mouse strains with tail vein injection followed by metastasis formation in the lungs (49, 50). BC cell lines cultured *in vitro* (median diameter 20um) are larger than BC circulating tumor cells (CTCs, median diameter 12um) that arise from invasive primary tumor cells (51); therefore, TNBC cell lines cultured *in vitro* and then immediately injected into the mouse teil vein would first arrive in the heart via inferior vena cava, then travel

to the lungs, get stuck in the thin pulmonary capillaries (avg diameter 6um) and lose their chance to exit the lung and travel to other organs to form metastases. This experimental strategy 1) makes it impossible to study the first part of the metastatic cascade where primary tumor cells undergo phenotypic changes to become invasive and enter circulation to form spontaneous metastases and 2) only allows for the study of lung metastases, it is therefore scientifically not preferable.

Here, I outline my *in vivo* experimental design involving orthotopic transplantation of stably Luciferase-expressing versions of the MDA-MB-231 and SUM159PT cells with shControl or shNNMT-1 into female NSG mouse inguinal mammary fat pad, surgical removal of the primary xenograft tumor and quantification of metastatic burden in multiple visceral organs with bioluminescence imaging. This experimental design allows for determination of NNMT's effect on tumor growth rate, overall metastatic burden and organ-specific metastatic burden (Figure 4.1).

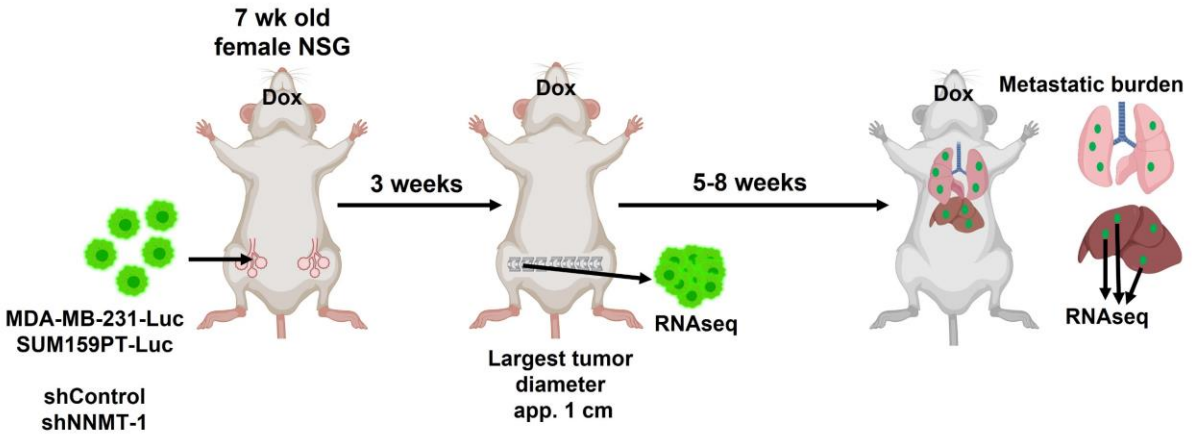

Figure 4.1. *In vivo* experimental design to investigate NNMT's role in TNBC xenograft primary tumor growth, metastatic potential, and organ tropism. **1)** Stably Luciferase-expressing MDA-MB-231 or SUM159PT cells with shControl or shNNMT-1 were cultured *in vitro* for 3 days with 100 ng/ml doxycycline to induce shRNA expression. **2)** Cells were implanted into the right inguinal mammary fat pads of 7-week-old female NSG mice. **3)** Tumors along with entire inguinal mammary gland were surgically removed when the largest diameter reached 1 cm. This allowed enough time for the primary tumors to become invasive and seed metastases. **4)** Metastatic burden was routinely monitored with bioluminescence imaging for 5-8 weeks. **5)** All mice were euthanized at the same time, visceral organs and metastatic nodules were collected for further analyses. *Mice were fed a doxycycline-containing diet throughout the experiment to maintain shRNA expression in primary tumors and metastatic cells.*

4.2 Results

4.2.1 NNMT is implicated as a metastasis-promoting protein in TNBC.

In this chapter, I will first report results on the MDA-MB-231 cell line and then will report results on the SUM15PT cell line. Prior to surgical removal of the primary MDA-MB-231 tumors, I performed bioluminescence imaging on each mouse to confirm that primary tumor cells exhibit Luciferase-based bioluminescence (Figure 4.2). This allowed me to confirm that I could monitor metastatic burden with bioluminescence imaging after primary tumor removal since primary tumor cells were bioluminescent and therefore metastatic cells would continue to be bioluminescent.

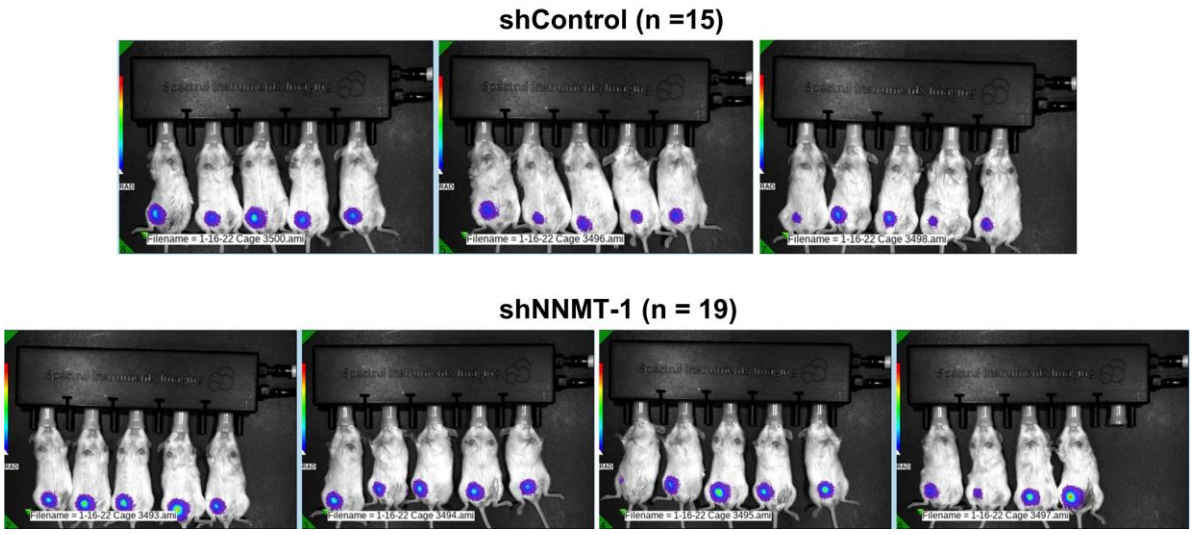

Figure 4.2. Luciferase-based bioluminescent imaging of MDA-MB-231 primary tumors with AMI-HTX *in vivo* imaging system. **1)** Mice were intraperitoneally injected with 150 mg/kg D-Luciferin. **2)** 2 minutes following Luciferin injection, anesthesia was induced and maintained with isoflurane. **3)** 8 minutes following Luciferin injection, mice were imaged on the AMI-HTX bioluminescence channel with 1 sec exposure.

Up until surgical removal of the MDA-MB-231 primary tumors, I measured the volume of each tumor with an electronic caliper to determine whether tumor NNMT expression is associated with time to tumor initiation and tumor growth rate. Primary tumor NNMT expression was associated with decreased time to tumor initiation but did not affect the growth rate of initiated

tumors (Figure 4.3). NNMT was depleted in the shNNMT-containing MDA-MB-231 cells prior to implantation, and tumor growth data suggest that NNMT depletion affected the tumor initiation capacity of these cells and thereby increased the time to tumor initiation. However, NNMT depletion did not affect the doubling rate once the tumors were established as the slope of the curves for NNMT-expressing and NNMT-depleted tumors are similar beyond day 17. Furthermore, I performed Western blots on an aliquot of the implanted cells and primary tumors to confirm that NNMT was depleted prior to implantation and in primary tumors (Figure 4.4).

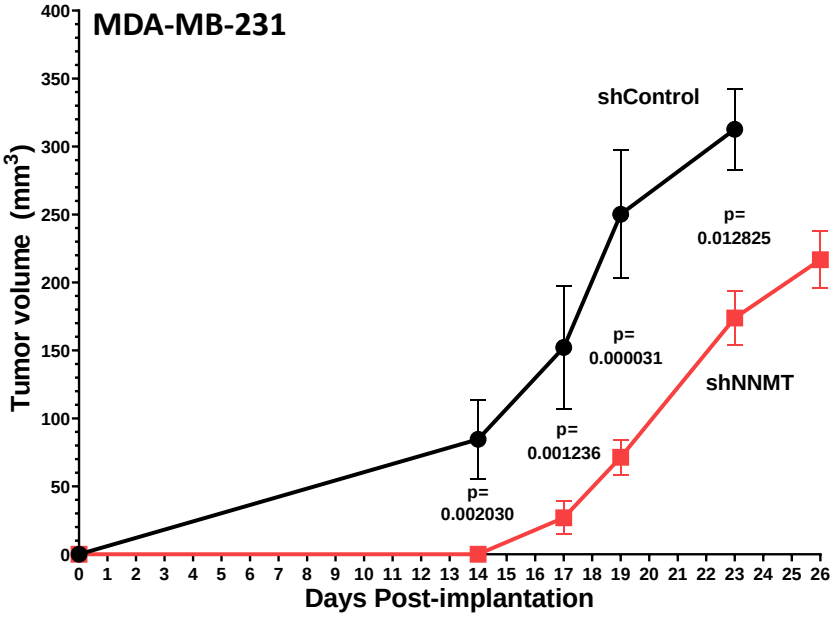

Figure 4.3. MDA-MB-231 primary tumor NNMT expression is associated with decreased time to tumor initiation but not with growth rate of already initiated tumors.

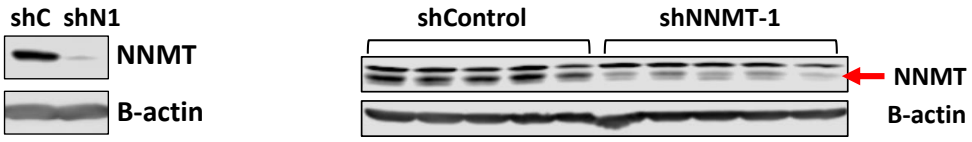

Figure 4.4. NNMT Western blot on MDA-MB-231 cells and primary tumors.

Immediately following surgical removal, I flash froze a portion of each primary tumor for RNAseq analysis and fixed the remaining portion for histology and IHC. Because the major aim of this experiment was to determine whether NNMT is associated with overall metastatic potential of TNBC cells in primary tumors, I aimed to determine whether primary tumor NNMT expression is associated with tumor cell proliferative index and viability since decreased tumor cell viability alone would be enough to explain the hypothesized decrease in overall metastatic potential upon NNMT depletion in the primary tumors. There were no significant differences in the level and intensity of Ki67 staining in NNMT-expressing and NNMT-depleted tumors, suggesting that NNMT expression does not affect the proliferative capacity of the MDA-MB-231 primary tumors

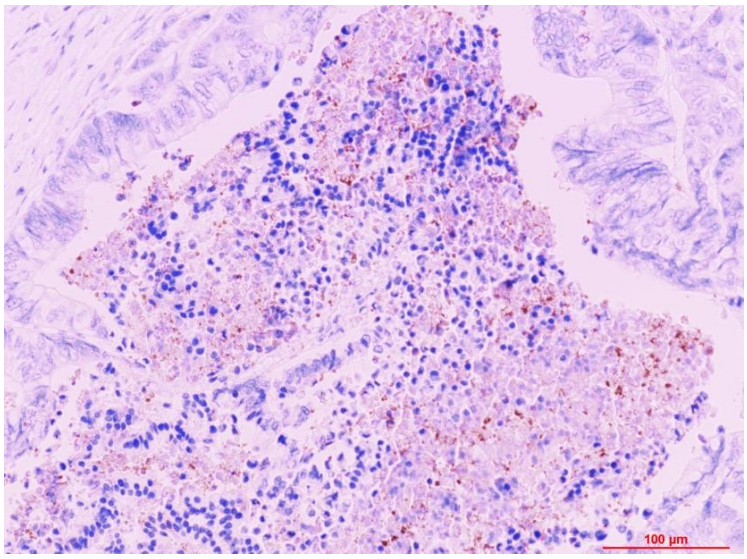

Figure 4.5. Cleaved caspase 3 staining on human tonsil as positive control for CC3 IHC on the MDA-MB-231 tumors.

(Figure 4.6). Furthermore, all tested NNMT-expressing and NNMT-depleted tumors stained completely negative for cleaved caspase 3 (CC3), suggesting that all tumors were non-apoptotic and that NNMT expression does not affect MDA-MB-231 primary tumor cell viability (Figure 4.6). Since all tested tumors were negative for CC3 staining, I provide CC3 staining on human tonsil as a positive control for CC3 IHC (Figure 4.5).

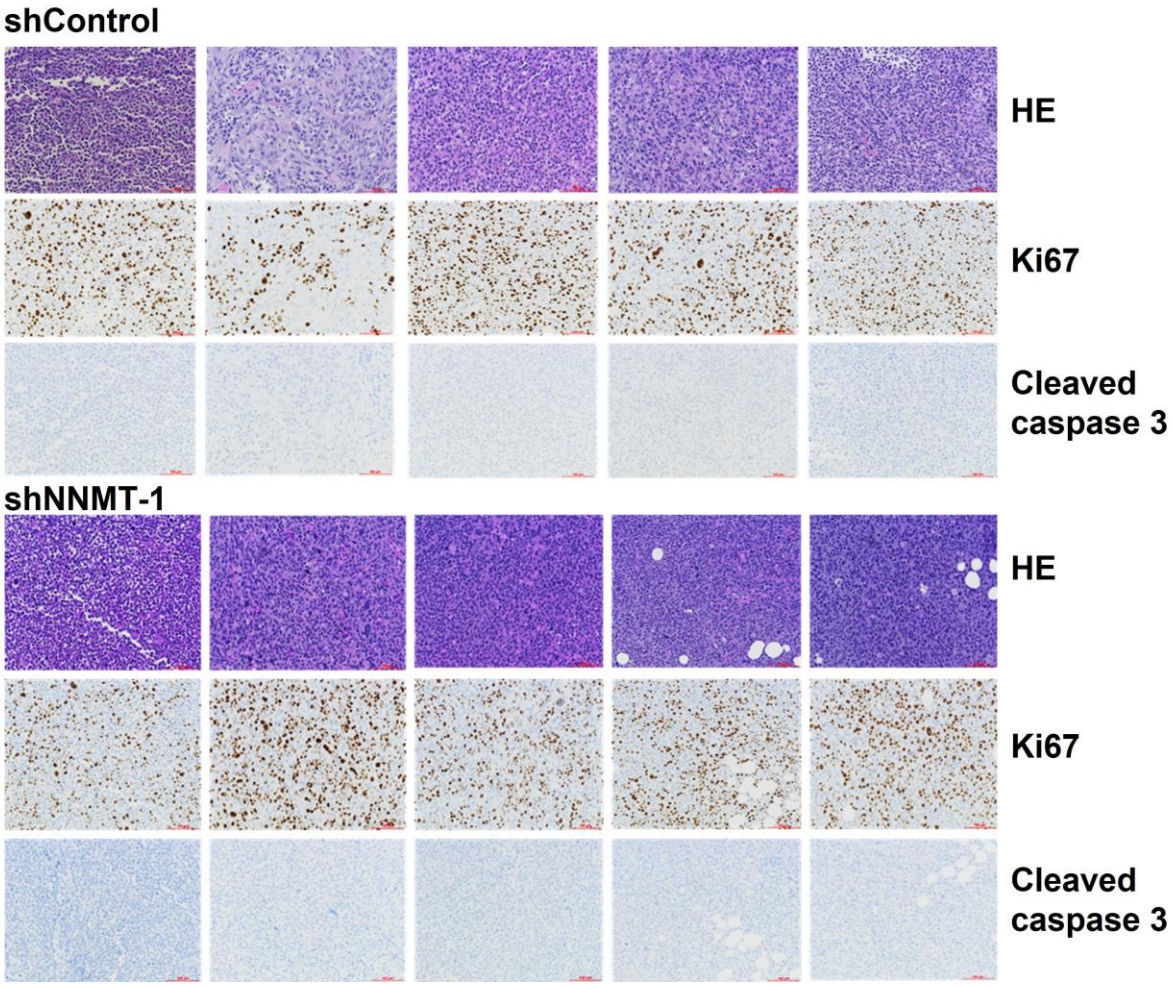

Figure 4.6. H&E, Ki67 and cleaved caspase 3 staining on NNMT-expressing and NNMT-depleted MDA-MB-231 primary tumors. Each column is an individual tumor.

I performed primary tumor removal surgery on 17 mice bearing NNMT-expressing tumors and 19 mice bearing NNMT-depleted primary tumors when the largest diameter of each tumor reached but did not exceed approximately 1 cm. Time to primary tumor removal surgery since the

day of implantation was on average 3 weeks for all mice, and all tumor removal surgeries were performed within the span of 1 week to minimize the variation in the duration of time each primary tumor resides in the mammary fat fad and continues to seed metastatic cells into the mouse circulation. It is also important to note that I removed as much of the inguinal mammary fat pad as I could after removing each primary tumor to minimize the possibility of primary tumor regrowth due to cancer cells that have infiltrated the inguinal mammary fat pad prior to the surgery. Several mice in both the shControl and shNNMT groups were euthanized to due post-surgical health concerns. I had 10 shControl mice and 13 shNNMT mice that were healthy after the surgeries and routinely monitored overall metastatic burden in these mice with bioluminescence imaging. Below are the major findings:

1) MDA-MB-231 cells were able to form peritoneal metastases, lung metastases, liver metastases, and primary tumor regrowth in this experimental model (Figure 4.7).

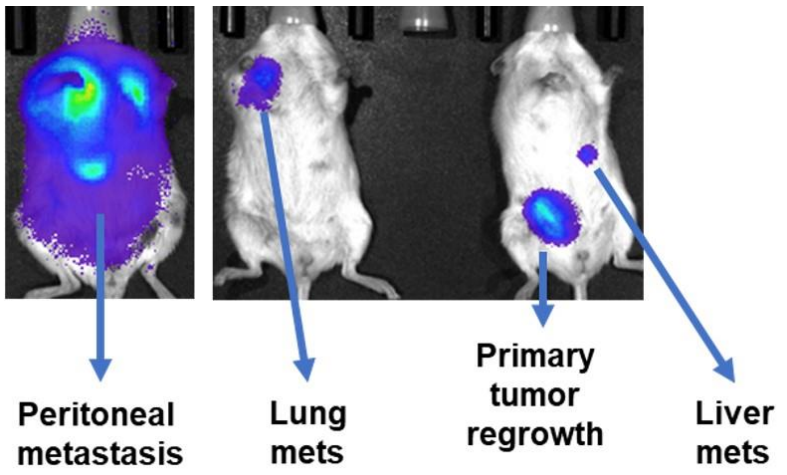

Figure 4.7. Bioluminescence imaging of post-surgical NSG mice demonstrating Luciferase signal emanating from metastatic MDA-MB-231 cells.

2) 7/10 mice in the shControl group developed extensive peritoneal metastasis resulting in poor health and thereby euthanasia. None of the mice in the shNNMT group developed peritoneal ascites (Figures 4.8, 4.9, 4.10).

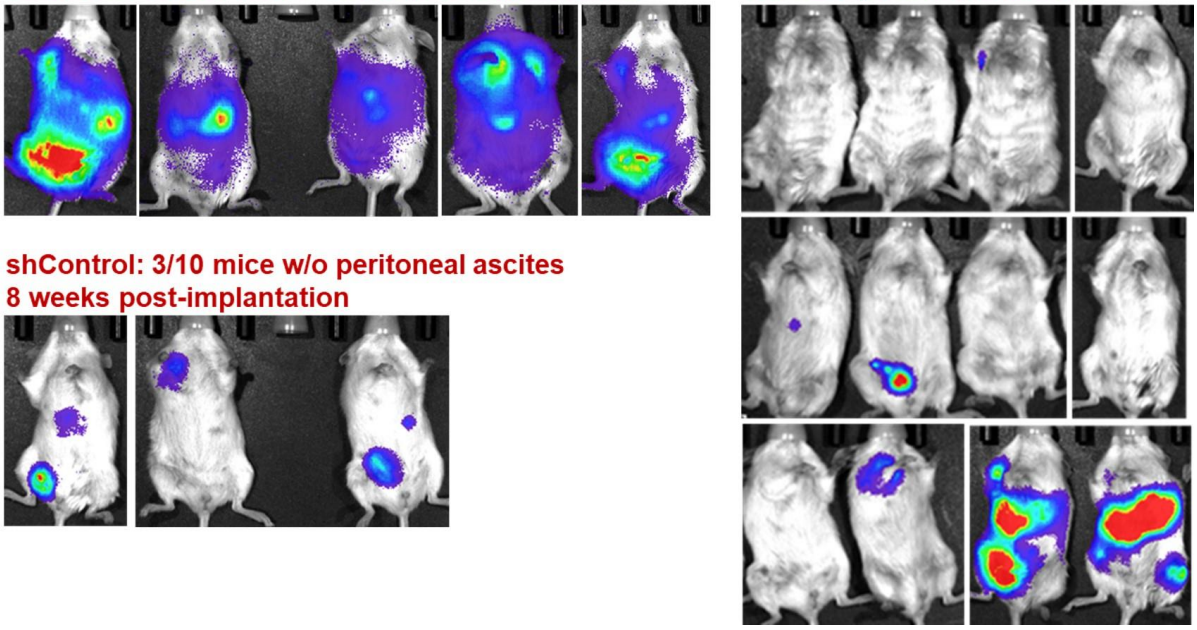

Figure 4.8. Bioluminescence imaging of post-surgical NSG mice demonstrating Luciferase signal emanating from metastatic MDA-MB-231 cells. 7/10 mice in the shControl group developed extensive peritoneal metastasis resulting in poor health and thereby euthanasia (2 shControl mice with peritoneal ascites not shown). None of the mice in the shNNMT group developed peritoneal ascites.

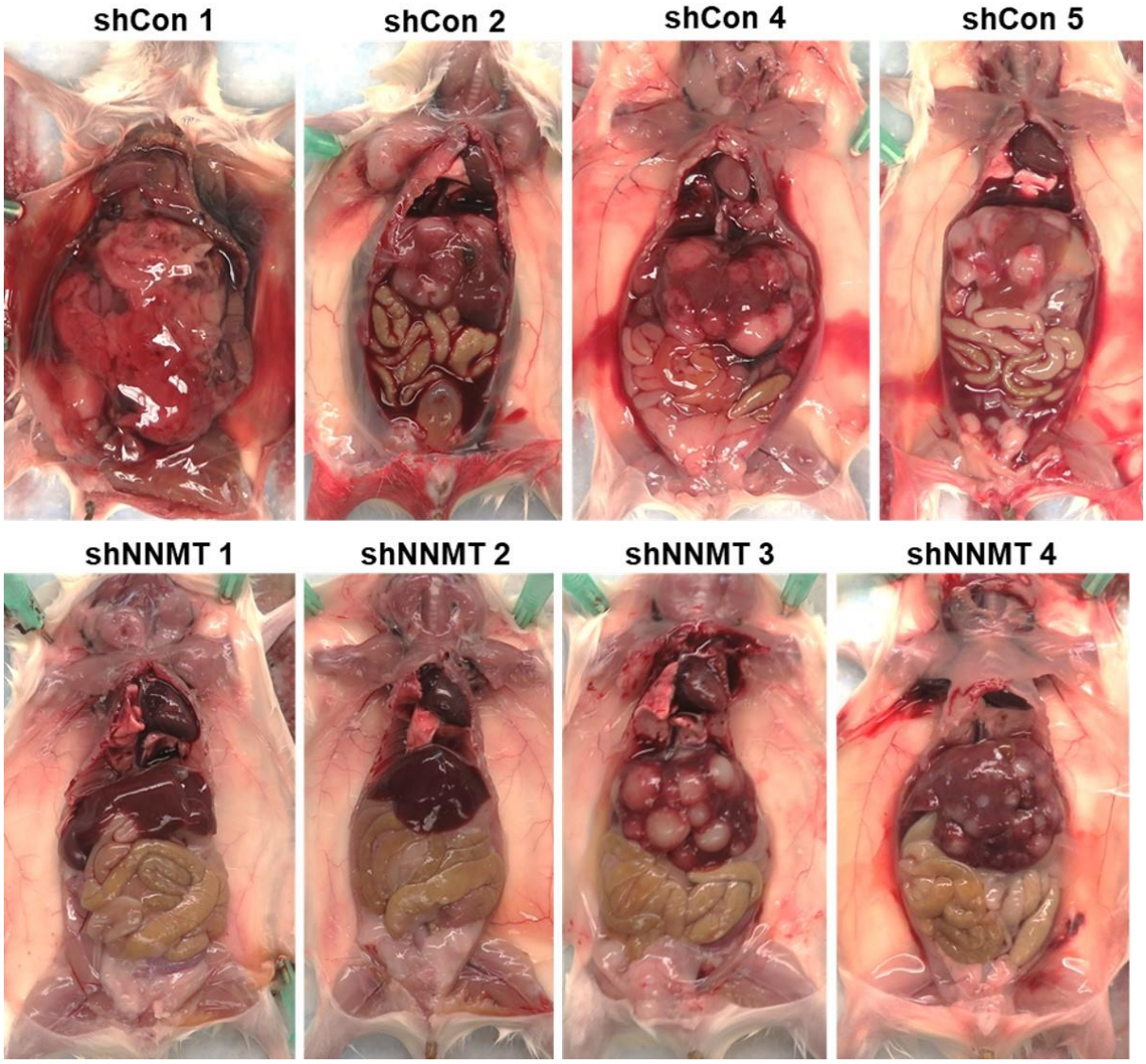

Figure 4.9. Representative abdominal photographs of 4 mice in the shControl group and 4 mice in the shNNMT group demonstrating the presence of peritoneal ascites in all mice that had NNMT-expressing primary tumors and lack of peritoneal ascites in all mice that had NNMT-depleted primary tumors.

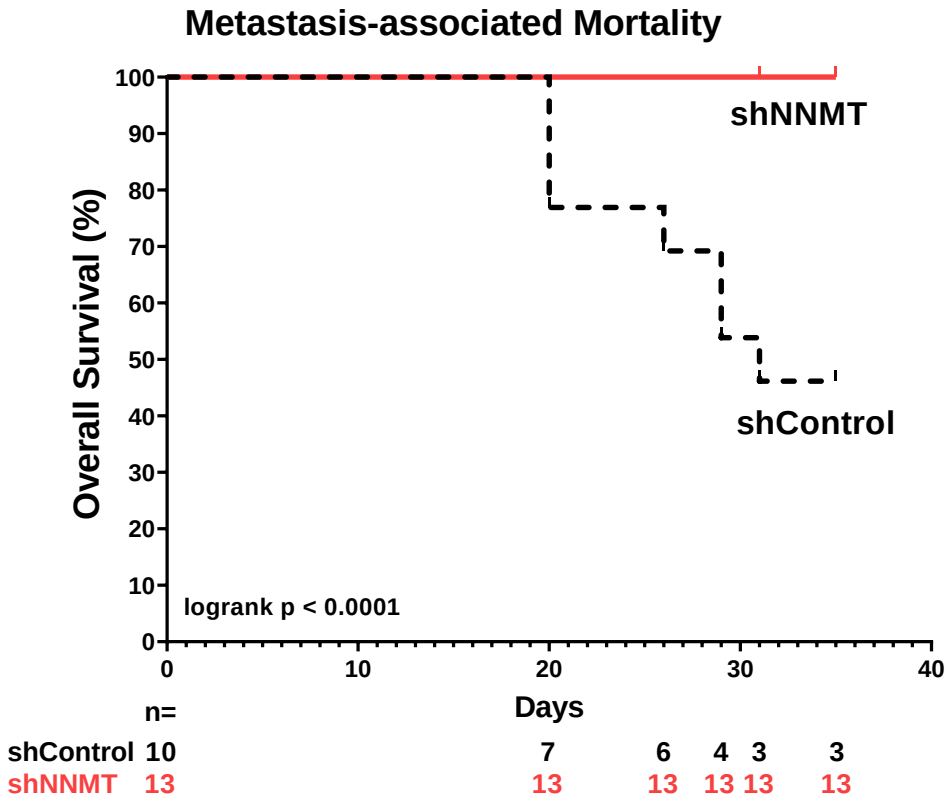

Figure 4.10. MDA-MB-231 primary tumor NNMT expression is associated with a significantly worse probability of overall survival due to metastasis-associated mortality. *Day 0 is the final day that primary tumor surgeries were performed.*

3) At the end of the study (8.5 weeks post-implantation) when all remaining mice were euthanized at the same time, while 0/10 mice in the shControl group were metastasis free, 6/13 mice in the shNNMT group were metastasis free based on the lack of Luciferase signal and lack of metastatic nodules on the lung and liver H&E slides.

4) I performed RNAseq on NNMT-expressing and NNMT-depleted MDA-MB-231 primary tumors to identify NNMT-associated primary tumor gene expression that may explain the strong association between primary tumor NNMT expression and increased

probability of metastasis formation. Similar to *in vitro* and TNBC patient tumor findings outlined in previous chapters, IPA analysis on NNMT depletion-induced DEGs showed that NNMT expression in MDA-MB-231 primary tumors is associated with increased expression of tumor-promoting genes (Invasion/EMT), and NNMT depletion is associated with increased expression of anabolic metabolism genes (lipogenesis (cholesterol biosynthesis), ribogenesis (many upregulated large and small ribosomal proteins categorized into EIF2 Signaling)) (Figure 4.11).

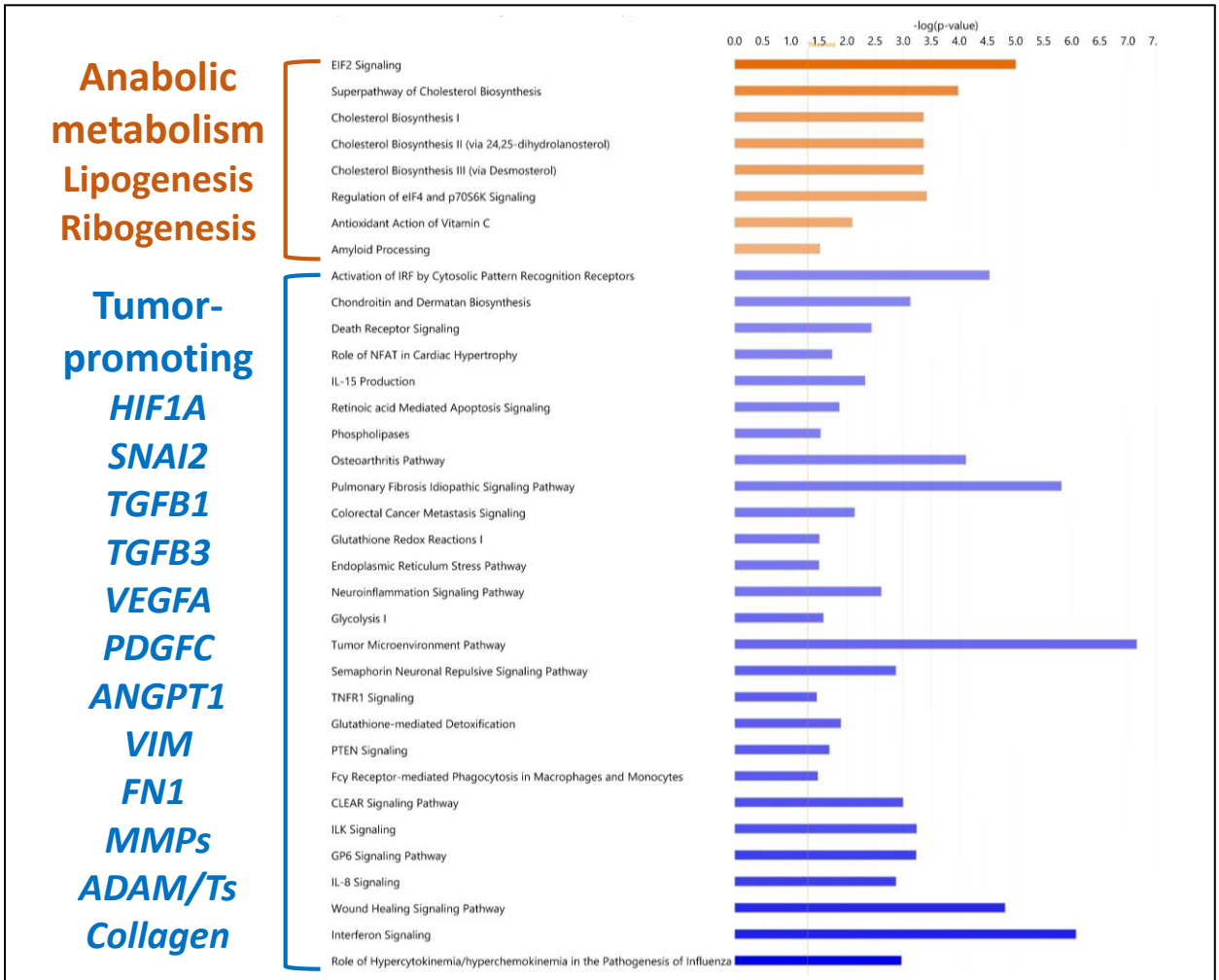

Figure 4.11. IPA canonical pathways whose activation levels are predicted to be upregulated (orange) or downregulated (blue) in association with NNMT depletion-induced DEGs in the MDA-MB-231 primary tumor RNAseq dataset (n = 10). *DEG filters: shControl TPM>5, FDR<0.05, Log_2FC >0.6 or <-0.6, IPA activation score -log(p-value) > 1.3.*

In summary, MDA-MB-231 xenograft primary tumor NNMT expression is associated with increased probability of metastasis formation *in vivo*, increased probability of metastasis-associated mortality, and these phenotypes are associated with significantly higher expression of invasion/EMT-promoting genes (i.e., *HIF1A*, *SNAI2*, *VEGFA*, *MMPs*) in the NNMT-expressing primary tumors. Importantly, NNMT-depletion associated decrease in metastasis formation is not due to decreased primary tumor cell viability as both NNMT-expressing and NNMT-depleted tumors were non-apoptotic, suggesting that NNMT may promote enhanced TNBC cell metastatic potential by invasion/EMT gene expression-induced upregulation of invasive capacity of primary tumor cells.

The SUM159PT cell line yielded metastasis-associated phenotypes similar to those of the MDA-MB-231 cell line in the same experimental model. Below are the major findings:

1) I performed Western blots on an aliquot of the implanted SUM159PT cells and primary tumors to confirm that NNMT was depleted prior to implantation and in primary tumors (Figure 4.12). Furthermore, all primary tumors exhibited Luciferase-based bioluminescence, and this allowed me to confirm that I could monitor metastatic burden with bioluminescence imaging after primary tumor removal since primary tumor cells were bioluminescent and therefore metastatic cells would continue to be bioluminescent (Figure 4.13).

2) 1 million implanted MDA-MB-231 cells are able to grow into tumors in this experimental model, while 10 million SUM159PT cells are needed to be implanted for primary tumor formation in the inguinal mammary fat pad, suggesting that SUM159PT cells have lower tumor initiation capacity compared to MDA-MB-231 cells. While all MDA-MB-231 tumors have become palpable 2 weeks following implantation,

SUM159PT tumors became palpable starting from 3 weeks post-implantation. Furthermore, once initiated, SUM159PT tumors grew too fast to assess differences in tumor growth between NNMT-expressing and NNMT-depleted conditions.

3) There were no significant differences in the level and intensity of Ki67 staining in NNMT-expressing and NNMT-depleted tumors, suggesting that NNMT expression does not affect the proliferative capacity of the SUM159PT primary tumors (Figure 4.14). Furthermore, all tested NNMT-expressing and NNMT-depleted tumors stained completely negative for cleaved caspase 3 (CC3), suggesting that all tumors were non-apoptotic and that NNMT expression does not affect SUM159PT primary tumor cell viability.

3) I had 15 shControl mice and 16 shNNMT mice that were healthy after the surgeries and routinely monitored overall metastatic burden in these mice with bioluminescence imaging. SUM159PT cells were able to form lung metastases, spleen metastases, thoracic mammary gland metastases, and primary tumor regrowth (Figure 4.15). None of the mice bearing SUM159PT primary tumors developed peritoneal ascites.

4) SUM159PT primary tumor NNMT expression was associated with a significantly higher probability of metastasis formation and increased probability of metastasis-associated mortality (Figures 4.16 and 4.17).

In summary, MDA-MB-231 and SUM159PT xenograft primary tumor NNMT expression is associated with increased probability of metastasis formation and increased probability of metastasis-associated mortality, implicating NNMT as a metastasis-promoting protein in TNBC.

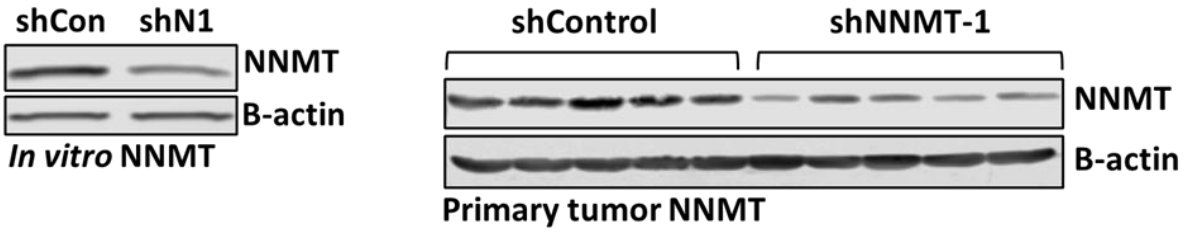

Figure 4.12. NNMT Western blot on SUM159PT cells prior to implantation and on SUM159PT primary tumors that have been surgically removed.

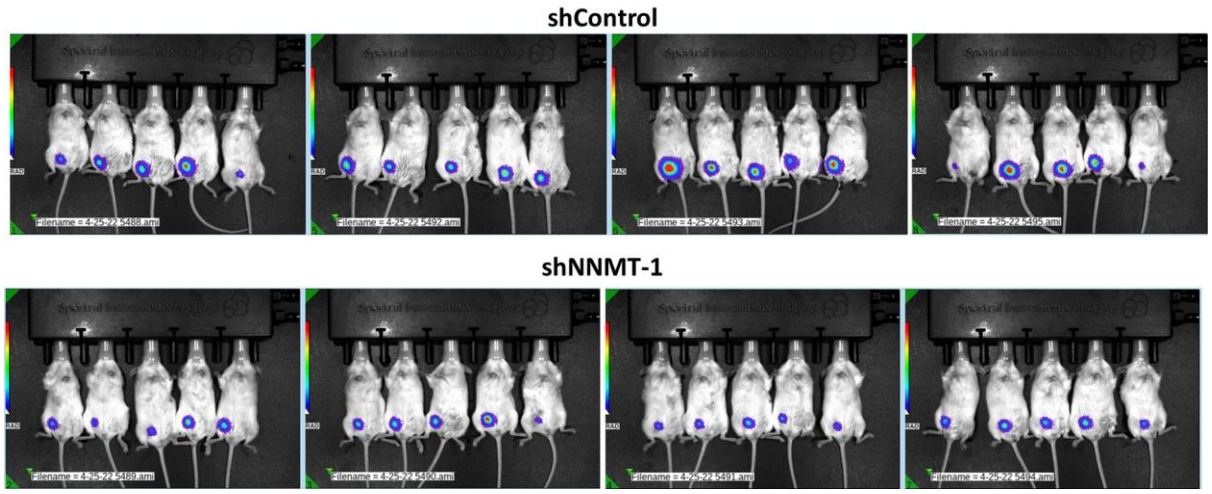

Figure 4.13. Luciferase-based bioluminescent imaging of SUM159PT primary tumors with AMI-HTX *in vivo* imaging system. **1)** Mice were intraperitoneally injected with 150 mg/kg D-Luciferin. **2)** 2 minutes following Luciferin injection, anesthesia was induced and maintained with isoflurane. **3)** 8 minutes following Luciferin injection, mice were imaged on the AMI-HTX bioluminescence channel with 1 sec exposure.

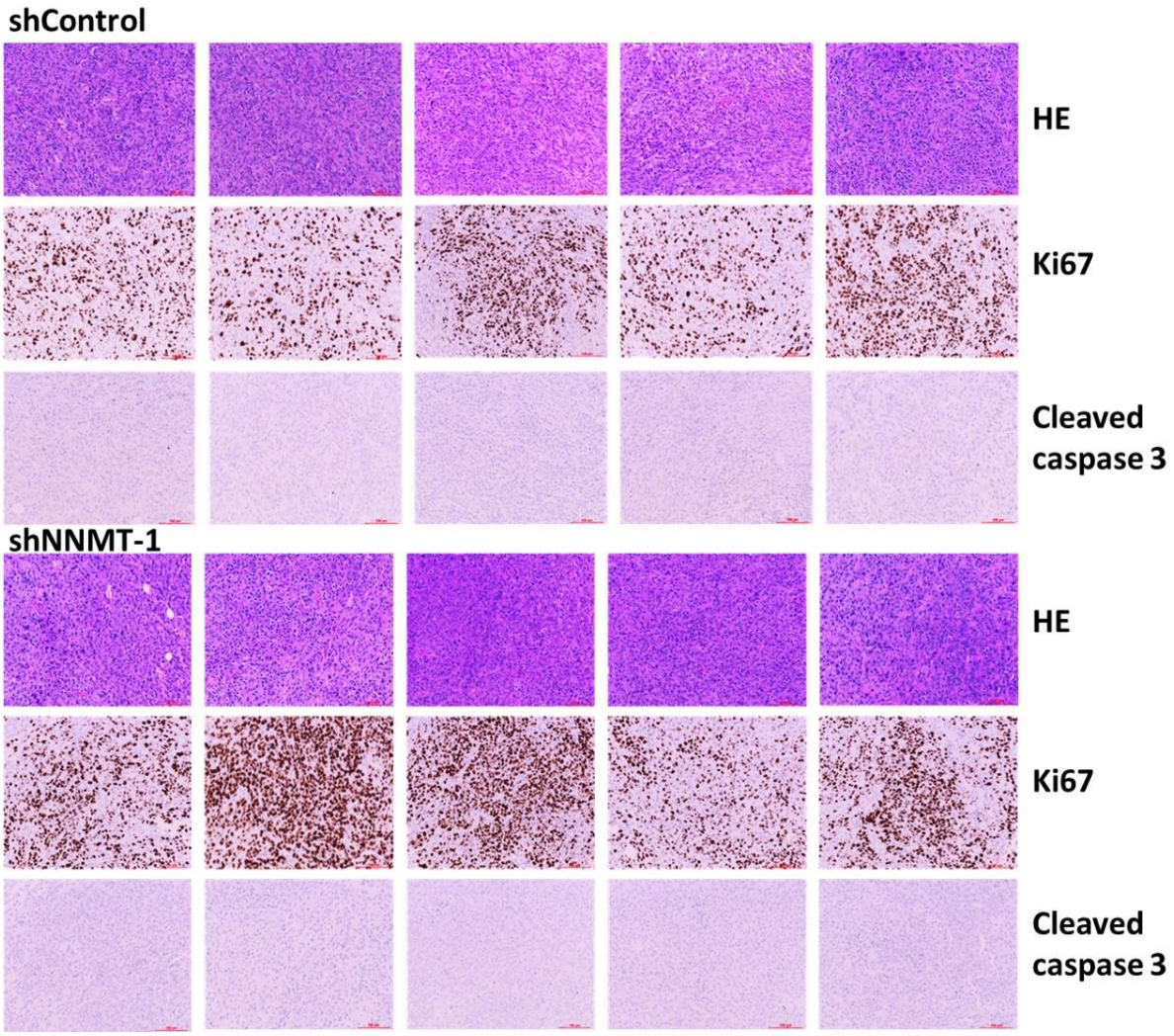

Figure 4.14. H&E, Ki67 and cleaved caspase 3 staining on NNMT-expressing and NNMT-depleted SUM159PT primary tumors. Each column is an individual tumor.

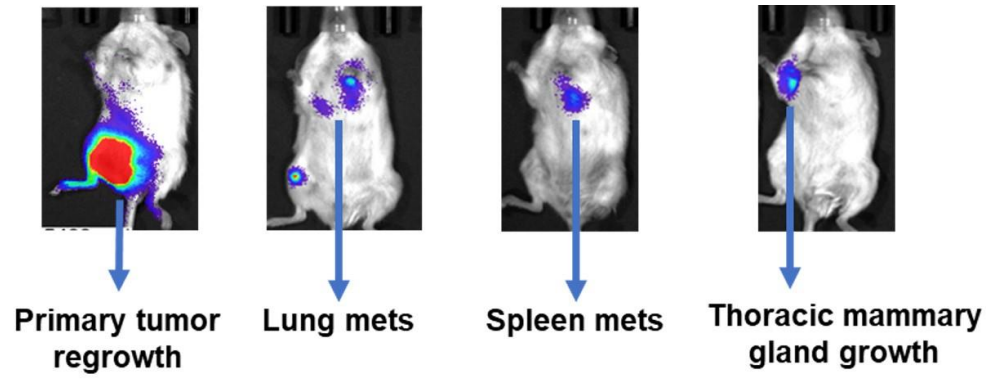

Figure 4.15. Bioluminescence imaging of post-surgical NSG mice demonstrating Luciferase signal emanating from metastatic SUM159PT cells.

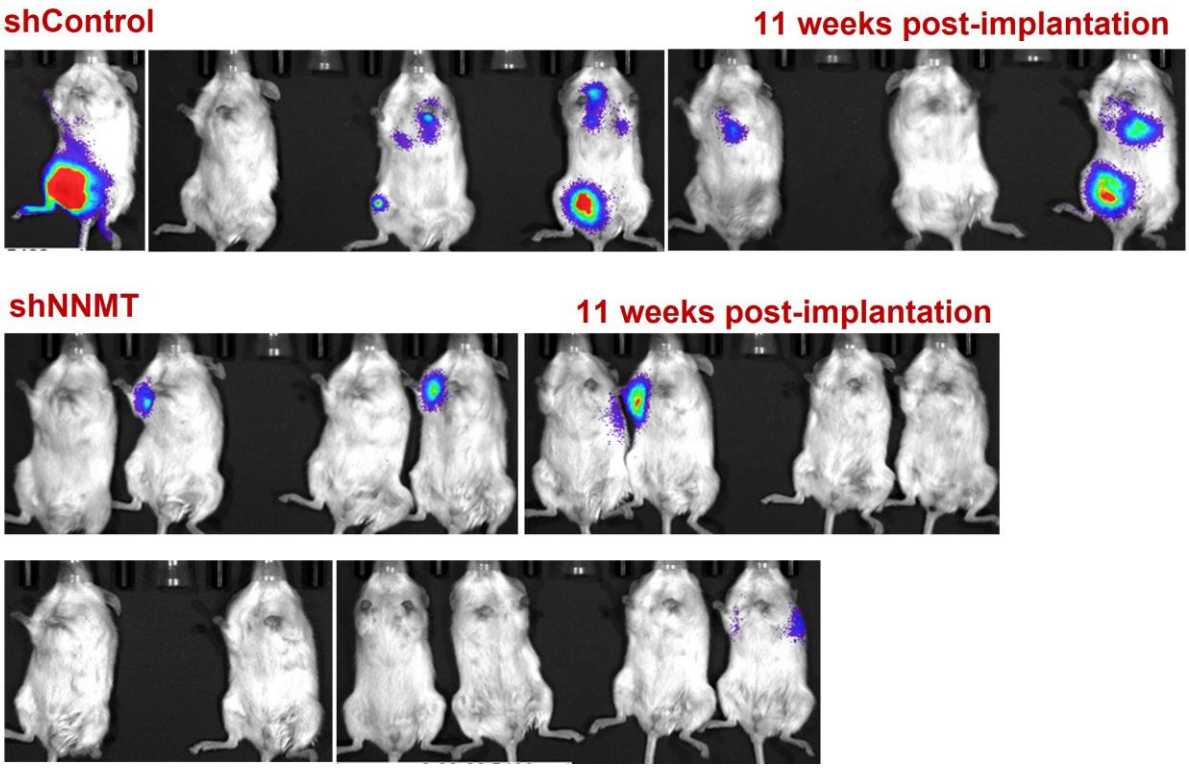

Figure 4.16. Bioluminescence imaging of post-surgical NSG mice demonstrating Luciferase signal emanating from metastatic SUM159PT cells. 11 weeks post-implantation, 2/15 mice in the shControl group lacked Luciferease signal, suggesting that they were metastasis free. In contrast, 9/16 mice in the shNNMT group lacked Luciferese signal, suggesting that they were metastasis free.

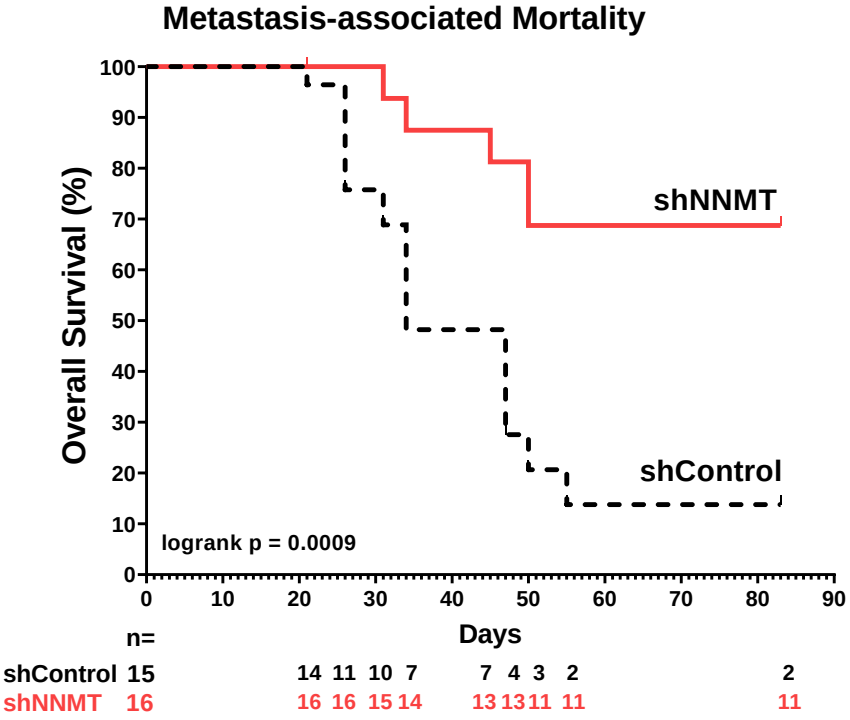

Figure 4.17. SUM159PT primary tumor NNMT expression is associated with a significantly worse probability of overall survival due to metastasis-associated mortality. *Day 0 is the final day that primary tumor surgeries were performed.*

4.3 Discussion

MDA-MB-231 xenograft primary tumor NNMT expression is associated with increased probability of overall metastasis formation (peritoneal, lung and liver), and increased probability of peritoneal metastasis-associated mortality. While lung and liver are TNBC metastatic cell targets in patients, TNBC primary tumor-induced peritoneal metastasis do not occur in women and is an artificial phenotype stemming from the mouse anatomy. The site of TNBC cell line implantation (inguinal mammary fat pad) is in direct contact with the peritoneum in mice, which is an anatomical characteristic not applicable to the human female anatomy. NNMT-expressing MDA-MB-231 primary tumors cells with enhanced invasive capability due to increased expression of invasion/EMT genes would have the physical opportunity to invade through the peritoneum and then passively spread into the entire abdominal cavity in a mouse. While NNMT-associated peritoneal metastasis is an artificial phenotype created by the mouse anatomy, it can still be concluded that NNMT expression in primary tumor cells is associated with increased invasiveness since only NNMT-expressing MDA-MB-231 primary tumor cells were able to invade through the peritoneum and into the abdomen. Importantly, SUM159PT xenograft primary tumor NNMT expression is also associated with increased probability of metastasis formation and increased probability of metastasis-associated mortality mostly due to formation of extensive lung metastasis or large thoracic mammary gland tumors. These findings altogether implicate NNMT as a metastasis-promoting protein in TNBC.

Furthermore, NNMT-depletion associated decrease in metastasis formation is not due to decreased primary tumor cell viability as both NNMT-expressing and NNMT-depleted MDA-MB-231 and SUM159PT tumors were non-apoptotic, suggesting that NNMT may promote enhanced TNBC cell metastatic potential by invasion/EMT gene expression-induced upregulation of

invasive capacity of primary tumor cells. I hypothesize that constitutive SAM depletion in high NNMT-expressing TNBC cells result in global DNA and/or histone hypomethylation and associated constitutive overexpression of genes that had possessed transcriptionally repressive DNA and/or histone methylation at their regulatory regions. Some of these genes upregulated downstream of NNMT-induced SAM depletion and repressive DNA/histone methylation depletion may happen to be master regulator genes that promote EMT such as *SNAI2* and genes that promote angiogenesis such as *HIF1A* (Figure 4.18). Upregulated expression of other genes associated with EMT (i.e., *VIM*, *FN1*, *MMPs*) and angiogenesis (i.e., *VEGF*, *PDGF*) phenotypes may then be explained by the upregulated expression of their upstream regulators (i.e., *SNAI2*, *HIF1A*). Investigating these potential epigenetic gene expression regulation mechanisms downstream of NNMT-induced SAM depletion is beyond the scope of my dissertation research.

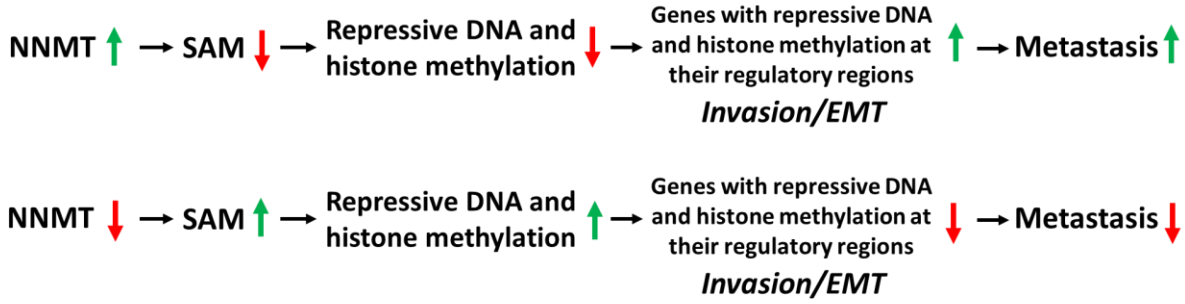

Figure 4.18. Working model of hypothesis.

CHAPTER 5

NNMT-ASSOCIATED TNBC ORGAN TROPISM PHENOTYPES

5.1 Introduction

Metastasis is a highly inefficient process with a minute percentage of CTCs arising from primary solid tumors having the ability to form distant organ metastases. The complete set of factors that contribute to primary tumor cell invasion, intravasation, survival in circulation, extravasation, homing and survival in the unique niches of distant organ microenvironments remains elusive. An intriguing observation regarding metastasis is that distinct tumor types have the proclivity to colonize specific organs, suggesting that the primary properties of metastatic cells arising from different tumor types may meet the microenvironmental demands of specific organs. Each metastatic site presents different metabolic challenges to a colonizing cancer cell, ranging from nutrient availability to oxidative stress, and unique metabolic adaptations have been shown in literature to dictate distant organ-specific metastatic colonization (reviewed in (47, 52)). For example, in one study, liver-metastatic breast cancer cells have been shown to exhibit a distinct metabolic program of increased glycolysis which was not observed in bone or lung-metastatic breast cancer cells (53).

Based on my NNMT-associated TNBC gene expression findings, I had hypothesized that NNMT-expressing TNBC cells may have enhanced metastatic potential *in vivo* due to increased expression of invasion and EMT-promoting genes which I addressed experimentally. I also had hypothesized that depleting NNMT in TNBC cells may decrease their overall metastatic capacity by downregulating the expression of invasion/EMT genes but may also influence their organ tropism by altering their metabolism through upregulating anabolic gene expression and giving

these cells unpredictable advantages in unique microenvironments of distant organs that put distinct metabolic demands on the invading metastatic cells. In this chapter of my dissertation, I will delineate novel and intriguing findings on NNMT-associated TNBC organ tropism phenotypes that I uncovered as a result of experiments outlined in the previous chapter.

5.2 Results

5.2.1 NNMT depletion in TNBC cells is associated with increased liver tropism.

NNMT expression in both the MDA-MB-231 and SUM159PT xenograft primary tumors was associated with increased probability of metastasis formation. Intriguingly, while there were a significantly lower number of mice with NNMT-depleted MDA-MB-231 primary tumors that developed metastasis, the ones that developed metastasis had extensive liver-specific metastasis, which did not occur in any of the mice that had NNMT-expressing MDA-MB-231 primary tumors, suggesting that NNMT depletion is associated with increased liver tropism of the MDA-MB-231 cell line (Figure 5.1). It is important to note that mice that had NNMT-expressing MDA-MB-231 tumors and developed peritoneal ascites were excluded from this comparison to only investigate NNMT-associated mechanisms contributing to hematogenous metastatic cell spread and tropism, as hematogenous spread is the primary route of cancer cell spread in humans and cancer cells in peritoneal ascites would passively spread to abdominal organs (Figure 5.1).

MDA-MB-231 primary tumor NNMT depletion-induced enhanced liver tropism phenotype is reproducible as it was also observed in a previous independent experiment (Figure 5.2). The design of this *in vivo* experiment was identical to those outlined in chapter 4 with the exception that I did not remove the inguinal mammary fat pads during primary tumor removal surgeries. This experiment was the first iteration of the *in vivo* metastasis experiments, and I was not aware that the primary tumor cells infiltrating the inguinal mammary fat pad would result in

primary tumor regrowth in a majority of the mice following surgery. Even though differences in overall metastasis formation between NNMT-expressing and NNMT-depleted experimental conditions were not observed in this experiment most likely due to infiltrated mammary glands contributing to NNMT-expressing and NNMT-depleted primary tumor regrowth and continued metastatic seeding, NNMT depletion-induced enhanced liver tropism phenotype was observed.

I then aimed to determine which steps of the metastatic cascade MDA-MB-231 primary tumor NNMT depletion may be contributing to that results in enhanced liver tropism. I had FFPE slides from the posterior surface of each liver from the experiment in Figure 5.2 stained for Luciferase expression with IHC to identify the MDA-MB-231 metastatic cells in those livers. I assumed that any liver-metastatic cell would had to have been alive to express Luciferase and get stained with IHC at the time I collected these livers and placed them in formalin. I then counted the number of individual metastatic cells, metastatic cell cluster less <200um in diameter, and metastatic nodules >200um in diameter in livers with shControl metastatic cells and in livers with shNNMT metastatic cells. Below is the information I aimed to gain from each count (Figure 5.3):

1) Number of individual metastatic cells would provide information on whether NNMT depletion affects the ability of the metastatic MDA-MB-231 to extravasate into the liver, home in the liver, and survive in the liver.

2) Number of metastatic cell clusters would provide information on whether phenotypic properties conferred to the individual metastatic MDA-MB-231 cells upon NNMT depletion would affect whether they enter quiescence or proliferation and grow into cluster in the liver microenvironment.

3) Number of metastatic nodules would provide information on whether phenotypic properties conferred to the metastatic MDA-MB-231 cells upon NNMT depletion affect

their capacity for continuous growth in the liver microenvironment.

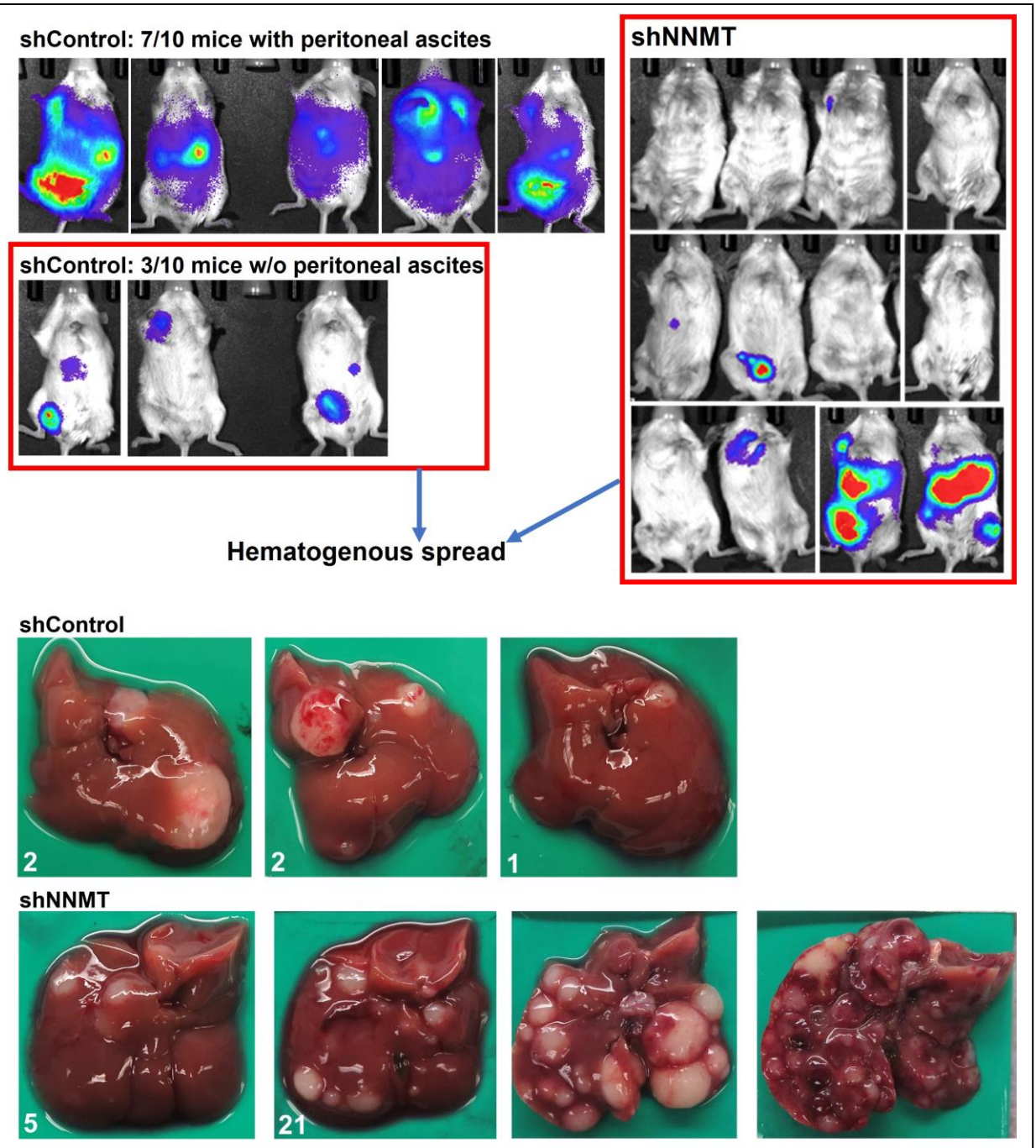

Figure 5.1. Livers of mice euthanized 8.5 weeks post-implantation with MDA-MB-231 cells (shControl or shNNMT-1). Livers of mice that had NNMT-depleted primary tumors had a significantly higher metastatic burden compared to livers of mice that had NNMT-expressing primary tumors and did not develop peritoneal ascites. *Numbers at the bottom left corner of each liver image denote the total number of metastatic nodules that was counted by eye on both surfaces of the liver. Two livers without these numbers were completely covered in metastatic nodules such that it was not possible to enumerate the number of metastatic nodules.*

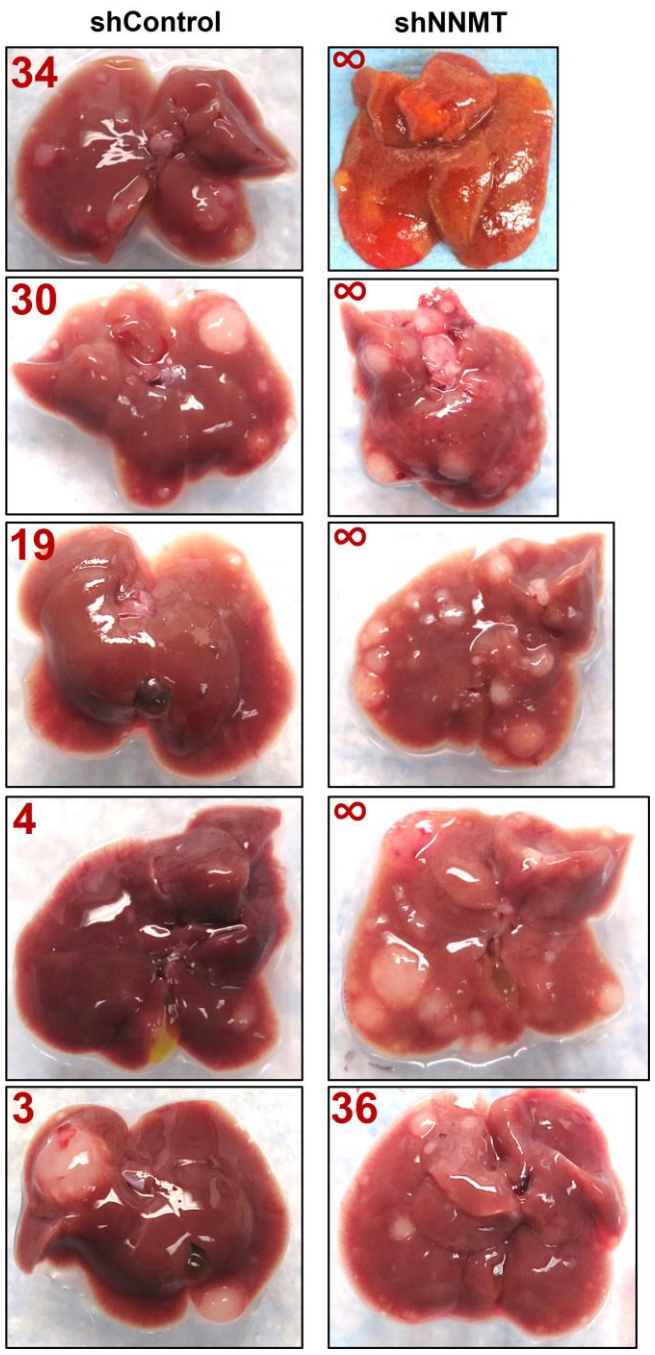

Figure 5.2. Photographs of all livers with visible metastatic nodules collected from mice without peritoneal ascites and euthanized 8 weeks post-implantation with MDA-MB-231 cells (shControl or shNNMT-1). *Numbers at the top left corner of each liver image denote the total number of metastatic nodules that was counted by eye on both surfaces of the liver. Livers with the infinity sign were completely covered in metastatic nodules such that it was not possible to enumerate the number of metastatic nodules.*

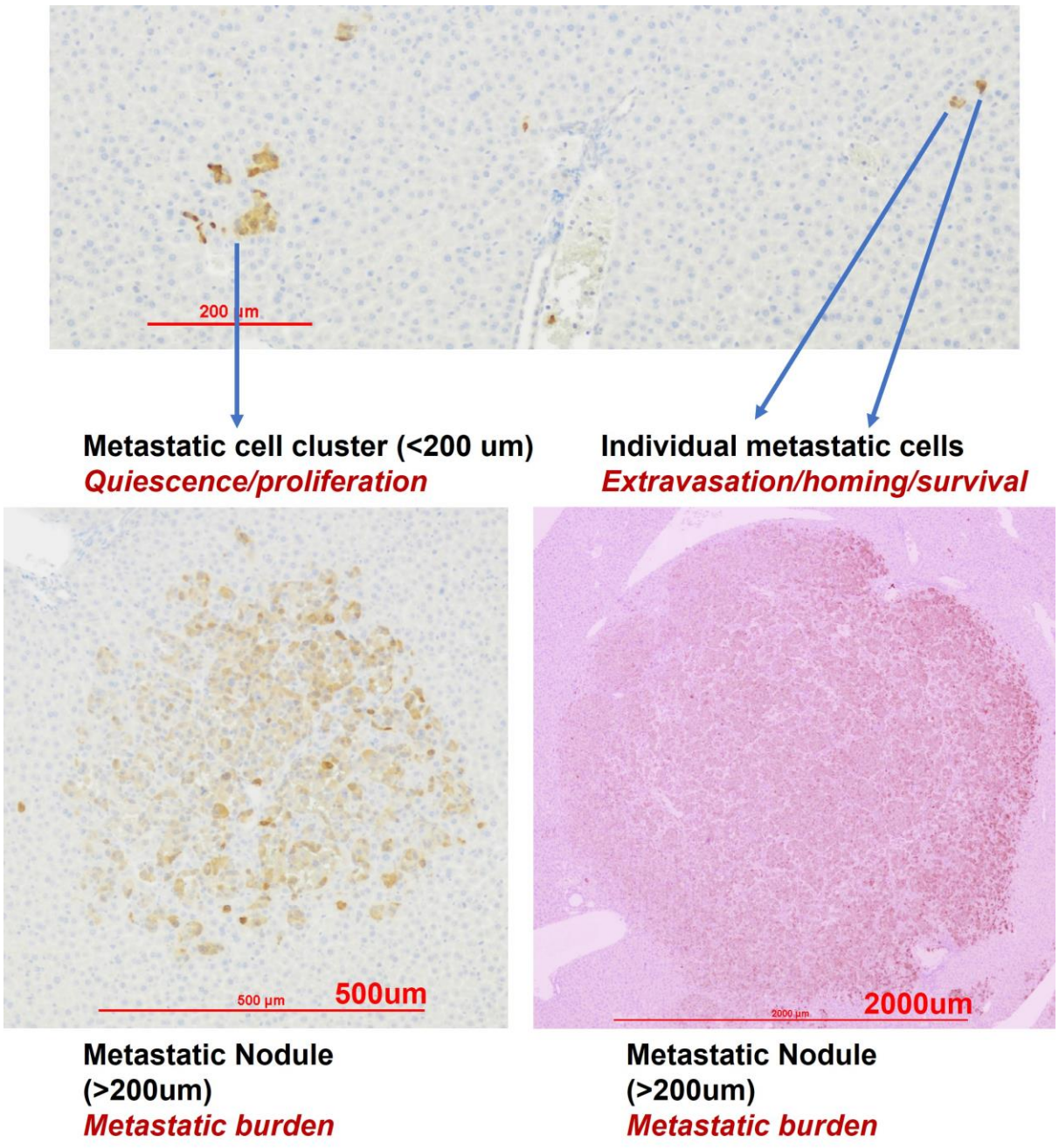

Figure 5.3. Representative Luciferase IHC images of livers with metastatic MDA-MB-231 cells, clusters and nodules and the type of information quantifying each of them would provide regarding which steps of the metastatic cascade MDA-MB-231 primary tumor NNMT depletion may be contributing to that results in enhanced liver tropism.

By counting the number of individual metastatic cells, metastatic cell cluster less <200um in diameter, and metastatic nodules >200um in diameter in livers with shControl metastatic cells and in livers with shNNMT metastatic cells (Figure 5.4), I determined that NNMT depletion in the MDA-MB-231 primary tumor cells

1) is not associated with their ability to extravasate/home/survive in the liver microenvironment as the number of individual shControl and shNNMT metastatic cells in these livers are not significantly different.

2) is associated with increased proclivity towards proliferation upon arrival in the liver microenvironment as there is a significantly higher number of shNNMT metastatic cell clusters compared to shControl metastatic cell clusters.

3) is associated with increased proclivity towards continuous growth in the liver microenvironment as there is a significantly higher number of shNNMT metastastic nodules compares to shControl metastatic nodules.

In summary, NNMT depletion in the MDA-MB-231 primary tumors is associated with decreased probability of metastasis formation in association with decreased invasion/EMT gene expression and increased liver tropism in association with increased proclivity towards proliferation and continued growth into metastatic modules upon arrival in the liver microenvironment.

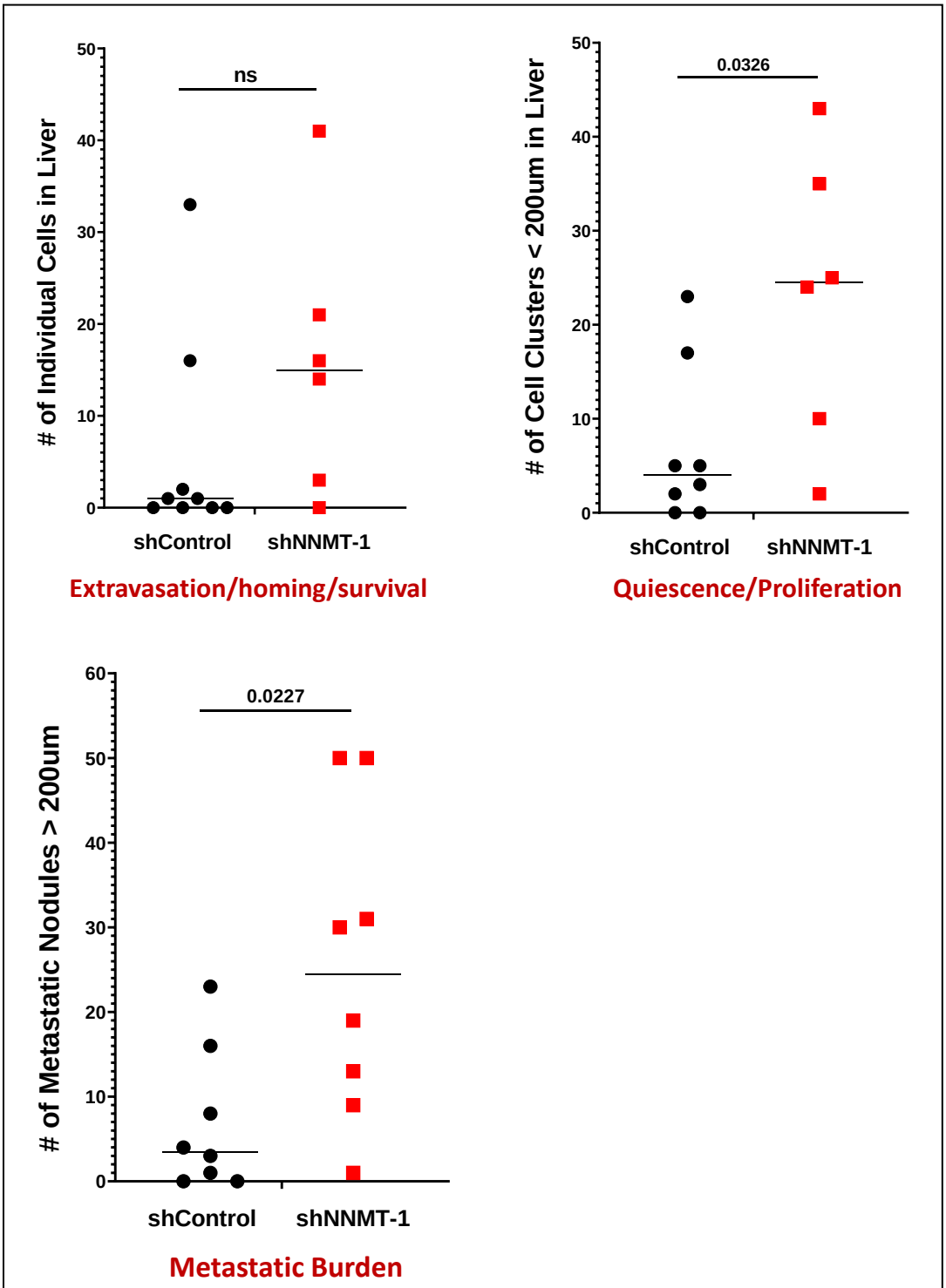

Figure 5.4. Number of individual metastatic cells, metastatic cell clusters, and metastatic nodules in livers of mice that had NNMT-expressing or NNMT-depleted MDA-MB-231 primary tumors.

5.3 Discussion

My research findings implicate that NNMT expression in TNBC cells increases their metastasis-forming efficiency. Multiple decades of research on primary tumor progression have shown that molecular mechanisms that promote angiogenesis and EMT phenotypes (i.e., motility) contribute to primary tumor cell invasion and overall metastatic potential (reviewed in (45, 46)). It is therefore conceivable that NNMT-associated increase in the expression of important upstream promoters of angiogenesis and EMT such as HIF1A and SNAI2 may underlie the NNMT-associated enhancement in the metastasis formation ability of the TNBC cell lines by allowing them to become invasive, exit the primary tumor site and enter circulation.

Interestingly, decreasing the overall metastasis-forming efficiency of NNMT-expressing primary tumor cells of TNBC cell lines by NNMT depletion was not a straightforward metastasis prevention strategy in my *in vivo* experimental models. While NNMT depletion in the SUM159PT xenograft primary tumors rendered a significant majority of shNNMT tumor-bearing mice metastasis free until the end of study, NNMT depletion in the MDA-MB-231 xenograft primary tumors had an undesired side effect of increased liver tropism, suggesting that an additional molecular mechanism(s) contributing to NNMT-depleted MDA-MB-231 cell liver tropism needs to be targeted along with NNMT in the primary tumors to effectively decrease overall metastasis formation.

Furthermore, the fact that I observed the NNMT depletion-induced enhanced liver tropism phenotype only with the MDA-MB-231 cell line opens up a discussion on whether this phenotype is a cell line specific phenomenon and therefore not generalizable to TNBC patient tumor biology. While this is plausible, it can also be debated that the possibility of this phenotype occurring even in a minute portion of TNBC patient primary tumor cells with a biology similar to that of the

MDA-MB-231 cell line would be enough to create unwanted liver metastases in patients upon NNMT inhibition in the TNBC primary tumors as a metastasis prevention treatment strategy. Investigation of the molecular mechanisms contributing to NNMT depletion-induced enhanced liver tropism is therefore warranted.

CHAPTER 6

MOLECULAR MECHANISMS POTENTIALLY UNDERLYING NNMT DEPLETION-ASSOCIATED TNBC LIVER TROPISM

6.1 Introduction

Despite significant developments in our understanding of cancer biology and improvements in primary tumor treatment over the last couple of decades, metastasis still is the most lethal feature of cancer and remains as a major obstacle to improving clinical outcomes of cancer patients. Clinically overt metastases of solid tumors remain incurable, which highlights the importance of uncovering molecular mechanisms that contribute to each step of the metastatic cascade for the development of effective metastasis prevention strategies. Distant organ colonization is the most understudied step of the metastatic cascade due to limitations in experimental models that enable investigation of the molecular interactions between a single metastatic cell and the evolving host organ microenvironment that result in metastatic cell viability or death, and quiescence or outgrowth (reviewed in (54). Metastatic cells of the primary tumor need to possess an intrinsic phenotypic state that can meet the unique demands posed by the microenvironment of the host organ they are colonizing.

Due to the presence of a wide array of distinct niches in each host organ that are in an ever-changing state in response to environmental stimuli and due to the large number unique phenotypic states possessed by individual metastatic cells, conceivably innumerable combinations of metastatic cell-intrinsic and host organ-intrinsic phenotypic states can complement each other that result in colonizing metastatic cell survival and outgrowth. This opens up a discussion on whether distant organ colonization can ever become a practical clinical target for metastasis prevention as

a large multitude of molecular mechanisms underlying organ colonization cannot be individually pharmacologically targeted in a patient without introducing lethal off-target toxicity. Therefore, the current desire in modern cancer research is to push the limits of experimental models and technology to continue identifying molecular mechanisms underlying colonizing metastatic cell survival, quiescence, and outgrowth for all combinations of primary tumor types and host organs such that we can begin to understand whether there are a smaller number of essential molecular mechanisms underlying organ tropism that are indispensable across multiple solid tumor types and host organs. If there are molecular mechanisms that commonly promote the metastatic cell survival, escape from quiescence, and entrance into proliferation of multiple primary solid tumor types in multiple host organs, then it may be feasible to pharmacologically target these smaller number of molecular mechanisms in large groups of cancer patients to either kill the colonizing cells entirely or perpetually lock them in quiescence such that they never become proliferative and go on to form incurable overt metastases.

There is accumulating evidence demonstrating that unique metabolic adaptations of metastatic cells dictate distant organ-specific metastatic colonization. For example, liver-metastatic breast cancer cells have been shown to exhibit a distinct metabolic program of increased glycolysis which was not observed in bone or lung-metastatic breast cancer cells (53). In another study, brain metastases originating from a wide array of primary tumors including breast cancer have been shown to efficiently oxidize the locally available acetate as an energy source (55). Because NNMT depletion increases anabolic gene expression in both MDA-MB-231 and SUM159PT cell lines and because NNMT depletion in the MDA-MB-231 primary tumors is associated with increased proclivity towards proliferation and continued growth into metastatic modules in the liver microenvironment, I dedicated the final chapter of my dissertation to

investigating the potential NNMT depletion-induced metabolic mechanisms contributing to increased MDA-MB-231 metastatic potential in the unique liver metabolic microenvironment.

6.2 Results

6.2.1 Comparison of gene expression in NNMT-expressing and NNMT-depleted MDA-MB-231 xenograft primary tumors and liver metastatic nodules.

To gain insight into the potential NNMT depletion-induced mechanisms contributing to increased MDA-MB-231 metastatic potential in the liver, I compared gene expression via RNAseq in NNMT-expressing and NNMT-depleted MDA-MB-231 liver metastatic nodules shown in Figure 5.1 and their primary tumors. I first determined with principal component analysis (PCA) that NNMT-expressing tumors and their liver metastatic nodules, and NNMT-depleted tumors and their liver metastatic nodules form four distinct groups based on their gene expression patterns (Figure 6.1). According to PCA, primary tumors are distinctly separated into two groups based on whether they express NNMT, suggesting that NNMT expression level was the primary determinant of primary tumor gene expression. Liver metastatic nodules of NNMT-expressing and NNMT-depleted tumors are also separated into two groups based on whether their primary tumors express NNMT; however, they are not tightly grouped together as the primary tumors, suggesting that both NNMT expression level and the liver microenvironment where these individual nodules existed were determinants of metastatic nodule gene expression.

I then investigated NNMT mRNA expression in shControl tumors and shControl liver metastatic nodules, and shNNMT tumors and shNNMT liver metastatic nodules. First, I confirmed that NNMT expression was successfully downregulated in shNNMT tumors and shNNMT liver metastatic nodules compared to shControl tumors (Figure 6.2). Interestingly, I observed that

NNMT expression was also downregulated in shControl liver metastatic nodules compared to shControl tumors, suggesting that NNMT depletion is selected for in the MDA-MB-231 metastatic cells colonizing the liver and may provide a survival and/or growth advantage in the liver microenvironment (Figure 6.2).

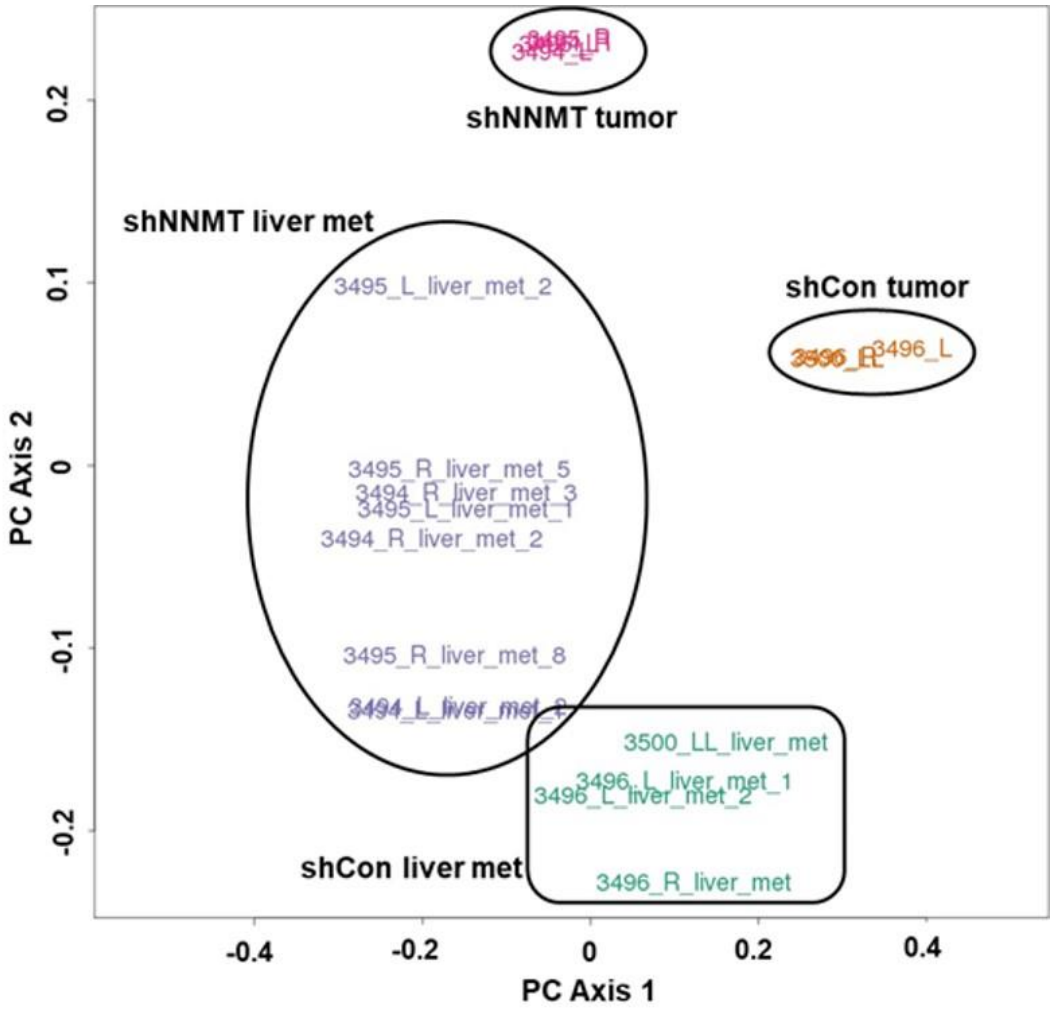

Figure 6.1. Principal component (PC) analysis on the RNAseq-based gene expression of MDA-MB-231 NNMT-expressing tumors (shCon tumor, n=3) and their liver metastatic nodules (shCon liver met, n=4), and NNMT-depleted tumors (shNNMT tumor, n = 4) and their liver metastatic nodules (shNNMT liver met, n=8).

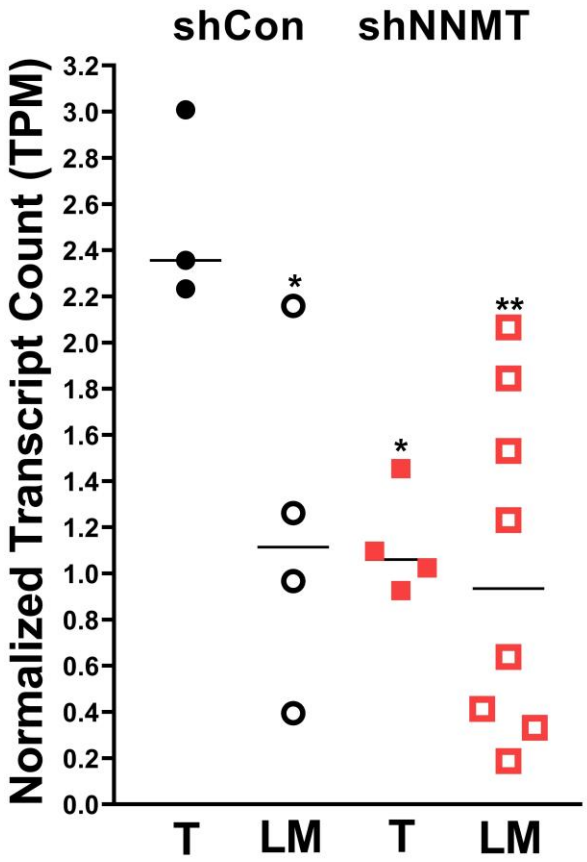

Figure 6.2. Normalized RNAseq *NNMT* mRNA expression (transcripts per million) in MDA-MB-231 NNMT-expressing tumors (shCon tumor) and their liver metastatic nodules (shCon liver met), and NNMT-depleted tumors (shNNMT tumor) and their liver metastatic nodules (shNNMT liver met). *T = primary tumor, LM = liver metastatic nodule, *p<0.05, **p<0.01.*

To begin to gain insight into potential molecular mechanisms contributing to MDA-MB-231 liver tropism, I identified IPA pathways enriched in DEGs in shControl liver metastatic nodules compared to shControl primary tumors to determine gene expression patterns that naturally arise in the metastatic MDA-MB-231 cells with an innate capacity for colonizing the liver (Figure 6.3). In the IPA analysis, I observed that DEGs in shControl liver metastatic nodules compared to shControl primary tumor are mostly associated with IPA pathways whose activation levels are predicted to be downregulated and that the pathways predicted to have the lowest level of activation are related to fibrosis that results in excessive ECM deposition into the stroma of an

organ. In other words, MDA-MB-231 liver metastatic nodules are enriched for downregulated expression of ECM components (i.e., collagens) and ECM remodeling enzymes (i.e., MMPs) compared to shControl primary tumors. Importantly, one study that characterized the transcriptional landscape of breast cancer metastases compared to primary tumors determined that liver metastases displayed unique transcriptional profiles enriched in downregulation of ECM component genes (i.e., collagen), suggesting that ECM gene downregulation in BC metastatic cells is of biological significance and potentially provides a survival and/or growth advantage in the liver microenvironment (56). Also importantly, I determined that DEGs in shNNMT primary tumors compared to shControl primary tumors are also associated with the IPA pathways whose activation levels are predicted to be downregulated by the DEGs in shControl liver metastatic nodules compared to shControl primary tumors (i.e., downregulated fibrosis (ECM) genes). These findings demonstrate that NNMT depletion in the primary tumors mimics gene expression patterns that naturally arise in the shControl MDA-MB-231 metastatic cells (i.e., downregulated ECM genes) with an innate capacity for colonizing the liver, which potentially contributes to NNMT depletion-induced enhanced liver tropism of MDA-MB-231 cells (Figure 6.4).

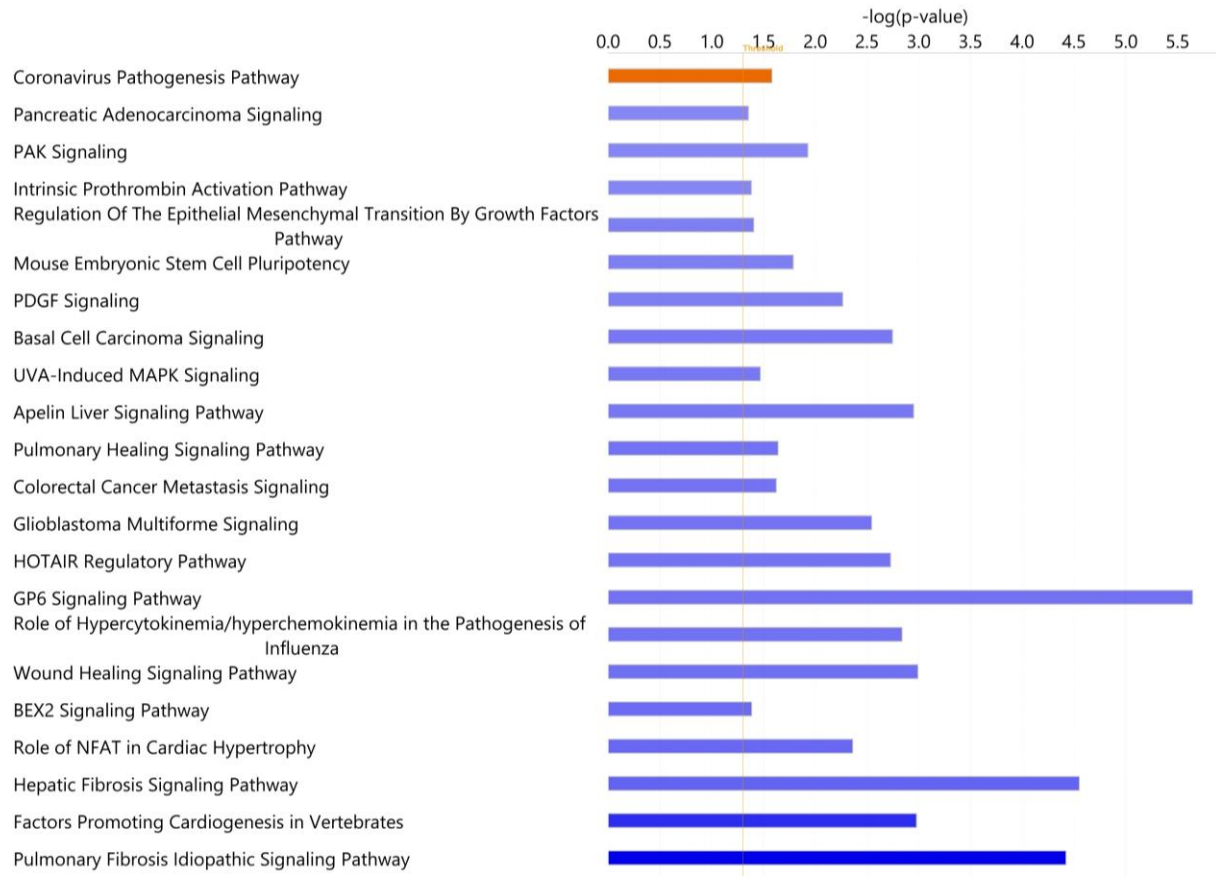

Figure 6.3. IPA canonical pathways whose activation levels are predicted to be upregulated (orange) or downregulated (blue) in association with DEGs in MDA-MB-231 shControl liver metastatic nodules compared to shControl primary tumors. *Activation score -log(p-value) > 1.3.*

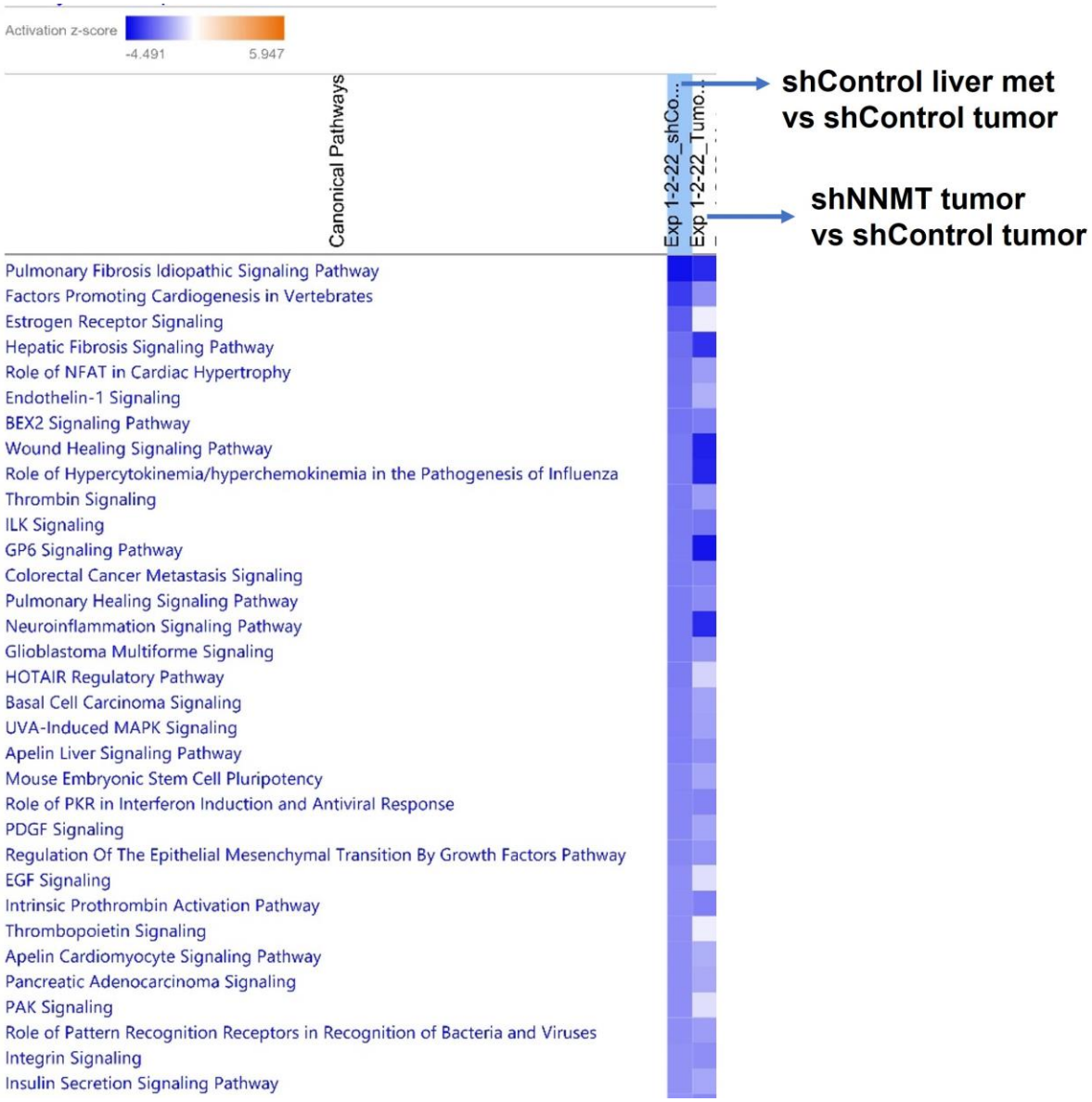

Figure 6.4. IPA canonical pathways whose activation levels are predicted to be upregulated (orange) or downregulated (blue) in association with 1) DEGs in MDA-MB-231 shControl liver metastatic nodules compared to shControl tumors, and 2) DEGs in MDA-MB-231 shNNMT tumors compared to shControl tumors. *Activation score -log(p-value) > 1.3.*

Liver is composed of functional units called lobules (Figure 6.5), and liver lobules are composed of various cell types that perform liver's vital metabolic functions (i.e., gluconeogenesis and glucose output into circulation) (reviewed in (57)). Importantly, parenchyma of the liver lobules contains minimal ECM components (i.e., collagen) that is hypothesized to be an evolutionary advantageous trait facilitating free flow of macromolecules within the lobular structures as unobstructed substance exchange between hepatocytes and circulation within liver lobules is crucial for organismal homeostasis (reviewed in (58)). I therefore hypothesize that downregulated expression of ECM components is selected for in the control liver metastatic MDA-MB-231 cells to preserve the ECM-deficient stroma of the liver lobules and allow free flow of nutrients (i.e., glucose, glutamine) into the colonizing cells providing them a survival and/or proliferative advantage (Figure 6.5). Accordingly, NNMT-depleted MDA-MB-231 metastatic cells of the shNNMT primary tumors would arrive in the liver lobules already depleted of ECM component gene expression, which may contribute to their enhanced survival, proliferation and thereby tropism to the liver. These molecular mechanisms hypothetically contributing to NNMT depletion-induced enhanced liver tropism of MDA-MB-231 cells unfortunately cannot be experimentally tested as current experimental models and technology are not sufficient to investigate interactions between a single metastatic colonizing cell and the host organ microenvironment.

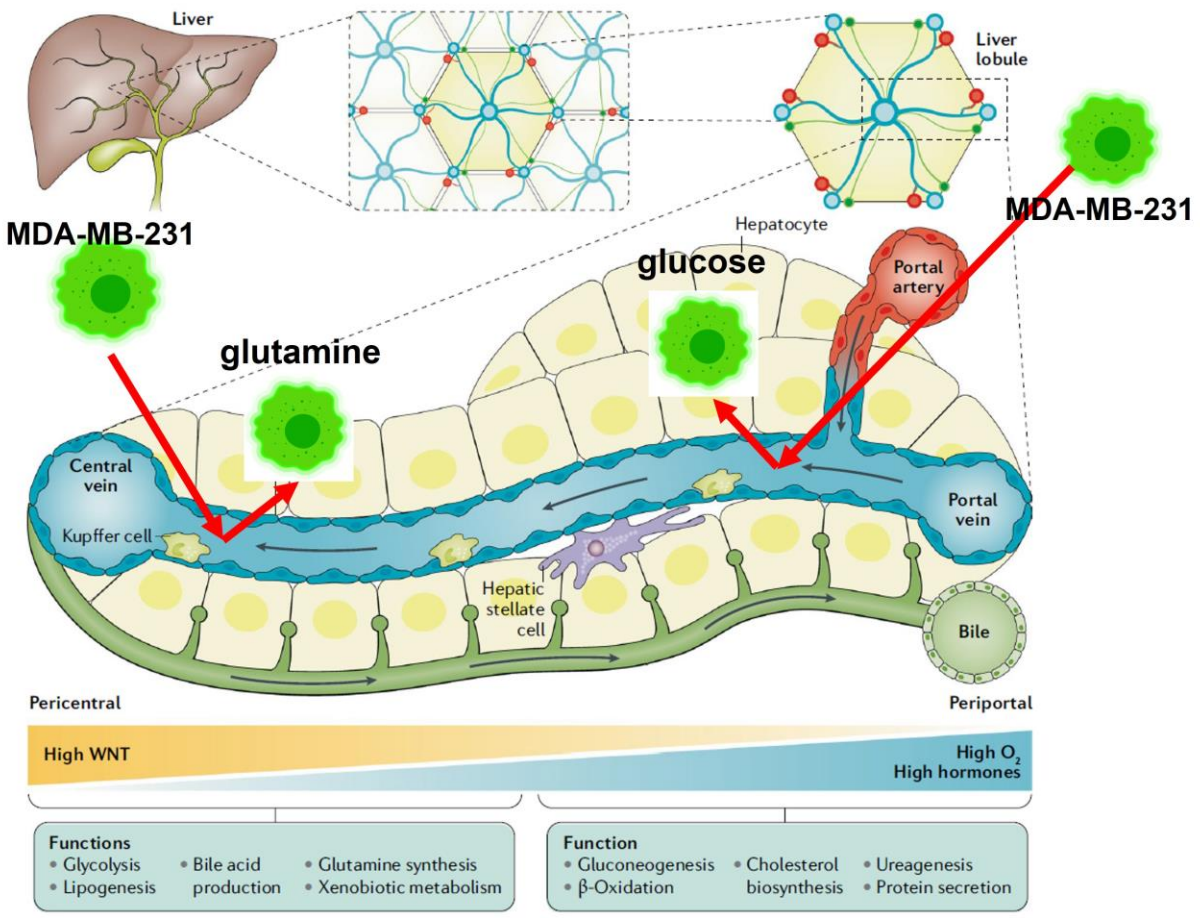

Figure 6.5. Liver lobule anatomy and hematogenous arrival routes for metastatic cells (Ben-Moshe et al., 2019).

6.2.2 Comparison of anabolic gene expression in NNMT-expressing and NNMT-depleted MDA-MB-231 xenograft primary tumors and liver metastatic nodules.

NNMT depletion in the MDA-MB-231 primary tumors is associated increased number of metastatic cell clusters in the liver, suggesting that molecular mechanisms downstream of NNMT depletion in the liver-colonizing MDA-MB-231 cells promote their escape from quiescence and entrance into proliferation in the liver microenvironment. While combination of a multitude of liver microenvironment-intrinsic and NNMT-depleted metastatic MDA-MB-231 cell-intrinsic molecular mechanisms may contribute to this phenotype, it is plausible that NNMT depletion-

induced ECM component downregulation in the metastatic MDA-MB-231 cells may be a major contributor to this phenotype as outlined in the previous section of this chapter. Importantly, NNMT depletion in the MDA-MB-231 primary tumors is also associated increased number of metastatic nodules in the liver, suggesting that additional combinations of liver microenvironment-intrinsic and NNMT-depleted metastatic MDA-MB-231 cell-intrinsic molecular mechanisms may contribute to outgrowth of metastatic cell clusters into overt metastatic nodules.

Because NNMT depletion in MDA-MB-231 cells is associated with upregulated anabolic gene expression, I hypothesized that the liver parenchyma with interstitial fluid enriched in hepatocyte-secreted glutamine and glucose may enhance anaplerosis (TCA cycle intermediate replenishment with glutamine or glucose uptake) in NNMT-depleted MDA-MB-231 liver metastatic cells and metastatic cell clusters, resulting in higher energy (ATP) and building block (i.e., Acetyl-CoA) production that can meet the demands of anabolism-induced cell growth. NNMT depletion-induced anabolic gene expression in MDA-MB-231 cells consists of upregulated expression of rate-limiting enzymes in *de novo* cholesterol synthesis and upregulation of a multitude of large and small ribosomal proteins. I first aimed to determine whether NNMT-depleted MDA-MB-231 primary tumors and metastatic nodules exhibit an anabolic phenotype in association with anabolic gene expression and began this investigation by focusing on *de novo* cholesterol synthesis.

De *novo* cholesterol synthesis (mevalonate pathway) uses Acetyl-CoA, NADPH and ATP to produce sterols including free cholesterol that is essential for plasma membrane structure and therefore cell growth and proliferation (reviewed in (59)). The production of Acetyl-CoA occurs following glucose, glutamine or acetate consumption which is then converted into mevalonic acid by the rate-limiting enzymes HMGCS1 and HMGCR followed by a series of enzymatic reactions

that produce mevalonate pathway intermediates such as lanosterol and eventually sterols such as free cholesterol (Figure 6.6). *HMGCS1* and *HMCGR* expression was upregulated in MDA-MB-231 shNNMT primary tumors compared to shControl primary tumors and downregulated in shNNMT liver metastatic nodules compared to shNNMT primary tumors (Figure 6.7). When excess free cholesterol accumulates intracellularly, HMGCS1 and HMGCR get downregulated in expression and activity in a negative feedback loop; I therefore hypothesized that NNMT-depleted primary tumors with upregulated *de novo* cholesterol synthesis gene expression could produce excess free cholesterol in the liver microenvironment such thatHMGCS1 and HMGCR expression got downregulated specifically in the shNNMT liver metastatic nodules.

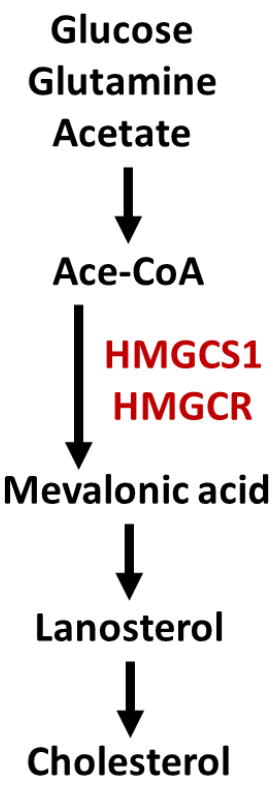

Figure 6.6. Overview of *de novo* cholesterol synthesis (mevalonate) pathway.

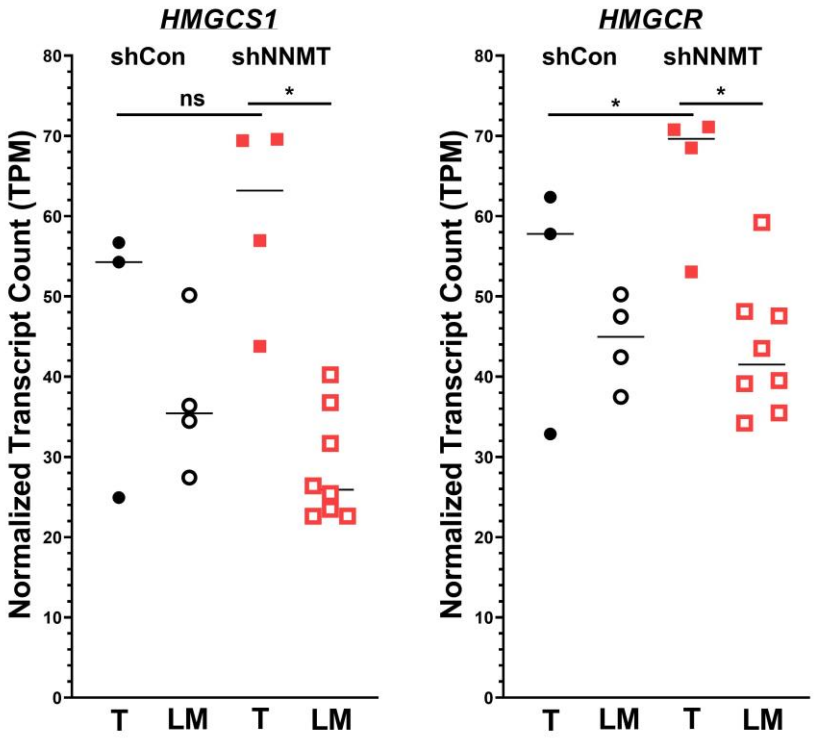

Figure 6.7. Normalized RNAseq *HMGCS1 and HMGCR* mRNA expression (transcripts per million) in MDA-MB-231 NNMT-expressing tumors (shCon tumor) and their liver metastatic nodules (shCon liver met), and NNMT-depleted tumors (shNNMT tumor) and their liver metastatic nodules (shNNMT liver met). *T = primary tumor, LM = liver metastatic nodule, *p<0.05.*

These results support a role for the liver microenvironment in sustaining NNMT depletion-induced anabolic metabolism in MDA-MB-231 metastatic cells. I then quantified free cholesterol along with *de novo* cholesterol synthesis intermediates with mass spectrometry in shControl and shNNMT primary tumors and liver metastatic nodules and determined that both shNNMT primary tumors and shNNMT liver metastatic nodules had significantly higher levels of intracellular free cholesterol compared to shControl primary tumors and liver metastatic nodules (Figure 6.8).

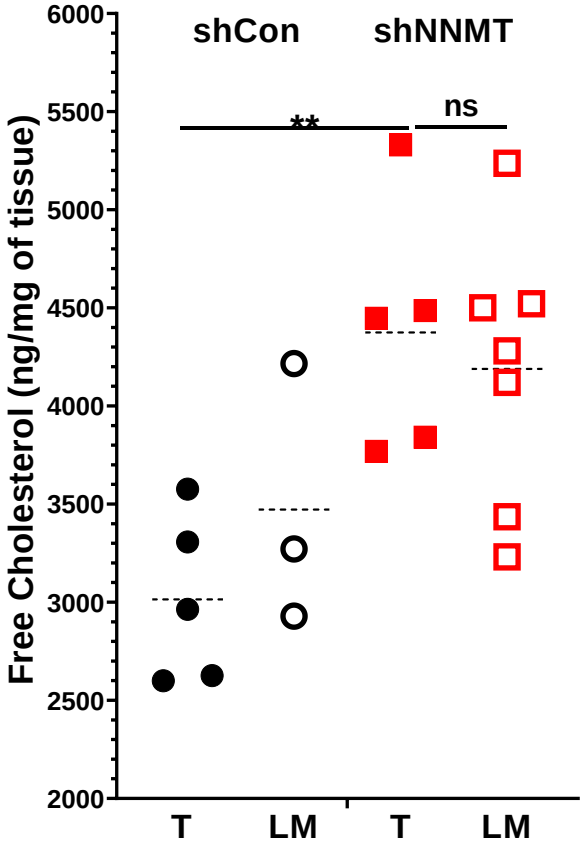

Figure 6.8. Intracellular free cholesterol quantification with mass spectrometry in MDA-MB-231 NNMT-expressing tumors (shCon tumor) and their liver metastatic nodules (shCon liver met), and NNMT-depleted tumors (shNNMT tumor) and their liver metastatic nodules (shNNMT liver met). *T = primary tumor, LM = liver metastatic nodule, *p<0.05, **p<0.01*

The fact that shNNMT liver metastatic nodules had intracellular free cholesterol levels similar to that of shNNMT tumors even though shNNMT liver metastatic nodules had downregulated *HMGCS1* and *HMCGR* expression compared to shNNMT tumors supports the hypothesis that metastatic cells of NNMT-depleted primary tumors with upregulated *HMGCS1* and *HMGCR* expression were able to produce excess free cholesterol specifically in the liver microenvironment such that *HMGCS1* and *HMGCR* expression got downregulated in a negative feedback loop as the metastatic cells proliferated into clusters and eventually nodules that were collected for RNAseq and lipidomics (Figure 6.9).

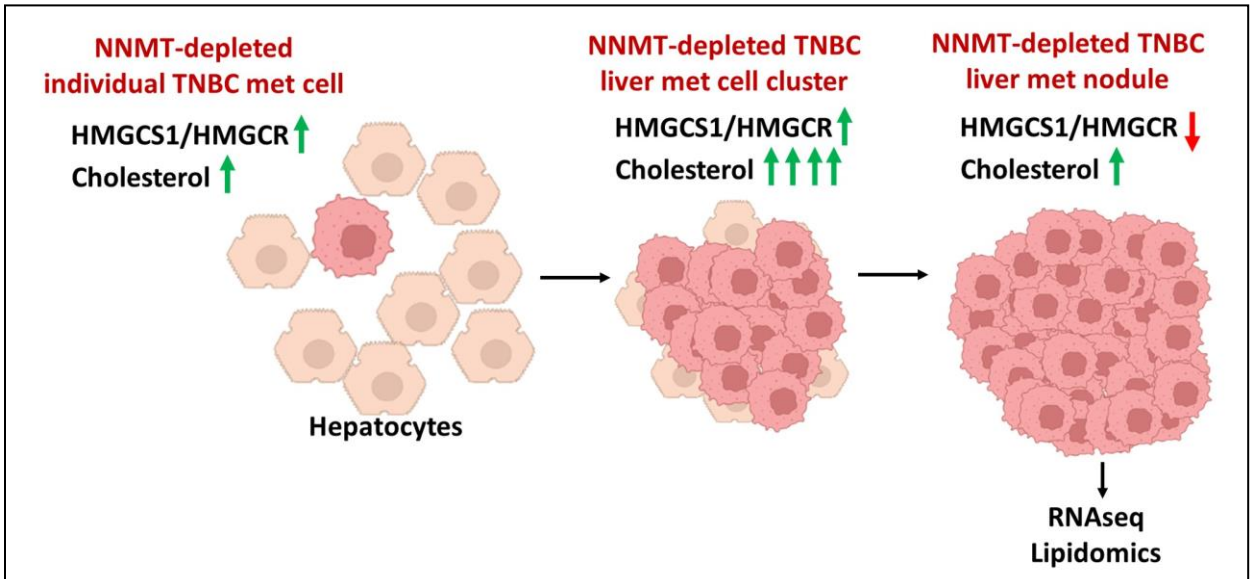

Figure 6.9. Pictorial explanation of interpretation of the data figures 6.7 and 6.8.

After determining that NNMT depletion in the MDA-MB-231 primary tumors and liver metastatic nodules is associated with increased intracellular free cholesterol, I determined that *de novo* cholesterol synthesis-specific intermediates (lanosterol, FF-MAS, T-MAS) are also upregulated in the MDA-MB-231 primary tumors and liver metastatic nodules compared to control tumors and metastatic nodules, suggesting that NNMT depletion upregulates intracellular free cholesterol by increasing *de novo* cholesterol synthesis (Figure 6.10).

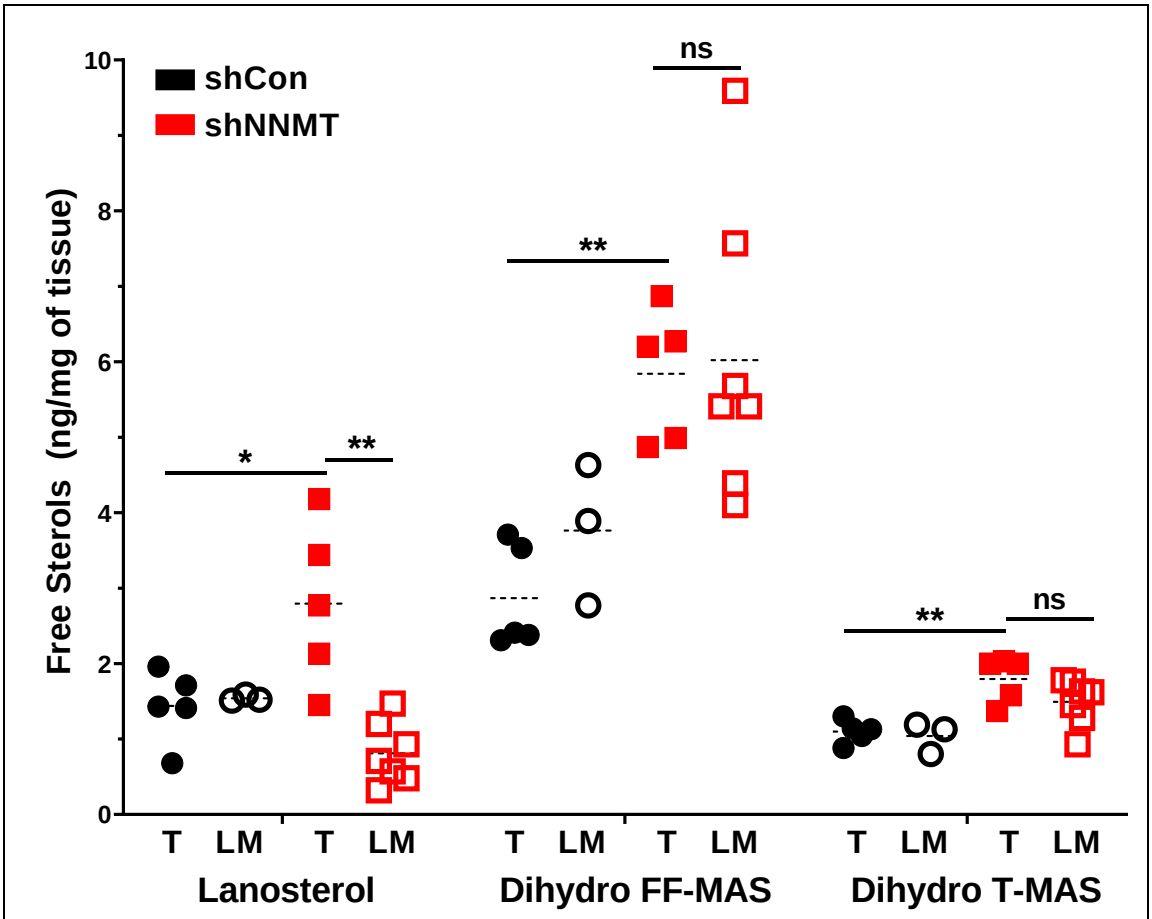

Figure 6.10. Intracellular *de novo* cholesterol synthesis intermediate quantification with mass spectrometry in MDA-MB-231 NNMT-expressing tumors (shCon tumor) and their liver metastatic nodules (shCon liver met), and NNMT-depleted tumors (shNNMT tumor) and their liver metastatic nodules (shNNMT liver met). *T = primary tumor, LM = liver metastatic nodule, *p<0.05, **p<0.01*

Because NNMT depletion in MDA-MB-231 cells is associated with upregulated anabolic gene expression, I had hypothesized that the liver parenchyma with interstitial fluid enriched in hepatocyte-secreted glutamine and glucose may enhance anaplerosis (TCA cycle intermediate replenishment with glutamine or glucose uptake) in NNMT-depleted MDA-MB-231 liver metastatic cells and metastatic cell clusters, resulting in higher energy (ATP) and building block (i.e., Acetyl-CoA) production that can meet the demands of anabolism-induced cell growth. Data in Figure 6.10 regarding intracellular lanosterol, FF-MAS and T-MAS levels in NNMT-depleted tumors vs their metastatic nodules strongly support this hypothesis. Lanosterol, FF-MAS and T-

MAS are consecutive intermediates, meaning that FF-MAS is synthesized directly from lanosterol, and T-MAS is directly synthesized from FF-MAS. Importantly, shNNMT liver metastatic nodules had a significantly lower steady-state level of lanosterol compared to shNNMT tumors; however, even with a lower lanosterol level, shNNMT metastatic nodules had intracellular FF-MAS and T-MAS levels similar to that of shNNMT tumors. The most plausible explanation of this finding is that lanosterol in the shNNMT liver metastatic nodules has a lower steady-state level, but higher turnover rate compared to lanosterol in the shNNMT tumors. Furthermore, increased lanosterol turnover rate in the shNNMT liver metastatic nodules that can sustain elevated FF-MAS and T-MAS synthesis can be achieved by enhanced metastatic MDA-MB-231 cell anaplerosis in the liver parenchyma with interstitial fluid enriched in hepatocyte-secreted glutamine and glucose; increased glucose/glutamine uptake-mediated anaplerosis would result in increased Acetyl-CoA synthesis that can increase the rate at which used up lanosterol molecules are replaced with new lanosterol molecules to sustain elevated FF-MAS and T-MAS synthesis.

Based on the research findings so far, below is my working model of hypothesis to explain NNMT depletion-induced enhanced liver tropism of MDA-MB-231 cells (Figure 6.11):

1) NNMT-depleted metastatic MDA-MB-231 cells with downregulated ECM component gene expression deposit minimal ECM (i.e., collagen) into the liver parenchyma upon arrival via liver circulation, which preserves the integrity and functionality of the liver microenvironment (i.e., free flow of macromolecules in the liver lobules).

2) Preservation of the liver microenvironment (ME) facilitates increased glucose and/or glutamine uptake by the NNMT-depleted MDA-MB-231 metastatic cells as hepatocytes in the liver lobular structures synthesize and secrete glucose and glutamine

into the surrounding interstitial fluid that is then directly accessible to the colonizing cancer cells. Increased nutrient uptake facilitates proliferation of the metastatic cells into cell clusters.

3) Increased glucose and/or glutamine uptake also supports anaplerosis (replenishment of TCA cycle intermediates), resulting in increased ATP and building block (i.e., Acetyl-CoA for *de novo* cholesterol synthesis) synthesis.

4) Enhanced ATP and building block synthesis sustains anabolic pathways including *de novo* cholesterol synthesis and rapid growth of metastatic cells and clusters into metastatic nodules.

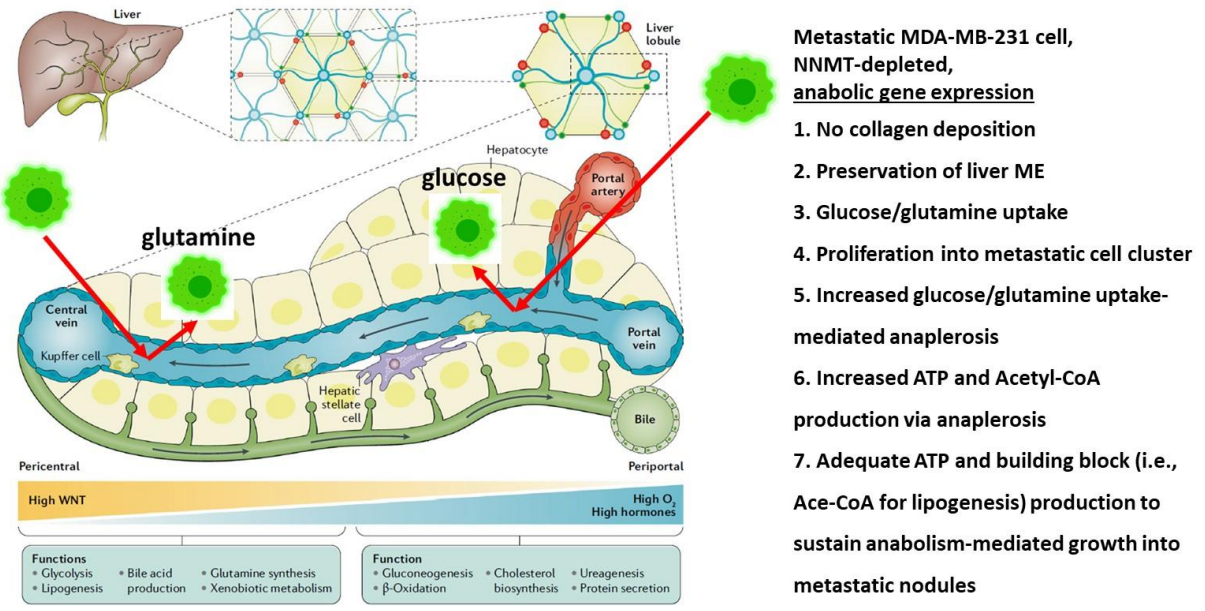

Figure 6.11. Working model of hypothesis (Ben-Moshe et al., 2019).

It is important to repeat that due to the presence of a wide array of distinct niches in each host organ that are in an ever-changing state in response to environmental stimuli and due to the large number unique phenotypic states possessed by individual metastatic cells, conceivably innumerable combinations of metastatic cell-intrinsic and host organ-intrinsic phenotypic states

can complement each other that result in colonizing metastatic cell survival and outgrowth. However, my cumulative research findings support the above hypothesis which should be further tested by, for example, quantifying TCA cycle intermediates in tumors and liver metastatic nodules to determine whether only NNMT-depleted MDA-MB-231 cells have increased levels of TCA cycle intermediates specifically in the liver.

6.2.3 In vitro findings demonstrate that mTOR is downstream of NNMT depletion-induced changes in HMGCS1 expression and free cholesterol levels in TNBC cells.

I next sought to identify molecular mechanisms contributing to increased anabolic gene expression and *de novo* cholesterol synthesis downstream of NNMT depletion in the TNBC cell lines to determine whether there is a potentially targetable molecular mechanism that can be inhibited along with NNMT in the MDA-MB-231 xenograft primary tumors to both decrease overall probability of metastasis formation and liver tropism.

Based on RNAseq DEG findings in NNMT-depleted vs NNMT-expressing TNBC cells, I had hypothesized that NNMT depletion-induced SAM upregulation may upregulate mTOR signaling leading to increased anabolic gene expression including *de novo* cholesterol synthesis gene expression. mTORC1 regulates anabolic metabolism and cell growth in response to multiple environmental cues including growth factors and nutrients such as amino acids. The Sabatini Lab discovered that SAMTOR acts as a nutrient sensor for SAM in lieu of methionine upstream of mTOR (42). During methionine depletion and thereby SAM depletion, free SAMTOR acts to inhibit mTORC1. When methionine and thereby SAM levels are replete, SAM binds SAMTOR and SAM-bound SAMTOR undergoes conformational changes that inhibits SAMTOR from interacting with the mTORC1 complex, releasing the repression on mTORC1 and activating canonical mTORC1 targets that upregulate anabolism and cell growth.

First, I determined that NNMT depletion with multiple shRNAs results in increased HMGCS1 expression in MDA-MB-231 and SUM159PT cell lines *in vitro*, demonstrating that NNMT inhibits HMGCS1 expression in these TNBC cell lines (Figure 6.12). Next, I determined that NNMT depletion with all three shRNAs significantly alters intracellular free cholesterol levels in both TNBC cell lines, demonstrating that NNMT regulates intracellular free cholesterol levels in these TNBC cell lines. (Figure 6.12). While SUM159PT intracellular free cholesterol levels were increased in accordance with increased HMGCS1 expression, it was surprising that NNMT

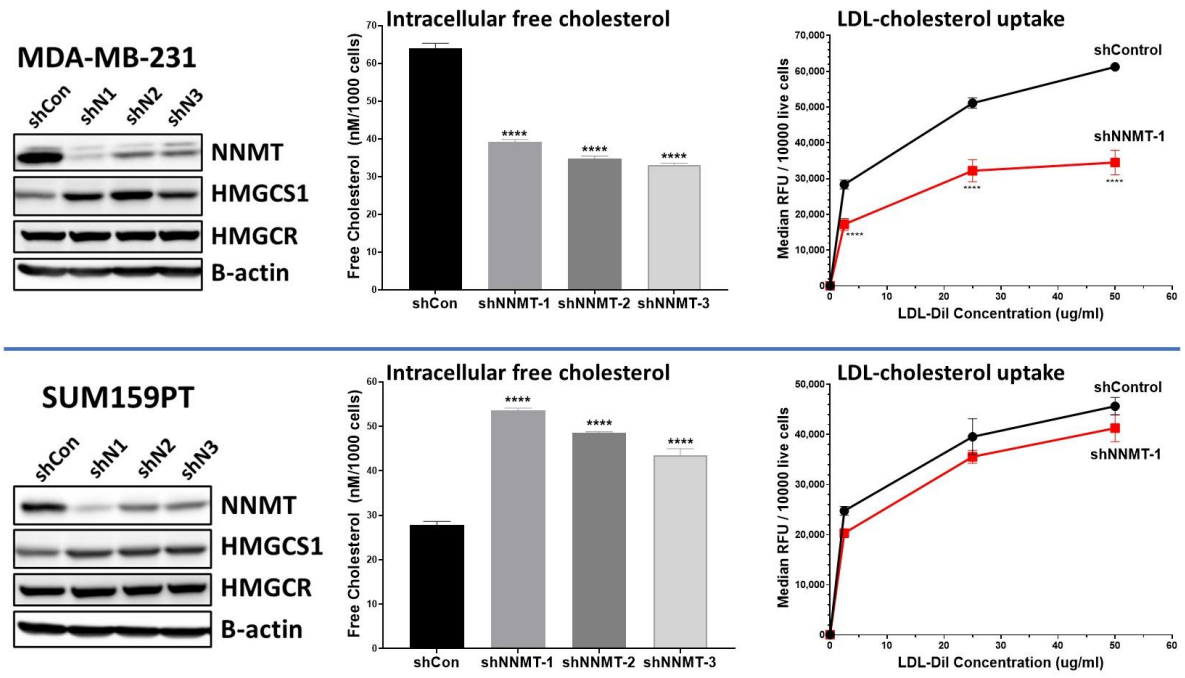

Figure 6.12. NNMT depletion with multiple shRNAs results in increased HMGCS1 expression in MDA-MB-231 and SUM159PT cell lines *in vitro*, demonstrating that NNMT inhibits HMGCS1 expression in these TNBC cell lines. NNMT depletion with all three shRNAs significantly alters intracellular free cholesterol levels in both TNBC cell lines, demonstrating that NNMT regulates intracellular free cholesterol levels in these TNBC cell lines. While SUM159PT intracellular free cholesterol levels were increased in accordance with increased HMGCS1 expression, NNMT depletion in the MDA-MB-231 cells decreased intracellular free cholesterol levels even though HMCGS1 expression was upregulated with NNMT depletion in this cell line. Only in the MDA-MB-231 cell line, LDL uptake is significantly decreased with NNMT depletion, suggesting that LDL-cholesterol uptake contributes more significantly to intracellular free cholesterol levels compared to *de novo* synthesis in MDA-MB-231 cells *in vitro*. *n = 3 for intracellular free cholesterol and LDL uptake quantification, ****p<0.0001.*

depletion in the MDA-MB-231 cells decreased intracellular free cholesterol levels even though HMCGS1 expression was upregulated with NNMT depletion in this cell line. While majority of intracellular free cholesterol is acquired by *de novo* synthesis, cells can also acquire cholesterol by uptaking LDL-cholesterol from circulation (reviewed in (60)). I therefore quantified the level of fluorescently labeled LDL-cholesterol uptake by NNMT-expressing and NNMT-depleted MDA-MB-231 and SUM159PT cell lines and determined that only in the MDA-MB-231 cell line, LDL uptake is significantly decreased with NNMT depletion (Figure 6.12). These findings suggest that LDL-cholesterol uptake contributes more significantly to intracellular free cholesterol levels compared to *de novo* synthesis in MDA-MB-231 cells *in vitro.*

Second, I determined that mTOR and *de novo* cholesterol synthesis are downstream of NNMT depletion-induced changes in HMGCS1 expression and intracellular free cholesterol levels in the MDA-MB-231 and SUM159PT cell lines (Figure 6.13). mTOR inhibition with rapamycin (RAPA) reverses NNMT depletion-induced upregulation in HMGCS1 expression, demonstrating that mTOR is downstream of NNMT depletion-induced increase in HMGCS1 expression in the MDA-MB-231 and SUM159PT cell lines. mTOR inhibition with rapamycin reverses NNMT depletion-induced changes in intracellular free cholesterol levels, demonstrating that mTOR is downstream of NNMT depletion-induced alterations in free cholesterol levels in the MDA-MB-231 and SUM159PT cell lines. HMGCR inhibition with lovastatin reverses NNMT depletion-induced changes in intracellular free cholesterol levels, demonstrating that *de novo* cholesterol synthesis activation is downstream of NNMT depletion-induced alterations in free cholesterol levels in the MDA-MB-231 and SUM159PT cell lines. These findings support the hypothesis that NNMT depletion in TNBC cells, potentially via SAM upregulation, results in mTOR-mediated

activation of *de novo* cholesterol synthesis, which is an important mediator of anabolic metabolism and cell growth.

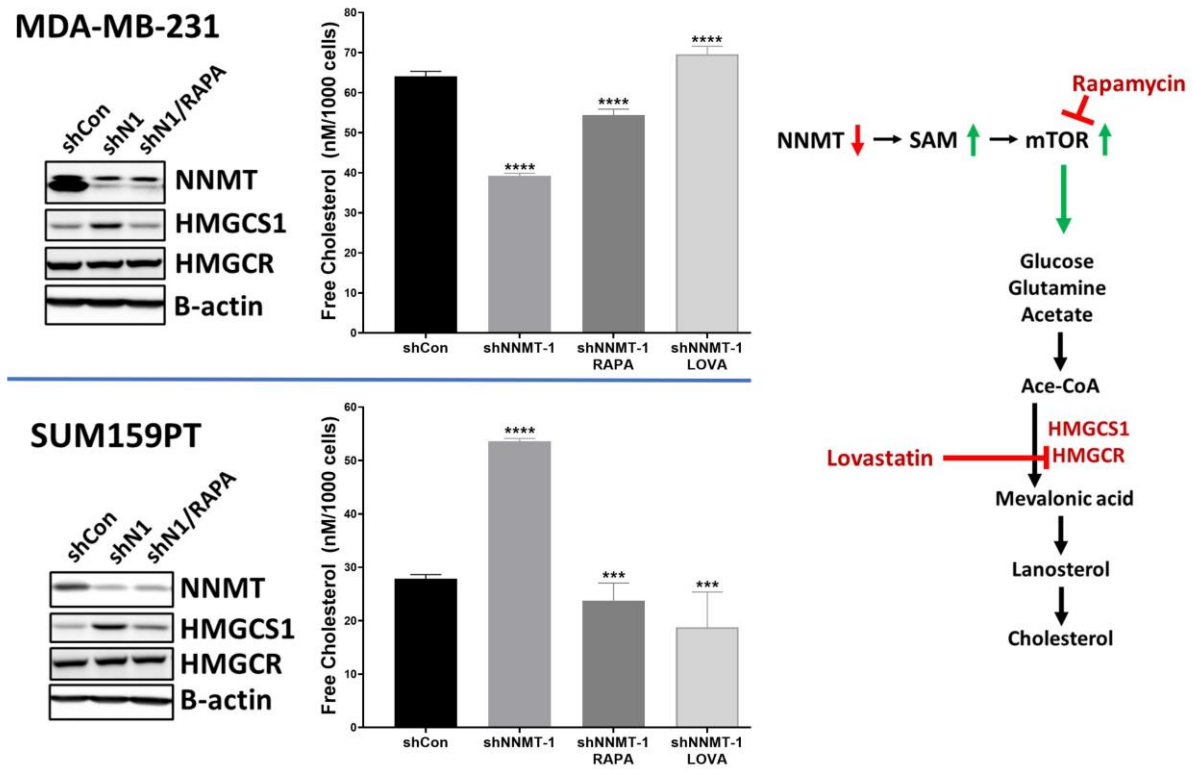

Figure 6.13. mTOR inhibition with rapamycin (RAPA) reverses NNMT depletion-induced upregulation in HMGCS1 expression, demonstrating that mTOR is downstream of NNMT depletion-induced increase in HMGCS1 expression in the MDA-MB-231 and SUM159PT cell lines. mTOR inhibition with rapamycin (RAPA) reverses NNMT depletion-induced changes in intracellular free cholesterol levels, demonstrating that mTOR is downstream of NNMT depletion-induced alterations in free cholesterol levels in the MDA-MB-231 and SUM159PT cell lines. HMGCR inhibition with lovastatin (LOVA) reverses NNMT depletion-induced changes in intracellular free cholesterol levels, demonstrating that *de novo* cholesterol synthesis activation is downstream of NNMT depletion-induced alterations in free cholesterol levels in the MDA-MB-231 and SUM159PT cell lines. These findings support the hypothesis that NNMT depletion in TNBC cells, potentially via SAM upregulation, results in mTOR-mediated activation of *de novo* cholesterol synthesis, which is an important mediator of anabolic metabolism and cell growth. *n = 3 for intracellular free cholesterol quantification, ***p<0.001, ****p<0.0001.*

6.3 Discussion

Below are my conclusions on NNMT's role in TNBC metastasis based on my dissertation research (Figure 6.14):

1) NNMT expression in xenograft primary tumors of the patient-derived MDA-MB-231 and SUM159PT TNBC cell lines is associated with increased probability of distant metastasis formation in female immunocompromised mice. NNMT's association with increased expression of invasion and EMT genes (i.e., *HIF1A, SNAI2, MMPs*) in these cells may underlie this phenotype by increasing their metastatic potential via enhancing their ability to invade, intravasate and survive in circulation. Importantly, NNMT expression is associated with invasion/EMT gene expression in untreated early-stage TNBC tumors, suggesting that NNMT-associated tumor-promoting gene expression may have relevance to TNBC patient tumor biology. While investigating the molecular mechanisms underlying NNMT's association with TNBC tumor-promoting gene expression was beyond the scope of my dissertation research, it is plausible that NNMT-induced SAM depletion downregulates repressive DNA and/or histone methylation at the regulatory regions of genes such as *HIF1A* and *SNAI2*, resulting in alleviation of transcriptional repression and thereby upregulation of their transcription.

2) The fact that NNMT expression in both the MDA-MB-231 and SUM159PT xenograft primary tumors is associated with increased probability of metastasis formation suggested that NNMT depletion in the primary tumors may be a viable metastasis prevention strategy. Intriguingly, while there were a significantly lower number of mice with NNMT-depleted MDA-MB-231 and SUM159PT primary tumors that developed metastasis, the ones with NNMT-depleted MDA-MB-231 primary tumors that

developed metastasis had extensive liver-specific metastasis, which did not occur in any of the mice that had NNMT-expressing MDA-MB-231 primary tumors, suggesting that NNMT depletion is associated with increased liver tropism of the MDA-MB-231 cell line.

3) The fact that I observed the NNMT depletion-induced enhanced liver tropism phenotype only with the MDA-MB-231 cell line opened up a discussion on whether this phenotype is a cell line specific phenomenon and therefore not generalizable to TNBC patient tumor biology. While this is plausible, it can also be debated that the possibility of this phenotype occurring even in a minute portion of TNBC patient primary tumor cells with a biology similar to that of the MDA-MB-231 cell line would be enough to create unwanted liver metastases in patients upon NNMT inhibition in the TNBC primary tumors as a metastasis prevention treatment strategy. Investigation of the molecular mechanisms contributing to NNMT depletion-induced enhanced liver tropism was therefore warranted to identify a pharmacologically targetable mechanism that can be inhibited along with NNMT in the primary tumors to significantly decrease the probability of overall and liver-specific metastasis formation in this experimental model.

4) While NNMT expression is associated with increased invasion/EMT gene expression, NNMT depletion is associated with increased anabolic gene expression, specifically increased expression of genes encoding a multitude of large and small ribosomal proteins and genes in the *de novo* cholesterol synthesis pathway. Anabolic pathways that facilitate cell growth and proliferation such as synthesis of new ribosomes (ribogenesis) and *de novo* cholesterol is downstream of mTOR activation in response to cell-extrinsic and cell-intrinsic stimuli indicative of replete nutrient, energy and growth factor levels. Hepatocytes synthesize glucose and glutamine and secrete them into

the liver interstitial fluid; glucose and glutamine then enter the circulation and get distributed to the entire body. Glucose and glutamine are the main drivers of anaplerosis (replenishment of TCA cycle intermediates) crucial for oxidative phosphorylation-mediated high level ATP production that can meet the high energy demand of anabolic metabolism. NNMT-depleted metastatic MDA-MB-231 cells may gain a proliferative advantage to rapidly grow into large nodules specifically in the liver microenvironment via the interstitial fluid that can provide these cells with high levels of glucose and glutamine to drive anaplerosis and thereby anabolism and cell growth.

5) It is important to repeat that due to the presence of a wide array of distinct niches in each host organ that are in an ever-changing state in response to environmental stimuli and due to the large number unique phenotypic states possessed by individual metastatic cells, conceivably innumerable combinations of metastatic cell-intrinsic and host organ-intrinsic phenotypic states can complement each other that result in colonizing metastatic cell survival and outgrowth. However, my research findings on *de novo* cholesterol synthesis intermediate and free cholesterol quantification in primary tumor and liver metastatic nodules of NNMT-expressing and NNMT-depleted MDA-MB-231 cells support the above hypothesis which should be further tested by, for example, quantifying TCA cycle intermediates in tumors and liver metastatic nodules to determine whether only NNMT-depleted MDA-MB-231 cells have increased levels of TCA cycle intermediates specifically in the liver.

6) I next sought to identify molecular mechanisms contributing to increased anabolic gene expression and *de novo* cholesterol synthesis downstream of NNMT depletion in the TNBC cell lines to determine whether there is a potentially targetable

molecular mechanism that can be inhibited along with NNMT in the MDA-MB-231 xenograft primary tumors to both decrease overall probability of metastasis formation and liver tropism. I determined that NNMT depletion in TNBC cells, potentially via SAM upregulation, results in mTOR-mediated activation of *de novo* cholesterol synthesis, which is an important mediator of anabolic metabolism and cell growth as free cholesterol is a required plasma membrane component. These findings suggest that dual NNMT and mTOR inhibition in the MDA-MB-231 xenograft primary tumors can be tested to determine whether their dual inhibition significantly downregulates overall metastasis formation by diminishing enhanced liver tropism that occurs as a side effect of NNMT depletion.

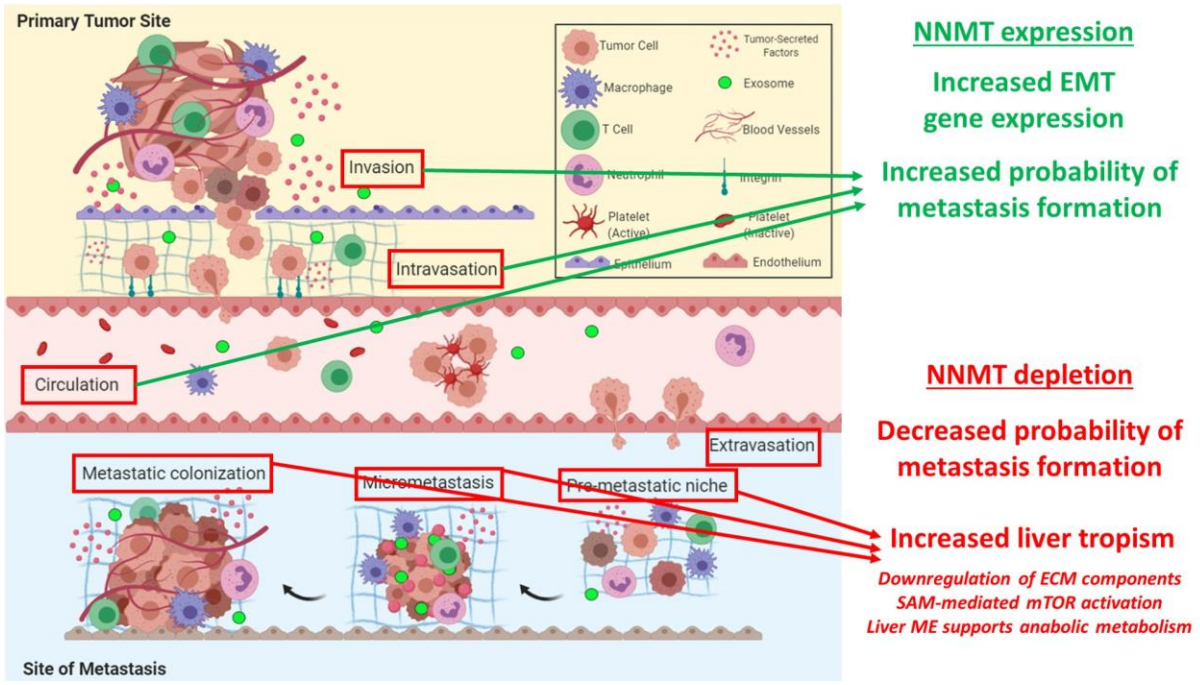

Figure 6.14. Overall working model of hypothesis for NNMT's role in TNBC metastasis (61).

CHAPTER 7

SIGNIFICANCE AND FUTURE DIRECTIONS

7.1 Significance

Clinically overt metastasis formation is the last step of the metastatic cascade, remains incurable and is the cause of death in 90% of cancer patients. This highlights the importance of uncovering potentially targetable molecular mechanisms that contribute to the earlier steps of the metastatic cascade prior to metastatic outgrowth (invasion, intravasation, survival in circulation, extravasation, distant organ colonization). As CTCs have been detected in the circulation of patients with early-stage primary tumors and without clinically detectable metastases, it is conceivable that primary tumors seed metastatic cells into distant organs in the earlier stages of disease progression (62). These distant organ-colonizing metastatic cells remain quiescent for an unpredictable amount of time followed by entry into proliferation and metastatic outgrowth. Therefore, investigating molecular mechanisms contributing to metastatic cell survival, quiescence, proliferation and outgrowth in distant organs is of utmost importance to devise new metastasis prevention strategies that involve either killing the quiescence cells completely or perpetually locking them in quiescence such that they never go on to form incurable metastatic nodules.

As a wide array of metastatic cell-intrinsic and host organ-intrinsic phenotypic states can complement each other that result in colonizing metastatic cell survival and outgrowth, it can be discussed whether distant organ colonization can ever become a practical clinical target for metastasis prevention as a large multitude of molecular mechanisms underlying organ colonization cannot be individually targeted in a patient without introducing intolerable side effects. However,

if novel molecular mechanisms underlying colonizing metastatic cell survival, quiescence, and outgrowth for all combinations of primary tumor types and host organs are continued to be identified, we can eventually begin to understand whether there are patterns of essential molecular mechanisms underlying organ tropism that are indispensable across multiple solid tumor types and host organs. If there are such molecular mechanisms that commonly promote the metastatic cell survival, escape from quiescence, and entrance into proliferation of multiple primary solid tumor types in multiple host organs, then it may be feasible to pharmacologically target these smaller number of molecular mechanisms in large groups of cancer patients to prevent metastasis formation.

Research on cancer organ tropism and colonization is in its infancy and there is much to uncover. My dissertation findings point to a previously unknown possibility that when a metastasis-promoting SAM-dependent methyltransferase (i.e., NNMT) is inhibited in primary tumors to prevent metastasis formation, resultant upregulation in intracellular SAM levels may activate mTOR signaling and anabolism, providing the tumor cells with a new-found proliferative advantage in the liver microenvironment. Research findings such as this one should make cancer researchers cognizant of the possibility that when a metastasis-promoting molecular mechanism is inhibited in patient tumors to decrease their overall metastatic potential, inhibition of that molecular mechanism may endow the tumor cells a novel phenotypic state that may be advantageous in a specific niche of a distant organ. In order to be effective, metastasis prevention strategies need to account for the possibility that they may change the organ tropism of primary tumor cells in addition to decreasing their overall metastatic potential, resulting in unwanted organ-specific metastases as a side effect.

7.2 Future Directions

A major disadvantage of my *in vivo* experimental design is the lack of an immune microenvironment in NSG mice. Both innate and adaptive immune systems have extensively been shown to influence tumor biology, progression, and metastasis; therefore, studying the role of NNMT in TNBC metastasis using immunocompromised mice may yield artificial phenotypes (reviewed in (63)). My *in vivo* experiments should be repeated with NNMT-expressing syngeneic mouse models of TNBC to determine whether NNMT acts as a metastasis-promoting and whether NNMT depletion enhances liver tropism when both the primary tumor cells and metastatic cells exist in an intact physiological context.

The fact that I observed the NNMT depletion-induced enhanced liver tropism phenotype only with the MDA-MB-231 cell line opens a discussion on whether this phenotype is a cell line specific phenomenon and therefore not generalizable to TNBC patient tumor biology. While this is plausible, it can also be debated that the possibility of this phenotype occurring even in a minute portion of TNBC patient primary tumor cells with a biology similar to that of the MDA-MB-231 cell line would be enough to create unwanted liver metastases in patients upon NNMT inhibition in the TNBC primary tumors as a metastasis prevention treatment strategy.

It may be that cancer cells need to possess baseline liver tropism (i.e., extravasate into liver and survive) for NNMT depletion to upregulate liver metastatic burden as shControl MDA-MB-231 cells were able to form metastatic nodules in the liver while SUM159PT cells did not form liver metastases at all. My findings suggest that NNMT depletion in the MDA-MB-231 primary tumor cells is not associated with an increase ability to extravasate/home/survive in the liver microenvironment as the number of individual shControl and shNNMT metastatic cells in the livers were not significantly different. On the other hand, NNMT depletion in the MDA-MB-231

primary tumor cells is associated with increased proclivity towards proliferation upon arrival in the liver microenvironment as there was a significantly higher number of shNNMT metastatic cell clusters compared to shControl metastatic cell clusters. These findings suggest that MDA-MB-231 cells have an innate ability to extravasate and survive in the liver microenvironment, and that NNMT depletion in the MDA-MB-231 liver metastatic cells enhances their proliferation and growth. My *in vivo* experiments should be repeated with additional NNMT-expressing patient-derived TNBC cell lines that can metastasize in NSG mice to determine whether only TNBC cell lines with baseline liver tropism would exhibit NNMT depletion-induced enhanced liver tropism.

I sought to identify molecular mechanisms contributing to increased anabolic gene expression and *de novo* cholesterol synthesis downstream of NNMT depletion in the TNBC cell lines to determine whether there is a potentially targetable molecular mechanism that can be inhibited along with NNMT in the MDA-MB-231 xenograft primary tumors to both decrease overall probability of metastasis formation and liver tropism. I determined that NNMT depletion in TNBC cells, potentially via SAM upregulation, results in mTOR-mediated activation of *de novo* cholesterol synthesis, which is an important mediator of anabolic metabolism and cell growth as free cholesterol is a required plasma membrane component. These findings suggest that dual NNMT and mTOR inhibition in the MDA-MB-231 xenograft primary tumors can be tested to determine whether their dual inhibition significantly downregulates overall metastasis formation by diminishing enhanced liver tropism that occurs as a side effect of NNMT depletion. That being said, systemic pharmacological inhibition of mTOR in NNMT-depleted MDA-MB-231 cells *in vivo* would not allow us to determine whether TNBC cell-intrinsic NNMT depletion and downstream mTOR signaling activation contributes to increased liver-specific metastatic burden

because the systemic inhibition of mTOR activity would act at an organismal level and not just in the TNBC cells.

The hypothesized mechanism for NNMT depletion-induced enhanced liver tropism of MDA-MB-231 cells is SAM upregulation-induced mTOR and downstream anabolic metabolism activation that provides a proliferative advantage in the liver microenvironment. SAMTOR acts as a nutrient sensor for SAM in lieu of methionine upstream of mTOR. During methionine depletion and thereby SAM depletion, free SAMTOR acts to inhibit mTORC1. When methionine and thereby SAM levels are replete, SAM binds SAMTOR and SAM-bound SAMTOR undergoes conformational changes that inhibits SAMTOR from interacting with the mTORC1 complex, releasing the repression on mTORC1 and activating canonical mTORC1 targets that upregulate anabolism and cell growth. Therefore, it should first be determined whether NNMT-expressing MDA-MB-231 and SUM159PT cells exhibit upregulated free cholesterol levels upon shRNA-mediated SAMTOR depletion, as SAMTOR inhibition in NNMT-expressing and SAM-depleted cells should release SAMTOR-mediated inhibition on mTOR signaling. If this is the case, then it should be determined whether mTOR inhibition with rapamycin in NNMT-expressing and SAMTOR-depleted MDA-MB-231 and SUM159PT cells downregulates free cholesterol levels. If this is the case, these series of experiments would connect NNMT activity, intracellular SAM levels, SAMTOR activity and mTOR signaling as a mechanism regulating an aspect of TNBC cell anabolic mechanism (*de novo* cholesterol synthesis).

Expression of small and large ribosomal proteins are also upregulated upon NNMT depletion in MDA-MB-231 cand SUM159PT cells; ribogenesis and increased translation is another anabolic pathway downstream of mTOR signaling (reviewed in (64)). To determine whether NNMT depletion upregulates other aspects of anabolic mechanism and not just *de novo*

cholesterol synthesis, it should be determined whether NNMT depletion in MDA-MB-231 and SUM159PT cells results in increased protein synthesis with OP-puro labeling. If this is the case, then it should first be determined whether NNMT-expressing MDA-MB-231 and SUM159PT cells exhibit upregulated protein synthesis upon shRNA-mediated SAMTOR depletion, as SAMTOR inhibition in NNMT-expressing and SAM depleted cells should release SAMTOR-mediated inhibition on mTOR signaling. If this is the case, then it should be determined whether mTOR inhibition with rapamycin in NNMT-expressing and SAMTOR-depleted MDA-MB-231 and SUM159PT cells downregulates protein synthesis. If this is the case, these series of experiments would connect NNMT activity, intracellular SAM levels, SAMTOR activity and mTOR signaling as a mechanism regulating TNBC cell anabolic mechanism and not just *de novo* cholesterol synthesis.

Finally, it should be determined whether shRNA-mediated SAMTOR inhibition in NNMT-expressing and SAM-depleted MDA-MB-231 xenograft primary tumors increase their liver-specific metastatic potential to provide a more detailed molecular understanding for NNMT depletion and SAM upregulation-induced enhanced liver tropism. If this is the case, these findings would result in more outstanding questions to be experimentally addressed with important implications regarding metastasis prevention treatments focusing on inhibiting SAM-dependent methyltransferases. For example, would inhibition of other SAM-dependent methyltransferases upregulate intracellular SAM, mTOR signaling and anabolism, thereby altering cancer cell tropism of primary breast tumors and other solid tumors? In other words, does SAM upregulation downstream of any metastasis-promoting SAM-dependent methyltransferase inhibition as a metastasis prevention strategy has the potential side effect of altering cancer cell metabolism and increasing organ-specific metastasis? To address these questions, my *in vivo* experiments can be

repeated with patient-derived cell lines of TNBC and/or other solid tumors whose metastatic potential is upregulated by other SAM-dependent methyltransferases. Finally, my dissertation findings encourage the development of effective and selective small molecule activators of SAMTOR so that pharmacological SAMTOR activation can be tested in the proposed experiments to determine whether dual NNMT inhibition and SAMTOR activation (and resultant mTOR signaling inhibition) is a viable strategy to significantly downregulate overall metastatic burden by diminishing liver-specific increase in metastasis upon NNMT depletion alone.

APPENDIX A

Introduction

Hypothesized role of nicotinamide n-methyltransferase activity in the m6A mRNA modification-mediated post-transcriptional regulation of triple-negative breast cancer gene expression

Nicotinamide N-methyltransferase (NNMT), through depleting intracellular SAM with its SAM-dependent nicotinamide methylating activity, has the potential to regulate triple-negative breast cancer (TNBC) gene expression transcriptionally and post-transcriptionally by resulting in DNA, histone and RNA hypomethylation. NNMT-induced SAM depletion was initially found to result in histone hypomethylation associated with increased pro-oncogenic gene expression in cancer cell lines. Subsequent studies demonstrated that high NNMT expression results in DNA and PP2A phosphatase hypomethylation associated with increased cancer gene expression and oncogenic kinase activation, respectively. As a link between NNMT expression and RNA hypomethylation has not previously been established as a mechanism contributing to cancer progression, I began my dissertation research by investigating NNMT-induced RNA hypomethylation as a potential mechanism contributing to tumor-promoting gene expression and phenotypes in TNBC cells. My initial hypothesis was that high NNMT activity in TNBC cells 1) reduces m6A mRNA modification at the 3'UTR of oncogenic transcripts that regulate cell viability, motility and differentiation, preventing m6A-mediated mRNA degradation and thereby increasing steady-state transcript levels and subsequent translation, and 2) consequently contributes to enhanced cancer stem cell-like traits associated with metastatic potential and increased in vivo tumor-forming capacity.

m6A is an abundant and reversible SAM-dependent RNA methylation in eukaryotes that is mediated by the METTL3/METTL14 protein complex, and it has recently been brought to the forefront of scientific research due to the discovery of m6A-regulatory proteins that can add, remove, or preferentially bind to the m6A site on mRNA and alter important biological functions such as cell fate (reviewed in (65)). m6A-regulatory proteins and altered m6A methylation levels on mRNA are implicated in the progression of several human cancers via causing changes in post-transcriptional gene expression of cancer pathways (reviewed in (66)). Our co-investigator in the Department of Chemistry at the University of Chicago, Dr. Chuan He, discovered that m6A mRNA methylation can mediate post-transcriptional gene expression by two mechanisms. The first is accomplished by the YTHDF1 protein (YTH N6-Methyladenosine RNA Binding Protein 1) that recognizes m6A modification on mRNA and thereby regulates translational efficiency (67). The second, YTHDF2 (YTH N6-Methyladenosine RNA Binding Protein 2), also recognizes m6A modification but facilitates mRNA degradation (68). I therefore originally hypothesized that high NNMT-expressing TNBC cells exhibit relatively low m6A mRNA methylation, directly resulting in deregulated mRNA and protein expression involved in key cancer biological processes. Support for this hypothesis comes from the observation that reduced m6A modification of NANOG mRNA in TNBC cells was found to increase NANOG expression and was associated with BC stem cell phenotypes (69). I predicted that similar previously unknown mechanisms underlie the mechanism of high NNMT expression in TNBC in mediating tumor cell viability and metastases via modulation of mRNA methylation.

Results

In order to determine whether m6A depletion on RNA contributes to NNMT-induced gene expression and phenotypes in TNBC cells, I knocked down METTL3 in NNMT-expressing and

NNMT-depleted MDA-MB-231 and SUM159PT patient-derived TNBC cell lines with constitutively expressed shRNAs targeting *METTL3* mRNA. According to my hypothesis, METTL3 knockdown-mediated m6A depletion should, at least partially, rescue NNMT-induced phenotypes in TNBC cells with NNMT knockdown. METTL3 depletion resulted in significantly decreased growth and viability of TNBC cells regardless of whether NNMT was expressed or depleted concomitantly. Because METTL3-depleted TNBC cells were minimally viable as observed under the microscope, I concluded that m6A depletion on RNA downstream of NNMT-induced SAM depletion in TNBC cells cannot contribute to NNMT-induced tumor-promoting gene expression and phenotypes. In addition, differentially expressed transcripts and differentially m6A-methylated transcripts upon NNMT depletion did not overlap according to m6A immunoprecipitation-coupled RNAseq data, suggesting that NNMT-induced changes in transcript expression are not due to m6A-depletion mediated increase in transcript stability.

These results suggested that presence of m6A modification on RNA rather than its depletion is necessary for the growth and viability of the TNBC cells. Importantly, one of the m6A-binding proteins, YTHDF3, has been shown to induces the translation of m6A-enriched gene transcripts to promote breast cancer brain metastases *in vivo* (70). These findings warrant further investigation on the potential tumor-promoting roles of METTL3/METL14-mediated m6A modification on RNA in TNBC cells. m6A modification has been shown to be placed on different sections of mRNAs (i.e., 5' UTR and 3' UTR), and location of m6A modification has been shown to exhibit distinct effects on transcript fate (71-74). Below are the IPA canonical pathways enriched among non-m6A modified (2000) and m6A-modified transcripts (7000) among the 9000 expressed transcripts in NNMT-expressing MDA-MB-231 cells. Majority of expressed transcripts in these cells are m6A-modifed at unique locations with distinct functions and a multitude of

important cellular pathways are enriched among these groups of transcripts.

7000 m^{6}A-modified transcripts

Top Canonical Pathways		
Name	p-value	Overlap
EIF2 Signaling	1.23E-23	61.1 % 140/229
Protein Ubiquitination Pathway	2.09E-23	58.3 % 158/271
Sirtuin Signaling Pathway	7.03E-22	56.2 % 164/292
Molecular Mechanisms of Cancer	1.29E-18	50.3 % 198/394
Regulation of eIF4 and p70S6K Signaling	3.75E-13	56.4 % 93/165

2000 unmodified transcripts: housekeeping

Top Canonical Pathways		
Name	p-value	Overlap
Mitochondrial Dysfunction	1.35E-12	28.7 % 49/171
Oxidative Phosphorylation	2.87E-12	33.9 % 37/109

500 modified at the 5'UTR only (translational efficiency)

Top Canonical Pathways		
Name	p-value	Overlap
Sirtuin Signaling Pathway	6.42E-08	7.2 % 21/291
Protein Ubiquitination Pathway	4.76E-07	7.0 % 19/273
EIF2 Signaling	1.22E-05	6.7 % 15/224
Regulation of eIF4 and p70S6K Signaling	1.17E-04	7.0 % 11/157
Oxidative Phosphorylation	1.41E-04	8.3 % 9/109

3000 modified at the 3'UTR only (stability)

Top Canonical Pathways		
Name	p-value	Overlap
Molecular Mechanisms of Cancer	6.74E-15	26.3 % 103/391
Role of Tissue Factor in Cancer	9.22E-11	35.0 % 41/117
Senescence Pathway	1.05E-10	26.2 % 72/275
Rac Signaling	3.26E-10	34.8 % 39/112
IGF-1 Signaling	7.23E-09	33.7 % 35/104

2500 modified at exons only (translation elongation)

Top Canonical Pathways		
Name	p-value	Overlap
Mismatch Repair in Eukaryotes	1.32E-06	62.5 % 10/16
Unfolded protein response	2.37E-05	32.1 % 18/56
NGF Signaling	1.23E-04	23.7 % 27/114
Death Receptor Signaling	1.36E-04	25.3 % 23/91
Spermine and Spermidine Degradation I	1.58E-04	100.0 % 4/4

1000 modified at introns only (splicing)

Top Canonical Pathways		
Name	p-value	Overlap
Protein Ubiquitination Pathway	2.59E-11	14.7 % 40/273
EIF2 Signaling	3.08E-10	15.2 % 34/224
Mitochondrial Dysfunction	4.37E-10	17.0 % 29/171
Sirtuin Signaling Pathway	6.75E-10	13.4 % 39/291
Oxidative Phosphorylation	5.67E-08	18.3 % 20/109

Appendix A Figure 1. IPA pathways enriched among m6A-modified transcripts, m6A non-modified transcripts, and transcripts that are m6A-modified at unique locations in NNMT-expressing MDA-MB-231 cells. 5'UTR modification has been shown to regulate translational efficiency, 3'UTR modification has been shown to regulate transcript stability, exon modification has been shown to regulate translation elongation, and intron modification has been shown to regulate splicing.

Discussion

In vivo experiments outlined in the main chapters of my dissertation can be performed with METTL3-expressing and METTL3-depleted patient-derived TNBC cell lines to investigate whether METTL3/METTL14-mediated m6A modification on distinct locations on RNA and resultant post-transcriptional and translational gene expression regulation of cellular pathways contributes to unique phenotypes regarding TNBC primary tumor growth/viability, metastatic potential and organ tropism.

To update my original hypothesis and move my PhD research forward, I decided to inspect my RNAseq data to determine which transcripts were differentially expressed by NNMT-depletion in TNBC cells regardless of changes in m6A modification levels. NNMT-induced differential gene expression in TNBC cells can be explained by other mechanisms such as SAM depletion and resultant DNA/histone hypomethylation leading to transcriptional activation or repression of genes affected by the hypomethylation events. I observed that NNMT expression in MDA-MB-231 and SUM159PT cell lines is associated with tumor-promoting (invasion/EMT) gene expression and determined that higher NNMT expression in early-stage untreated ER-negative breast cancers is associated with a significantly worse distant metastasis free survival (DMFS). I subsequently hypothesized that NNMT may promote TNBC metastatic potential by upregulating the expression of tumor-promoting genes via a multitude of potential mechanisms including SAM-depletion induced decrease in transcriptionally repressive DNA and histone methylation at the regulatory regions of tumor-promoting genes. Experiments addressing this refined hypothesis comprise the main chapters of my dissertation.

REFERENCES

1. Hunt, Samantha Vicky, Aaron Jamison, and Raman Malhotra. “Oral nicotinamide for non-melanoma skin cancers: A review.” *Eye*, (March 15, 2022). doi.org/10.1038/s41433-022-02036-z.

2. Chen *et al*. “A Phase 3 Randomized Trial of Nicotinamide for Skin-Cancer Chemoprevention.” *N Engl J Med*, 373, no. 17 (October 22, 2015): 1618-1626. doi: https://10.1056/NEJMoa1506197.

3. Pissios, Pavlos. “Nicotinamide N-Methyltransferase: More Than a Vitamin B3 Clearance Enzyme.” *Trends in Endocrinology & Metabolism*, 28, no. 5 (May 2017): 340-353. doi: https://doi.org/10.1016/j.tem.2017.02.004.

4. Cantoni, GL. “Methylation of nicotinamide with soluble enzyme system from rat liver.” *J Biol Chem*, 189, no. 1 (March 1951): 203-216.

5. Parsons *et al*. “Expression of nicotinamide N-methyltransferase (E.C. 2.1.1.1) in the Parkinsonian brain.” *J Neuropathol Exp Neurol*, 61, no. 2 (February 2002): 111-124. doi: 10.1093/jnen/61.2.111.

6. Lee *et al*. “Microarray profiling of isolated abdominal subcutaneous adipocytes from obese vs non-obese Pima Indians: increased expression of inflammation-related genes.” *Diabetologia*, 48, no. 9 (August 2, 2005): 1776-1783. doi: 10.1007/s00125-005-1867-3.

7. Lim *et al*. “Overexpression of nicotinamide N-methyltransferase in gastric cancer tissues and its potential post-translational modification.” *Exp Mol Med*, 38, no. 5 (2006). doi: 10.1038/emm.2006.54.

8. Sartini *et al*. “Upregulation of tissue and urinary nicotinamide N-methyltransferase in bladder cancer: potential for the development of a urine-based diagnostic test.” *Cell Biochem Biophys*, 65, no. 3 (2013): 473-483. doi: 10.1007/s12013-012-9451-1.

9. Sartini *et al*. “Nicotinamide N-methyltransferase in non-small cell lung cancer: promising results for targeted anti-cancer therapy.” *Cell Biochem Biophys*, 67, no. 3 (2013): 865-873. doi: 10.1007/s12013-013-9574-z.

10. Xu *et al*. “Activation of nicotinamide N-methyltransferase gene promoter by hepatocyte nuclear factor-1beta in human papillary thyroid cancer cells.” *Mol Endocrinol*, 19, no. 2 (2005): 527-539. doi: 10.1210/me.2004-0215.

11. Sartini *et al*. “Identification of nicotinamide N-methyltransferase as a novel tumor marker for renal clear cell carcinoma.” *J Urol*, 176, no. 5 (October 31, 2006): 2248-2254. doi: 10.1016/j.juro.2006.07.046.

12. Kim *et al*. "Expression of nicotinamide N-methyltransferase in hepatocellular carcinoma is associated with poor prognosis." *J Exp Clin Cancer Res*, 28, no. 20 (February 17, 2009). doi: 10.1186/1756-9966-28-20.

13. Kanska *et al*. "Glucose deprivation elicits phenotypic plasticity via ZEB1-mediated expression of NNMT." *Oncotarget*, 8, no. 16 (April 17, 2017). doi: 10.18632/oncotarget.15429.

14. Tomida *et al*. "Stat3 up-regulates expression of nicotinamide N-methyltransferase in human cancer cells." *J Cancer Res Clin Oncol*, 134, no. 5 (2008): 551-559. doi: 10.1007/s00432-007-0318-6.

15. Kraus *et al*. "Nicotinamide N-methyltransferase knockdown protects against diet-induced obesity." *Nature Letter*, 508, (April 10, 2014): 258-262. https://doi.org/10.1038/nature13198.

16. Sampson *et al*. "Combined nicotinamide N-methyltransferase inhibition and reduced-calorie diet normalizes body composition and enhances metabolic benefts in obese mice." *Scientific Reports*, 11, no. 5637 (2021). https://doi.org/10.1038/s41598-021-85051-6.

17. Kannt *et al*. "Association of nicotinamide-N-methyltransferase mRNA expression in human adipose tissue and the plasma concentration of its product, 1-methylnicotinamide, with insulin resistance." *Diabetologia*, 58, (2015). doi: 10.1007/s00125-014-3490-7.

18. Liu *et al*. "Serum N1-Methylnicotinamide Is Associated With Obesity and Diabetes in Chinese." *J Clin Endocrinol Metab*, 100, no. 8 (August 2015): 3112-3117. doi: 10.1210/jc.2015-1732.

19. Wang *et al*. "Complex roles of nicotinamide N-methyltransferase in cancer progression." *Cell Death and Disease*, 13, no. 26 (March 25, 2022). https://doi.org/10.1038/s41419-022-04713-z.

20. Li *et al*. "Nicotinamide N-Methyltransferase: A Promising Biomarker and Target for Human Cancer Therapy." *Frontiers in Oncology*, 13, no. 26 (June 9, 2022). https://doi.org/10.3389/fonc.2022.894744.

21. Roberti, Annalisa, Agustin F Fernandez, and Mario F Fraga. "Nicotinamide N-methyltransferase: At the crossroads between cellular metabolism and epigenetic regulation." *Molecular Metabolism*, 45, (2020). https://doi.org/10.1016/j.molmet.2021.101165.

22. Kanakkanthara *et al*. "BRCA1 Deficiency Upregulates NNMT, Which Reprograms Metabolism and Sensitizes Ovarian Cancer Cells to Mitochondrial Metabolic Targeting Agents." *Cancer Research*, 79, no. 23 (December 1, 2019). doi: 10.1158/0008-5472.CAN-19-1405.

23. Komatsu *et al*. "NNMT activation can contribute to the development of fatty liver disease by modulating the NAD+ metabolism." *Scientific Reports*, 8, no. 8637 (June 5, 2018). https://doi.org/10.1038/s41598-018-26882-8.

24. Andrea *et al*. "Cancer stem cell overexpression of nicotinamide N-methyltransferase enhances cellular radiation resistance." *Radiotherapy Oncol*, 99, (June 29, 2011). doi: 10.1016/j.radonc.2011.05.086.

25. Ulanovskaya, Olesya A., Andrea M Zuhl, and Benjamin F Cravatt. "NNMT promotes epigenetic remodeling in cancer by creating a metabolic methylation sink." *Nature Chemical Biology*, 9, (June 2013): 300-306. https://doi.org/10.1038/nchembio.1204.

26. Jung *et al*. "Nicotinamide metabolism regulates glioblastoma stem cell maintenance." *JCI Insight*, 2, no. 10 (May 18, 2017). DOI: 10.1172/jci.insight.90019.

27. Eckert *et al*. "Proteomics reveals NNMT as a master metabolic regulator of cancer-associated fibroblasts." *Nature Letter*, 569, (May 30, 2019): 723-728. https://doi.org/10.1038/s41586-019-1173-8.

28. Palanichamy *et al*. "NNMT silencing activates tumor suppressor PP2A, inactivates oncogenic STKs and inhibits tumor forming ability." *Clin Can Res*, 23, no. 9 (May 1, 2017): 2325–2334. doi: 10.1158/1078-0432.CCR-16-1323.

29. Hong *et al*. "Nicotinamide N-methyltransferase regulates hepatic nutrient metabolism through Sirt1 protein stabilization." *Nature Medicine*, 21, no. 8 (May 1, 2017): 887-894. doi: 10.1038/nm.3882.

30. Xinyou *et al*. "Nicotinamide N-methyltransferase enhances resistance to 5-fluorouracil in colorectal cancer cells through inhibition of the ASK1-p38 MAPK pathway." *Oncotarget*, 7, no. 29 (June 13, 2016): 45837-45848. doi: 10.18632/oncotarget.9962.

31. Harbeck *et al*. "Breast cancer." *Nature Reviews Disease Primers*, 5, no. 66 (September 23, 2019). https://doi.org/10.1038/s41572-019-0111-2.

32. Bianchini, Giampolo, Carmine De Angelis, Luca Licata, and Luca Gianni. "Treatment landscape of triple-negative breast cancer - expanded options, evolving needs." *Nat Rev Clin Oncol*, 19, no. 2 (February 2022). doi: 10.1038/s41571-021-00565-2.

33. Wang *et al*. "Nicotinamide N-methyltransferase enhances chemoresistance in breast cancer through SIRT1 protein stabilization." *Breast Cancer Research*, 21, no. 64 (May 17, 2019). https://doi.org/10.1186/s13058-019-1150-z.

34. Yu *et al*. "Nicotinamide N-methyltransferase inhibits autophagy induced by oxidative stress through suppressing the AMPK pathway in breast cancer cells."

Breast Cancer Research, 20, no. 191 (May 24, 2020). https://doi.org/10.1186/s12935-020-01279-8.

35. Gast *et al*. "Surgical Procedures and Methodology for a Preclinical Murine Model of De Novo Mammary Cancer Metastasis." *J Vis Exp*, 29, no. 125 (July 29, 2017). doi: 10.3791/54852.

36. Paschall, Amy V, and Kebin Liu. "Surgical Procedures and Methodology for a Preclinical Murine Model of De Novo Mammary Cancer Metastasis." *J Vis Exp*, 114, no. 125 (August 14, 2016). doi: 10.3791/54040.

37. Luo, Kathy Q, and Donald C Chang. "The gene-silencing efficiency of siRNA is strongly dependent on the local structure of mRNA at the targeted region." *Biochem Biophys Res Commun*, 318, no. 1 (May 21, 2014): 303-310. doi: 10.1016/j.bbrc.2004.04.027.

38. Ibrahim *et al*. "Significantly Elevated Levels of Plasma Nicotinamide, Pyridoxal, and Pyridoxamine Phosphate Levels in Obese Emirati Population: A Cross-Sectional Study." *Molecules*, 25, no. 17 (August 28, 2020). doi: 10.3390/molecules25173932.

39. Zinellu *et al*. "Plasma methionine determination by capillary electrophoresis-UV assay: application on patients affected by retinal venous occlusive disease." *Anal Biochem*, 363, no. 1 (January 12, 2007): 91-96. doi: 10.1016/j.ab.2007.01.009.

40. Michalak *et al*. "The roles of DNA, RNA and histone methylation in ageing and cancer." *Nature Reviews Mol Cell Bio*, 20, (July 3, 2019): 573-589. https://doi.org/10.1038/s41580-019-0143-1.

41. Liu, Grace Y, and David M. Sabatini. "mTOR at the nexus of nutrition, growth, ageing and disease." *Nature Reviews Mol Cell Bio*, 21, (January 14, 2020): 183-203. https://doi.org/10.1038/s41580-019-0199-y.

42. Gu *et al*. "SAMTOR is an S-adenosylmethionine sensor for the mTORC1 pathway." *Science*, 10, no. 358 (November 2017): 813-818. doi: 10.1126/science.aao3265.

43. The Cancer Genome Atlas Network. "Comprehensive molecular portraits of human breast tumours." *Science*, 490, (September 23, 2012): 61-70. https://doi.org/10.1038/nature11412.

44. Lambert, Arthur W, Diwakar R. Pattabiraman, and Robert A. Weinberg. "EMERGING BIOLOGICAL PRINCIPLES OF METASTASIS." *Cell*, 168, no. 4 (February 9, 2017): 670-691. doi: 10.1016/j.cell.2016.11.037.

45. Dongre, Anushka, and Robert A. Weinberg. "New insights into the mechanisms of epithelial-mesenchymal transition and implications for cancer." *Nat Rev Mol Cell Biol*, 20, no. 2 (February 2019): 69-84. doi: 10.1038/s41580-018-0080-4.

46. Wilson, William R, and Michael P. Hay. “Targeting hypoxia in cancer therapy.” *Nat Rev Cancer*, 11, (May 24, 2011): 393-410. https://doi.org/10.1038/nrc3064.

47. Schild *et al*. “Unique Metabolic Adaptations Dictate Distal Organ-Specific Metastatic Colonization.” *Cancer Cell*, 33, no. 3 (March 12, 2018): 347-354. doi: 10.1016/j.ccell.2018.02.001.

48. Obradovic *et al*. “Glucocorticoids promote breast cancer metastasis.” *Nature*, 567, (March 13, 2019): 540-544. https://doi.org/10.1038/s41586-019-1019-4.

49. Guo *et al*. “Dual complementary liposomes inhibit triple-negative breast tumor progression and metastasis.” *Science Advances*, 5, no. 3 (March 20, 2019): 540-544. doi: 10.1126/sciadv.aav5010.

50. Thies *et al*. “The small G-protein RalA promotes progression and metastasis of triple-negative breast cancer.” *Breast Cancer Research*, 12, no. 23 (June 12, 2021). doi: 10.1186/s13058-021-01438-3.

51. Mendelaar *et al*. “Defining the dimensions of circulating tumor cells in a large series of breast, prostate, colon, and bladder cancer patients.” *Mol Oncology*, (September 18, 2020). https://doi.org/10.1002/1878-0261.12802.

52. Chen *et al*. “Organotropism: new insights into molecular mechanisms of breast cancer metastasis.” *NPJ Precis Oncol*, 16, no. 2 (February 16, 2018). doi: 10.1038/s41698-018-0047-0.

53. Dupuy *et al*. “PDK1-Dependent Metabolic Reprogramming Dictates Metastatic Potential in Breast Cancer.” *Cell Metabolism*, 22, no. 4 (October 6, 2015): 577-589. doi: 10.1016/j.cmet.2015.08.007.

54. Klein, Christoph A. “Cancer progression and the invisible phase of metastatic colonization.” *Nat Rev Cancer*, 20, no. 11 (November 2020): 581-694. doi: 10.1038/s41568-020-00300-6.

55. Mashimo *et al*. “Acetate is a Bioenergetic Substrate for Human Glioblastoma and Brain Metastases.” *Cell*, 159, no. 7 (December 18, 2014): 1603-1614. doi: 10.1016/j.cell.2014.11.025.

56. Kimbung *et al*. “Transcriptional Profiling of Breast Cancer Metastases Identifies Liver Metastasis-Selective Genes Associated with Adverse Outcome in Luminal A Primary Breast Cancer.” *Clin Cancer Research*, 22, no. 1 (January 1, 2016): 146-157. doi: 10.1158/1078-0432.

57. Ben-Moshe, Shani, and Shalev Itzkovitz. “Spatial heterogeneity in the mammalian liver.” *Nature Reviews Gastroenterology & Hepatology*, 16, (April 1, 2019): 395-410. https://doi.org/10.1038/s41575-019-0134-x.

58. Nystrom, Hanna. “Extracellular matrix proteins in metastases to the liver –

Composition, function and potential applications." *Seminars in Cancer Biology*, 71, (June 2021): 134-142. https://doi.org/10.1016/j.semcancer.2020.06.004.

59. Mullen *et al*. "The interplay between cell signalling and the mevalonate pathway in cancer." *Nat Rev Cancer,* 16, no. 11 (November 2016): 718-731. doi: 10.1038/nrc.2016.76.

60. Luo, Jie, Hongyuan Yang, and Bao-Liang Song. "Mechanisms and regulation of cholesterol homeostasis." *Nat Rev Molecular Cell Biology*, 21, (December 17, 2019): 225-245. https://doi.org/10.1038/s41580-019-0190-7.

61. Fares *et al*. "Molecular principles of metastasis: a hallmark of cancer revisited." *Signal Transduct Target Ther*, 5, no. 1 (March 12, 2020). doi: 10.1038/s41392-020-0134-x.

62. Krol et al. "Detection of clustered circulating tumour cells in early breast cancer." *British Journal of Cancer*, 125, (March 24, 2021): 23-27. https://doi.org/10.1038/s41416-021-01327-8.

63. Kitamura, Takanori, Bin-Zhi Qian, and Jeffrey W Pollard. "Immune cell promotion of metastasis." *Nat Rev Immunol*, 15, no. 2 (February h2015): 73-86. doi: 10.1038/nri3789.

64. Mayer *et al*. "Ribosome biogenesis and cell growth: mTOR coordinates transcription by all three classes of nuclear RNA polymerases." *Oncogene*, 25, (October 16, 2006): 6384-6391. https://doi.org/10.1038/sj.onc.1209883.

65. Fu *et al*. "Gene expression regulation mediated through reversible m(6)A RNA methylation." *Nat Rev Genet,* 15, no. 5 (May 2014): 293-306. doi: 10.1038/nrg3724.

66. Dai *et al*. "N6-methyladenosine links RNA metabolism to cancer progression." *Cell Death Dis*, 9, no. 124 (January 26, 2018). https://doi.org/10.1038/s41419-017-0129-x.

67. Wang *et al*. "N(6)-methyladenosine Modulates Messenger RNA Translation Efficiency." *Cell,* 161, no. 6 (June 4, 2015): 1388-1399. doi: 10.1016/j.cell.2015.05.014.

68. Wang *et al*. "N6-methyladenosine-dependent regulation of messenger RNA stability." *Nature*, 505, no. 7481 (January 2, 2014): 117-120. https://doi.org/10.1038/nature12730.

69. Zhang *et al*. "Hypoxia-inducible factors regulate pluripotency factor expression by ZNF217- and ALKBH5-mediated modulation of RNA methylation in breast cancer cells." *Oncotarget,* 7, no. 40 (October 4, 2016): 64527-64542. doi: 10.18632/oncotarget.11743.

70. Chang *et al*. "YTHDF3 Induces the Translation of m 6 A-Enriched Gene Transcripts to Promote Breast Cancer Brain Metastasis." *Cancer Cell,* 38, no. 6 (December 14, 2020): 857-871. doi: 10.1016/j.ccell.2020.10.004.

71. Coots *et al*. "m6A Facilitates eIF4F-Independent mRNA Translation." *Molecular Cell,* 68, (November 2, 2017): 504-514. doi :https://doi.org/10.1016/j.molcel.2017.10.002.

72. Wang *et al*. "N6-methyladenosine-dependent regulation of messenger RNA stability." *Nature*, 505, (November 27, 2013): 117-120. https://doi.org/10.1038/nature12730.

73. Louloupi *et al*. "Transient N-6-Methyladenosine Transcriptome Sequencing Reveals a Regulatory Role of m6A in Splicing Efficiency." *Cell Reports,* 23, (June 19, 2018): 3429–3437. doi :https://doi.org/10.1016/j.celrep.2018.05.077.

74. Mao *et al*. "m6A in mRNA coding regions promotes translation via the RNA helicase-containing YTHDC2." *Nat Comm*, 10, no. 5332 (November 25, 2019). https://doi.org/10.1038/s41467-019-13317-9.